| Title | Structural study of plant small G protein OsRac1 |
| --- | --- |
| Author(s) | 小佐見, 謙一 |
| Citation | 大阪大学, 2015, 博士論文 |
| Version Type | VoR |
| URL | https://doi.org/10.18910/52307 |
| rights | |
| Note | |

# Structural study of plant small G protein OsRac1

(植物の低分子量 G 蛋白質 OsRac1 の構造生物学的研究)

小佐見　謙一

大阪大学大学院

理学研究科化学専攻

蛋白質研究所　機能構造計測学研究室

(藤原　敏道　教授)

# Contents

# Abbreviations

| | |
|---|---|
| ABA | Abscisic acid |
| At | *Arabidopsis* |
| ATP | Adenosine-5'-triphosphate |
| Bis-Tris | Bis(2-hydroxyethyl)-amino-tris(hydroxymethyl)-methane |
| CA | Constitutively active |
| CBB | Coomassie Brilliant Blue |
| CRIB domain | Cdc42/Rac interactive binding domain |
| C-terminal | Carboxy-terminal |
| DN | Dominant negative |
| DTT | Dithiothreitol |
| *E. coli* | *Escherichia coli* |
| EDTA | Ethylenediaminetetraacetic acid |
| ETI | Effector-triggered immunity |
| GAPs | GTPase activating proteins |
| G domain | Guanine nucleotide binding domain |
| GMPPNP | Guanosine-5'-[$\beta,\gamma$-imido]triphosphate |
| G protein | Guanine nucleotide binding protein |
| GST | Glutathione S-transferase |
| GTP | Guanosine-5'-triphosphate |
| GTP$\gamma$S | Guanosine 5'-O-[gamma-thio]triphosphate |
| GPCR | G protein-coupled receptor |

| | |
|---|---|
| GppNHp | 5'-Guanylyl imidodiphosphate |
| HR | Hypersensitive response |
| HRV3C | Human rhinovirus 3C |
| Hs | *Homo sapiens* |
| HSQC | Heteronuclear single quantum coherence |
| IPTG | Isopropyl -d-1-thiogalactopyranoside |
| LB | Lysogeny broth |
| MES | 2-(N-morpholino)ethanesulfonic acid |
| NB | Nucleotide-binding |
| NMR | Nuclear magnetic resonance |
| NOXes | NADPH oxidases |
| Nt | *Nicotiana tabacum* |
| N-terminal | $NH_2$-terminal |
| NTP | Nucleotide triphosphate |
| NTPase | Nucleoside-5'-triphosphatase |
| O.D | Optical density |
| Os | *Oryza sativa* |
| PAMP | Pathogen-associated molecular pattern |
| pAsp | phosphoasparyate |
| PCD | Programmed cell death |
| PEG | Polyethylene glycol |
| PDB | Protein Data Bank |
| P-loop | Phosphate binding loop |

| | |
|---|---|
| PRONE | Plant-specific Rop nucleotide exchanger |
| PRR | pattern recognition receptor |
| pSer | phosphoserine |
| PTI | PAMP-triggered immunity |
| Rac/Rop | Rho-related GTPases from plant |
| Ras | Rat sarcoma |
| Rboh | Respiratory burst oxidase homolog |
| RMSD | Root mean square deviation |
| ROS | Reactive oxygen specie |
| RT-PCR | Reverse transcriptase polymerase chain reaction |
| SE | Sphingolipid elicitor |
| SDS PAGE | Sodiumdodecylsulfate polyacrylamide gel electrophoresis |
| Tris | Tris(hydroxymethyl)aminomethan |
| WT | Wild type |

# CHAPTER 1

**GENERAL INTRODUCTION**

# 1. GENERAL INTRODUCTION

## 1.1 Intracellular signaling

The cell activation molecules (ligand) such as hormones bind to the specific receptor. The receptors for some ligands are inside the cell, but many ligands receptors are located on the surface of the cell. A series of chain reaction occurs to induce stimulation into a cell from the receptor as the starting-point. As a result, metabolically changes, morphological changes and electrical changes take place in cells.

The process that the enzymatic reaction products of each stage activate the next stage is continually caused, which is referred to as cascade reaction (Figure 1-1). As the effect of a first-order reaction is enhanced largely or instantaneously with the several steps of enzymatic reaction, this amplification mechanism responses to weak environmental change in cells. In the "cascade reaction" of an intracellular signal transduction, the protein phosphorylation and G protein have important work in cell.

## 1.2 Effect of the phosphorylation

The protein phosphorylation has remarkable influence for target proteins and is one type of post-translational modification. Recent phosphoproteomic studies have suggested that the majority of proteins in a mammalian cell are phosphorylated (1). Phosphorylation induces an allosteric conformational change and can activate or inhibit enzyme activity. Additionally, phosphorylation lead to recognition site for other protein molecules. The protein phosphorylation reaction is caused instantly and reversibly and is one of the basic processes of the intracellular signal transduction as a main manner of active control.

In prokaryotic phosphorylation occurs on the serine, threonine and tyrosine residues and in prokaryotes histidine and aspartic acid are phosphorylated. The phosphoryl group (pKa of ~6.7) is dianionic at physiological pH (Figure 1-2). Phosphorylated residues can make the hydrogen-bond network and the salt bridge with basic amino acid residues for the property of a double negative charge and the capacity of the phosphoryl oxygen (Figure 1-3). Thereby, adding or removing a dianionic phosphate group in a protein induce the change of a local physicochemical properties, stability, kinetics and dynamics (2).

Two types predominate in interaction of the phosphate group. First, the interaction of the phosphate group with main-chain nitrogens often observed at the start of an a-helix. The phosphate group utilizes the positive charge of the helix dipole for charge neutralization (3). Secondly, at the tight binding sites using to stabilize a conformational site, phosphoryl group can form hydrogen bond and salt bridge with side-chain of arginine or lysine (Figure 1-4). Arginine usually forms stronger salt bridges with phosphorylated side chains than lysine. On one hand, phosphoserine (pSer) hydrogen-bond acceptor makes more stable interaction compared to phosphoasparyate (pAsp) acceptor (4).

As well as the protein phosphorylation, it is the important that proteins bind to guanosine triphosphate (GTP) and guanosine diphosphate (GDP). GTP and GDP are nucleotides and they exist in intracellular. The GDP is dianionic and GTP is trianionic. G proteins bind to GTP and GDP and regulate the intracellular signal transduction by inducing conformational change of G proteins (Figure 1-5).

## 1.3 Nucleotide triphosphate binding and hydrolyzing proteins

Nucleotide triphosphate (NTP) binding and hydrolyzing proteins are important in almost all facets of life. The mononucleotide-binding fold (P-loop NTPase fold) is the most prevalent domain of the several distinct nucleotide-binding protein folds. The P-loop NTPase proteins are α-β proteins that contain regularly recurring α-β units with the five β-strands (β1–β5). A central core is formed by the β-strands arranged in the order β(5-1-4-3-2) or β(5-1-3-4-2) and these β-strands were sandwiched by α-helices on both sides (5, 6). The P-loop NTPase fold as the most common reaction has the hydrolysis activity of the β-γ phosphate bond of a bound NTP.

The energy of NTP hydrolysis is utilized to induce conformational changes of P-loop NTPase proteins so that P-loop NTPase proteins play an important role in a variety of biochemical function.

**1.4 Trimeric G protein**

There are two classes of G proteins. The first is known as trimeric G proteins while the second is known as small GTPases. The trimeric G proteins play an important role on signal transduction in cells. The trimeric G proteins transmit signals from many hormones, neurotransmitters, smell, taste, light and extracellular other signaling factors to the intracellular. The trimeric G protein is comprised of Gα (39-52 kDa), Gβ (35-39 kDa), Gγ (6-8 kDa) and binds to guanosine triphosphate (GTP) or guanosine diphosphate (GDP) (7). In the steady state, GDP binds to the Gα and Gα exists as heterotrimer of the inactivated form with Gβ and Gγ (Figure 1-5 A). When the extracellular ligands bind to a domain of the G protein-coupled receptor (GPCR) located outside the cell, an intracellular GPCR domain is caused the structural change and GDP is dissociated from Gα. Then GTP binds to the Gα, and the trimeric G protein

dissociates in Gα and Gβγ subunits (Figure 1-5 B). GTP-bound form Gα and Gβγ subunits each transmit signals to the intercellular. Thereafter, GTP which bound to the Ga is hydrolyzed by the GTPase activity of Ga and Ga is returned to GDP bound form. GDP bound form Gα tightly associats with Gβγ subunits. Gα and Gβγ are returned to the trimeric G protein of the inactivated form.

## 1.5 Small GTPase (Small G protein)

Small GTPases (Small G proteins) are homologous to the Gα of trimeric G protein and also bind to GTP or GDP. They are small proteins (20-kDa to 25-kDa) and exist as monomers. Small GTPases play an important role in regulating the variety of biochemical function. Small GTPases exist in eukaryotes from yeast to human and constitute a super-family with at least five families (Ras, Rho, Rab, Sar / Arf and Ran) including more than 100 members (Figure 1-6) (8).

Ras protein plays an important role on signal transduction in cells. GDP-bound Ras protein exists as inactive states. When the extracellular ligands bind to a receptor located on the cell membrane, Ras protein is converted from GDP bound form to GTP bound form and becomes active. Activated Ras has emerged as a key of the phosphorylation reaction of proteins and activates the protein kinase activity (Figure 1-7) (9). The Rho family includes Cdc42, Rac and Rho proteins and regulates many fundamental cellular processes, including cell division, polarization, morphogenesis, and directionality (10).

Plants have only four of five families of small GTPase with lack of the Ras family. Plants have a plant-specific group of Rho family known as Rops (Rho-like GTPases from plants) (11, 12), which are sometimes called Racs in order to the high sequence

similarity with human Rac proteins (13). In plants, the Rops have attracted recent interest due to their function as molecular switches in the regulation of various cellular responses including cytoskeletal organization and dynamics, pollen tube growth and development, and vesicle traffic (Figure 1-8) (14). In recent years, evidence is accumulating that Rops/Racs also play an important role in the regulation of disease resistance.

## 1.6 The architecture of the G domain

The GTP binding and hydrolysis takes place in the highly conserved G domain common to all small GTPases. The conserved functional G domain has a universal structure and a universal switch mechanism. The human Ras (H-Ras) has done most of the biochemical and structural studies (15, 16). H-Ras consists of 189 amino acid residues and the G domain of H-Ras consists of 166 amino acid residues. The G domain of H-Ras folds into a central, curved six-stranded mixed ß-sheet, surrounded on both sides by five a-helices (Figure 1-9 A) (17, 18). This fold is conserved in GTP binding domains of bacterial elongation factor Tu (EF-Tu) and Gα subunit of the heterotrimeric G-proteins.

For nucleotide binding and GTP hydrolysis, the G proteins contain five polypeptide loops (G1-G5) and these sequence motifs are highly conserved (Figure 1-9B and Figure 1-10) (19). The G1 between the strand ß1 and the helices α1, also called phosphate binding loop (p-loop) is responsible for the binding of the phosphate groups. The G2 is located at switch I and contains a conserved threonine residue responsible for $\gamma$-phosphate and $Mg^{2+}$ ion binding. The G3 provides residues for $Mg^{2+}$ ion and phosphate groups binding and is contained just before the Switch II. The G4

14

contains the consensus sequence NKxD. The asparagine residue and the lysine residue have hydrogen bonds to guanine. The G5, although important for binding to the guanine base and often with the sequence motif SAK, is only weakly conserved. Especially, the loop region containing G2 between the helices α1 helix and the strand ß2 and the other loop region containing helices α2 between the strand ß3 and the strand ß4 are important for the conformational switch and are called switch I and switch II, respectively (20).

## 1.7 The mechanism of G domain switch and GTPase-catalyzed GTP hydrolysis

The small GTPases act as regulatory switches which cycle between ON and OFF states (Figure 1-11) (21). The switching between their ON and OFF states is determined by nucleotide binding and hydrolysis. The small GTPase is inactive when bound to GDP (Figure 1-11 a), but when the GDP is exchanged for GTP, the small GTPase switches to the ON-state until the endogenous GTPase activity hydrolyses GTP to GDP.

Although the mechanism of GTPase-catalyzed GTP hydrolysis is still controversially discussed, it is generally accepted that a water molecule acts as nucleophile and attacks the γ-phosphate of GTP in-line (22-24). The typical nucleophilic substitution reaction is caused by reaction mechanism of either SN1 or SN2. In small GTPase, it is thought that the hydrolysis of the GTP is caused by SN2 mechanism (Figure 1-12) (22, 23). For nucleophilic attack, the hydroxyl ion (nucleophilic reagent) is essential in GTPase-catalyzed GTP hydrolysis. The hydroxyl ion approaches phosphate group from backside of the GDP (leaving group), and the transition state is formed. Thereafter, GDP dissociates from phosphate group and GTP hydrolysis is finished.

It differs with enzymes how the hydroxyl ion is produced, and two mechanisms are

proposed. In first opinion, it is thought the hydroxyl ion is generated when a proton is pulled off from water molecules by the specific amino acid (Asp or Glu) (Figure 1-13). In this opinion, it is thought a specific amino acid (Asp or Glu) acts as the base. Previous studies have shown that one water molecule in the crystal structures of F1 of ATPase is close enough to the phosphate to perform the nucleophilic attack (25-27). This water molecule forms hydrogen bond with Glu188 on crystal structure (Figure 1-14). It is thought that Glu188 of F1 pulls off proton from water molecule and the produced hydroxyl ion attacks the γ-phosphate of ATP (28). In second opinion, γ-phosphate acid acts as a catalytic base (Figure 1-15). There are no glutamic acid residue and the aspartate residue which act as a catalytic base on the catalytic part in Ras and the Rho family of the small GTPase. Therefore, the oxygen of γ-phosphoric acid of the GTP attracts the proton of water molecule (22, 29). The water molecule which is deprived of a proton becomes the hydroxyl ion, and attacks the γ-phosphate, the transition state is formed (Figure 1-15). Thereafter, GDP dissociates from opposite sides of the hydroxyl ion, and GDP and phosphate group are produced, and GTP hydrolysis is finished (Figure 1-15).

## 1.8 Regulator of small GTPases

The release of GDP is intrinsically very slow, therefore small GTPases are activated by Guanine Nucleotide Exchange Factors (GEFs). GEFs which increase the dissociation rate of nucleotides accelerates the exchange of the bound GDP (Figure 1-11 b). In animal, most of GEFs contain Diffuse B-cell lymphoma-homology (DH) domain and Pleckstrin-homology (PH) domain, which referred to as DH-PH type GEF (30). However, plants lack DH-PH type GEFs. Therefore, different type GEFs have been

considered to regulate the activity of Rops.

The intrinsic rate of GTP hydrolysis is also intrinsically very slow, therefore small GTPases require the action of GTPase activating proteins (GAPs) to switch off rapidly when cellular conditions impose. GAPs accelerate the slow intrinsic rate of GTP hydrolysis (31).

The catalytic mechanism by GAP were first studied with RasGAP domain of p120GAP in complex with H-Ras-GDP- AlF4 (32) and the RhoGAP domain of p50-RhoGAP in complex with RhoA-GDP-AlF4 (33). They revealed each GAP of H-Ras and RhoA interacts with switch I and switch II in these structures.

The rate acceleration of GTP hydrolysis should be regulated not only by stabilization of the structure of switch I, switch II but by insertion of arginine residue of GAP (also called Arg finger) into the active site of GTPase (Arg finger model) (Figure 1-16) (34). This mechanism of GTP hydrolysis by arginine finger of GAP are as follows : (i) a positively charged arginine residue of GAP at the binding interface inserts into the active site of GTPase and neutralizes the developing negative charge in the transition state of GTP hydrolysis. (ii) Gln residues of GTPase, also called the catalytic glutamine (Q61 of Ras) forms hydrogen bond with the arginine finger of the GAP. This hydrogen bond stabilizes the catalytic glutamine. This Gln is thought to be important for GTP hydrolysis by positioning a water molecule which in turn acts as nucleophile and attacks the γ-phosphate (35). Thus, small GTPase inactivation is accelerated by GAPs.

## 1.9 Plant guanine exchange factors for ROP GTPases

Recently, a new type GEF has been identified in *Arabidopsis* (36). The GEF contains highly conserved region in the center, referred to as PRONE domain

(plant-specific Rop nucleotide exchanger). Rice contains 11 members of PRONE type GEF whereas 14 members are found in *Arabidopsis* (36, 37). It is known that PRONE type GEFs regulate Rop-dependent the morphogenesis of plant (38-41). This PRONE domain is plants specific, is not found in animals and yeasts.

## 1.10 Plant GTPase activating protein for Rop

RopGAPs are GTPase-activating proteins (GAPs) for plant Rho proteins (42). In *Arabidopsis*, 9 RopGAPs exist, which show about 27 % sequence homology to RhoGAPs in yeasts and animals (42). AtRop1-6 has Cdc42/Rac interactive binding domain (CRIB domain) in N-terminal and GAP domain in C-terminal (Figure 1-17) (42). Although CRIB domain is not found in RhoGAPs of yeasts or animals, GAP domain itself is very similar to RhoGAP of yeasts and animals. Because the catalytic arginine residue (the Arg finger) is conserved between plants and animals, it is thought that the RopGAP domain is functionally similar to RhoGAPs from yeast and animals.

## 1.11 Regulation of NADPH oxidase by small GTPase

NADPH oxidases (NOXes) plays a key role in the production of Reactive oxygen specie (ROS). Recent numerous studies have shown that ROS play an important role in many physiological functions including host defense, hormone biosynthesis and cellular signaling as a messenger (43- 45). In animals, gp91[phox] as known NADPH oxidase forms a complex with H-Rac1/2 and H-Rac1/2 play an essential role in activation of gp91[phox] (Figure 1-18 A) (46-49).

In plants, plant NADPH oxidase (Rboh, for respiratory burst oxidase homolog) has

been identified as the first homolog of gp91$^{phox}$ from many plant species including *rice*, *Arabidopsis*, *tobacco*, and *potato* (46, 50-54). All plant Rboh proteins have a cytosolic N-terminal region with two EF-hands that bind Ca$^{2+}$ (46, 55). Rop is known to interact with N-terminal region of Rboh localized on the plasma membrane and Rop binding to Rboh is required for activation of ROS production (Figure 1-18 B) (56).

### 1.12 In Plant, defense response system

Plants possess a highly efficient two-line in innate immune system that renders them resistant against most microbial pathogens (57-59). The first line of plant immunity is triggered by recognition of conserved microbial epitopes knows as pathogen-associated molecular patterns (PAMPs) (Figure 1-19 A) (60). PAMPs are recognized by pattern recognition receptors (PRRs) on their plasma membranes and this detection leads to PAMP-triggered immunity (PTI). PTI is the primary immune response, which effectively prevents colonization of plant tissues by non-pathogens (57). The second line of plant immunity is triggered by recognition of pathogen effectors and produced effector-triggered immunity (ETI) (Figure 1-19 B) (61). In ETI, plants recognize the pathogen effectors by resistance protein (R protein) and induce the programmed cell death (PCD) known as the hypersensitive response (HR) (57, 62). HR leads to rapid local cell death at the site in the local region surrounding an infection. In HR, plants produce superoxide anions and hydrogen peroxide known as ROS (43). The generation of ROS is a ubiquitous early part of the resistance mechanisms of plant cells (63). The increment in the ROS levels leads to inhibit the growth and spread of

pathogens to other parts of the plant. Therefore, plants resist pathogen invasion through a two innate immune system: PTI and ETI.

## 1.13 The roles of OsRac1 in rice innate immunity

Rice small GTPase OsRac1 is composed of 214 amino acids and has about masses of 25 kDa. OsRac1 is known that it plays important role in rice innate immunity (64-70). Transgenic rice expressing constitutively active OsRac1 (CA-OsRac1, OsRac1-G19V), but not transgenic rice expressing the dominant negative OsRac1 (DN-OsRac1, OsRac1-T24N), caused HR-like responses, enhanced resistance against blast fungus and bacterial blight (65). Further experiments demonstrate that transgenic rice expressing CA-OsRac1induced ROS production by fungal sphingolipid elicitor (SE) treatment as well. In contrast, transgenic rice expressing DN-OsRac1 blocked ROS production (71). Recent studies also have shown that CA-OsRac1, but not DN-Rac1, interacted with the N-terminus of rice NADPH oxidase OsRbohB (56, 72). These results indicate that OsRac1 are required for activation of ROS production in plant innate immunity and direct Rac–Rboh interaction may activate NADPH oxidase activity in plants.

## 1.14 Aim to this study

OsRac1 is the Rop family of plant small GTPases and has emerged as a key activator of downstream defense processes. Numerous studies suggest OsRac1 plays an important role as a molecular switch in plant innate immunity. However, the molecular mechanisms by which OsRac1 is activated in innate immunity remain largely unknown. Therefore, the aim of the present doctoral thesis is to investigate the basic biochemical

and structural features of OsRac1. Based on these findings, the work should create the molecular basis for further *in vivo* and *in vitro* studies of OsRac1 as a first step for better understanding the molecular mechanisms of defense in plants.
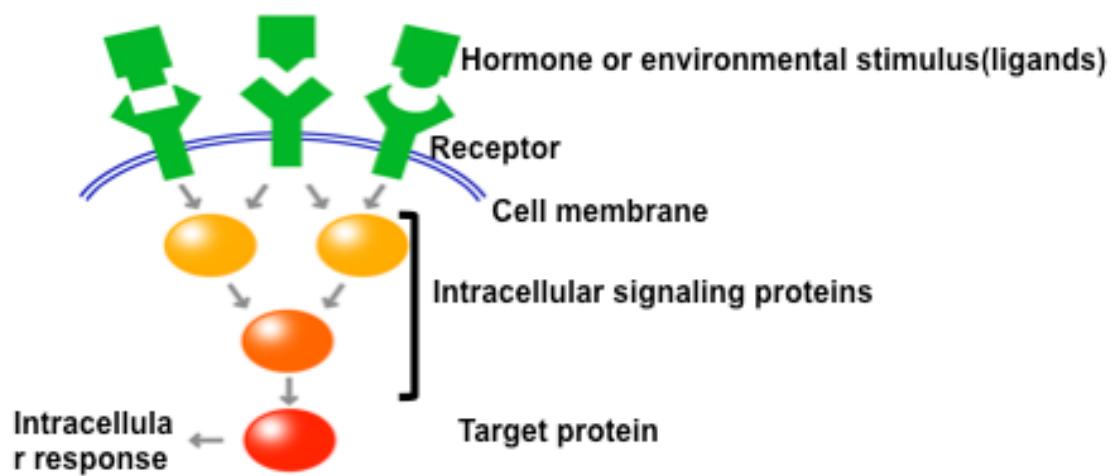
**Figure 1-1. Signal transduction pathways.**
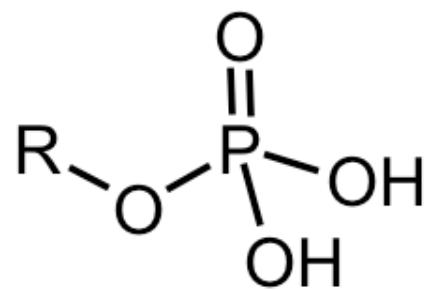


**Figure 1-2. Phosphoryl group.** P, O, H indicates phosphorus, nitrogen, oxygen atoms, respectively.

**Non-Phosphorylated form**

**Phosphorylated form**

Phosphorylated residue

phosphate dependent site of protein
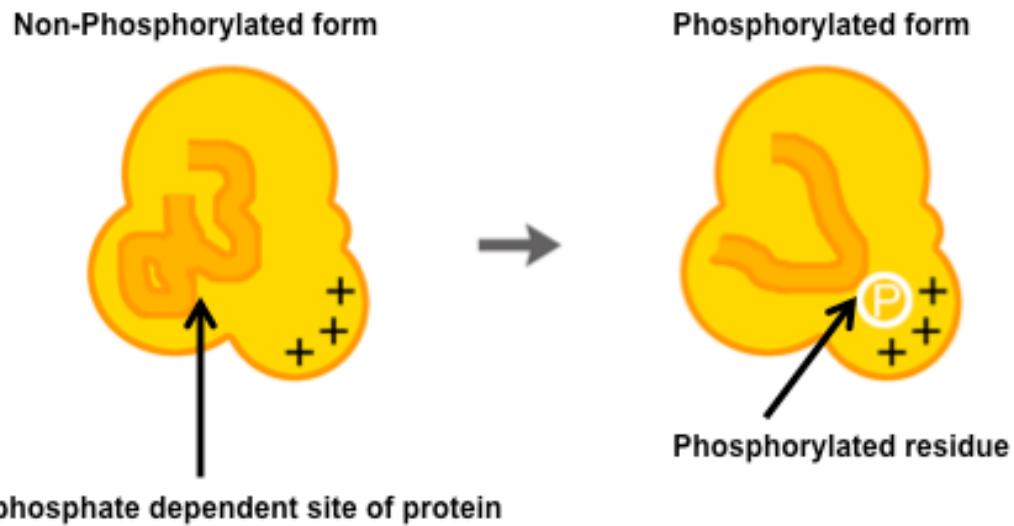
**Figure 1-3. Conformation changes caused by phosphorylation.** P indicates the phosphorylation.



GDP binding form

GTP binding form

G protein

GDP

GTP

GDP/GTP exchange

Target protein

Interaction
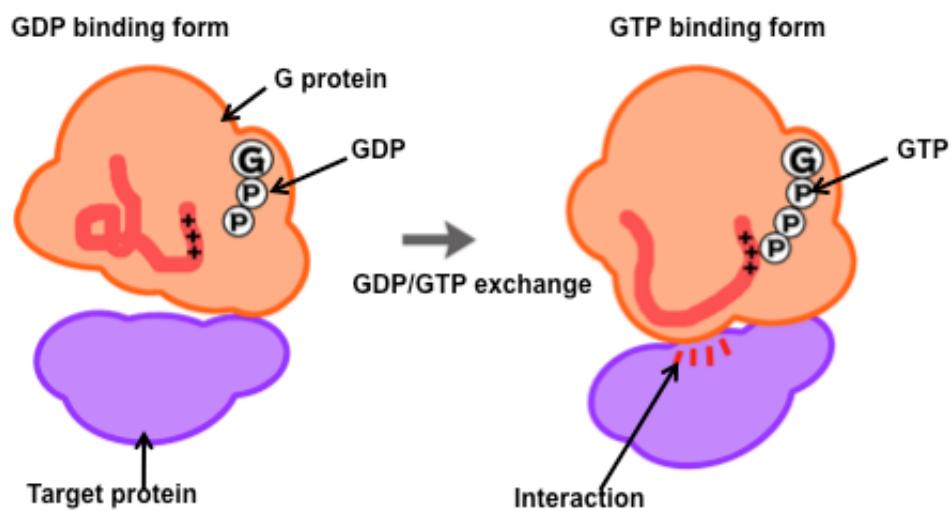
**Figure 1-4. Conformation changes caused by GDP/GTP exchange.**
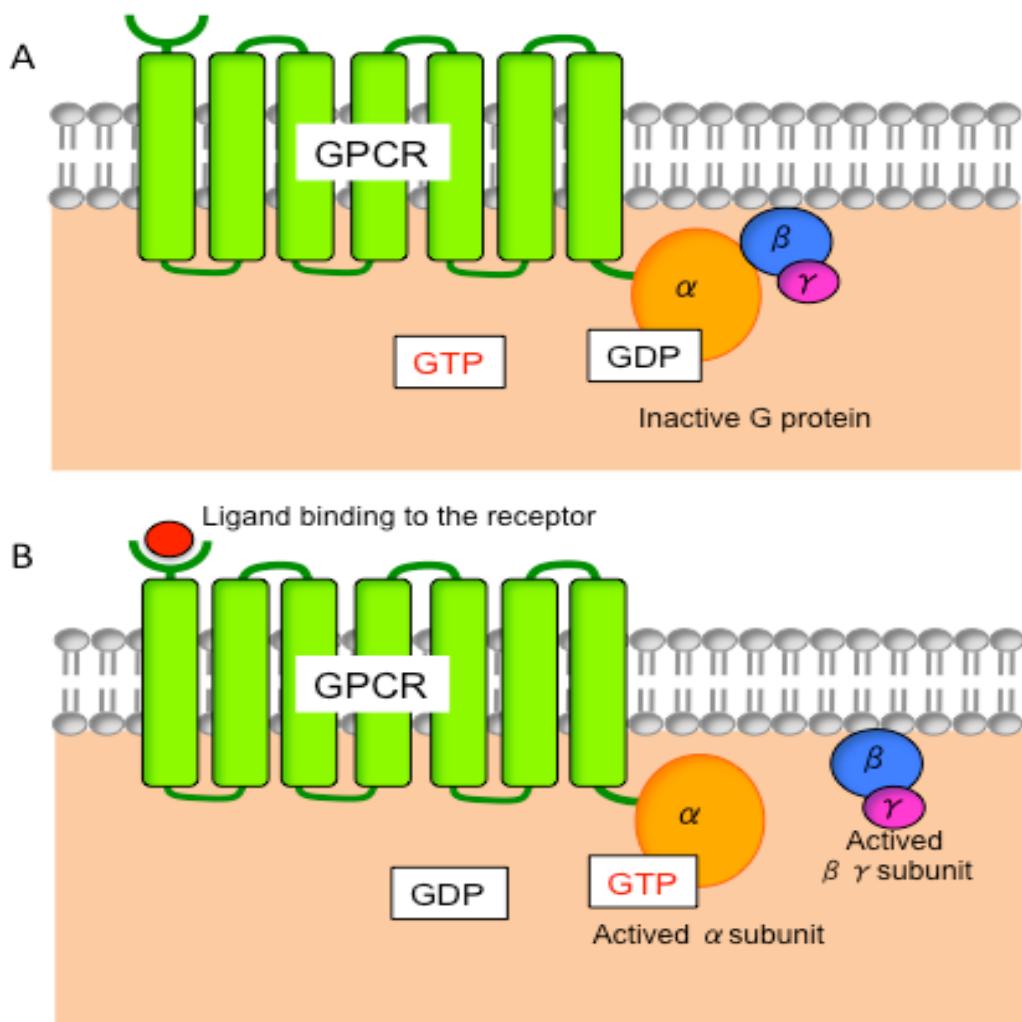
**Figure 1-5. Schematic illustrations of a G protein-coupled receptor (GPCR).** A trimeric GTP-binding protein (G protein) consisting of three subunits called α, β and γ is associated with GPCR (A) When no ligand is present, the α subunit of G protein binds to GDP and the trimeric G protein is inactive. (B) When ligands interact with the receptor of GPCR, a conformational change of the GPCR occurs. This leads the α subunit to exchange its bound GDP to GTP. This causes the βγ subunit to dissociate and activates the α subunit and the βγ subunit. Figure is adapted from (73).
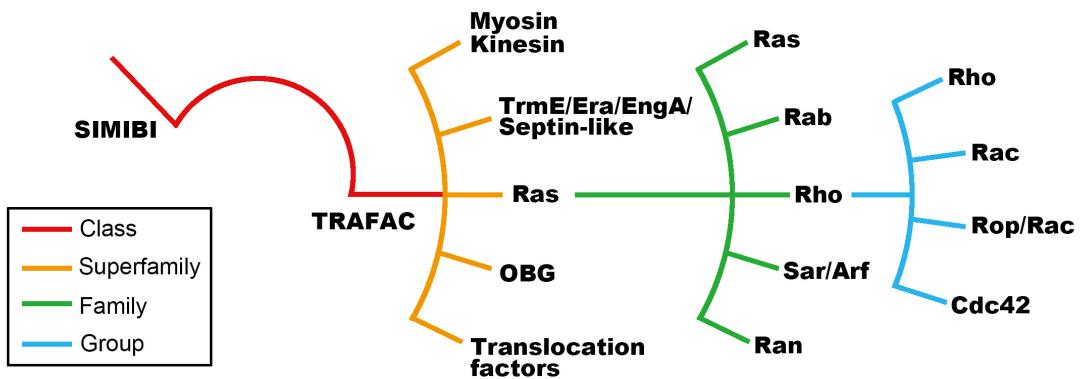
**Figure 1-6. Positioning of the paraseptin clade in the P-loop NTPase superclass.**
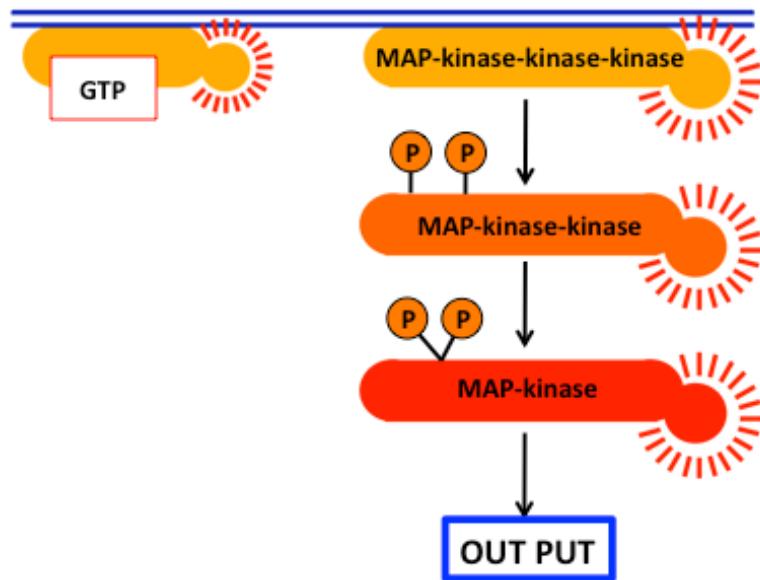


**Figure 1-7. Activated phosphorylation cascade by Ras.** P shows the phosphorylation. Activation of proteins are represented by arcs with spokes.
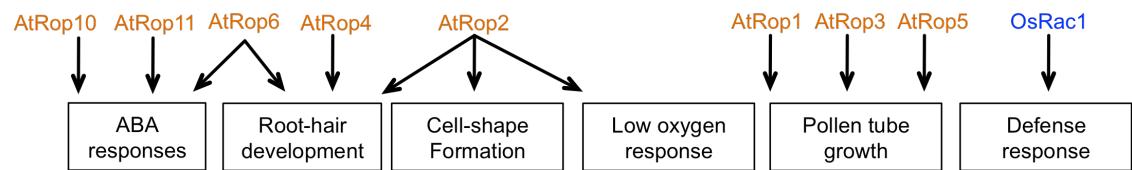
**Figure 1-8. The role of small GTPases in plant.**
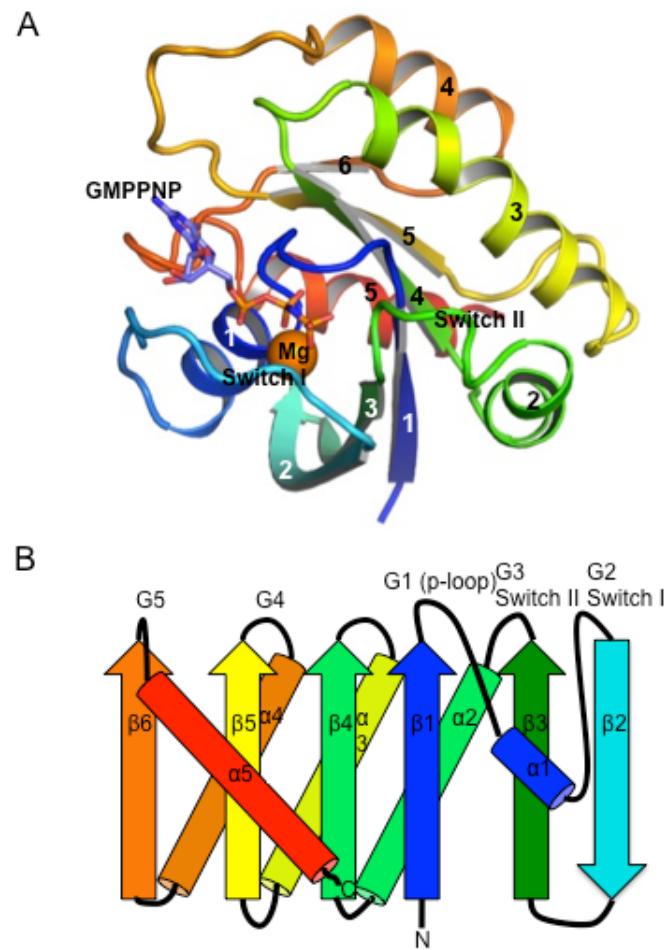
**Figure 1-9. Schematic representations of the G domain fold.** (A) Cartoon representation of the H-ras p21 (PDB code: 5P21). The nucleotide analog is shown in ball-and-stick representation and colored according to atom types. Carbon atoms are colored white, nitrogen blue, oxygen red and phosphorous orange. The magnesium ion is shown as orange sphere. (B) Topology of the G domain fold. Secondary structure elements are shown and colored as in A. conserved motifs and their amino acid residues are indicated.
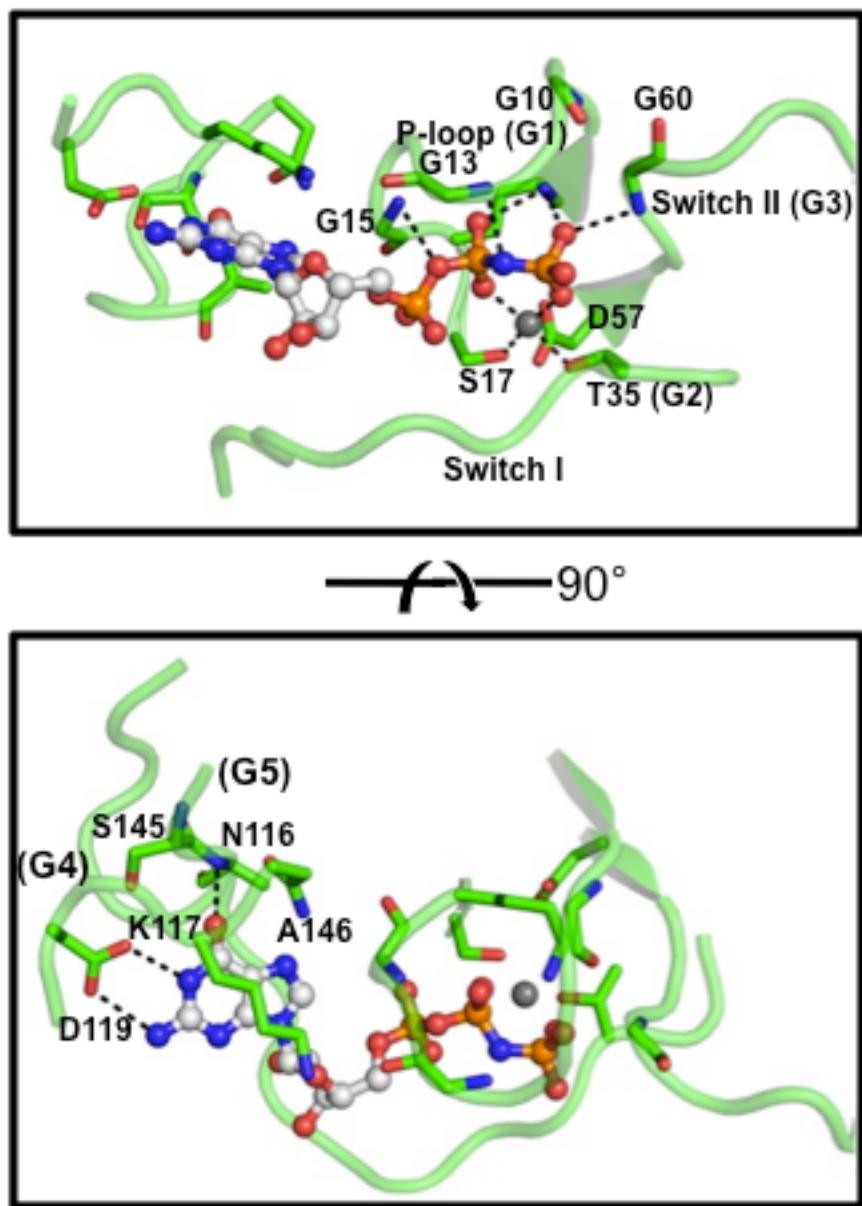
**Figure 1-10. Detailed view of the H-Ras p21 nucleotide-binding site** (see also Figure 1-3). Loops involved in GMP-PNP-binding are shown as green tubes, and selected amino acid residues are represented as sticks with carbon atoms colored green, nitrogen blue and oxygen red. The nucleotide analog is shown as in Figure 1-3. Protein-GMPPNP interactions are indicated as dotted.
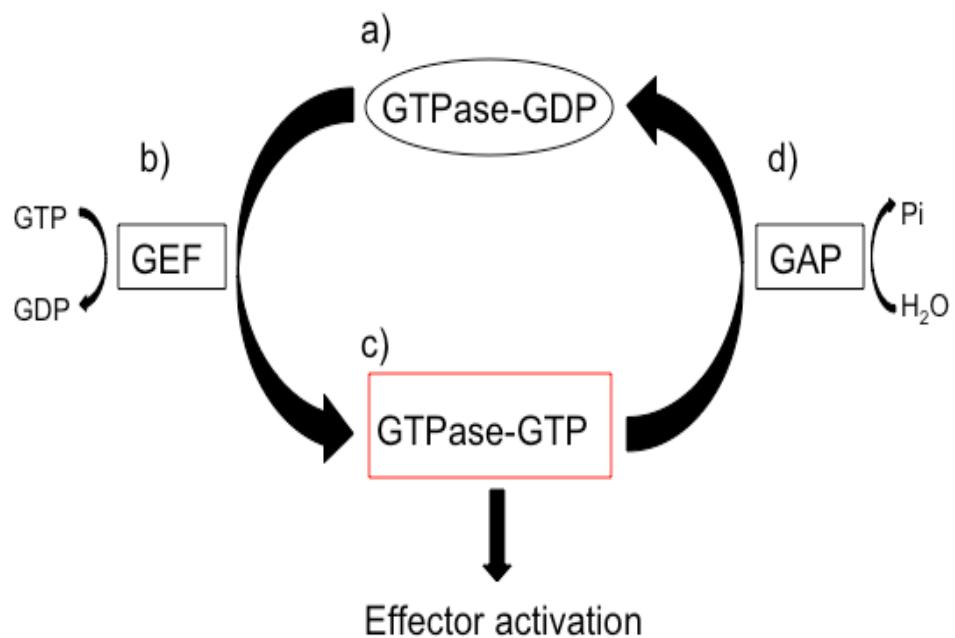
**Figure 1-11. Schematic view of the G domain switch mechanism of small GTPases.**
The GDP-bound OFF-state is indicated as black ellipse, the GTP-bound ON-state as red rectangle. The events a-d are described in the text. GEF-guanine nucleotide exchange factor, GAP-GTPase-activating protein.
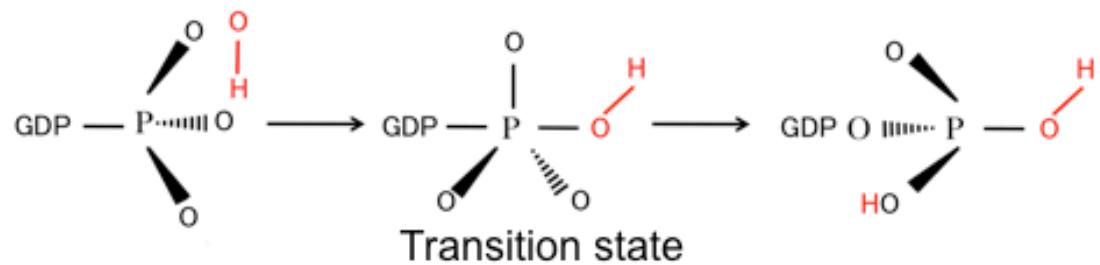
**Figure 1-12. Mechanistic principle of phosphoryl transfer in GTPases.** (A) Ground state of the reaction. (B) Transition state of the reaction, where bond lengths for a fully dissociative or fully associative state are given (see text). (C) Reaction products.
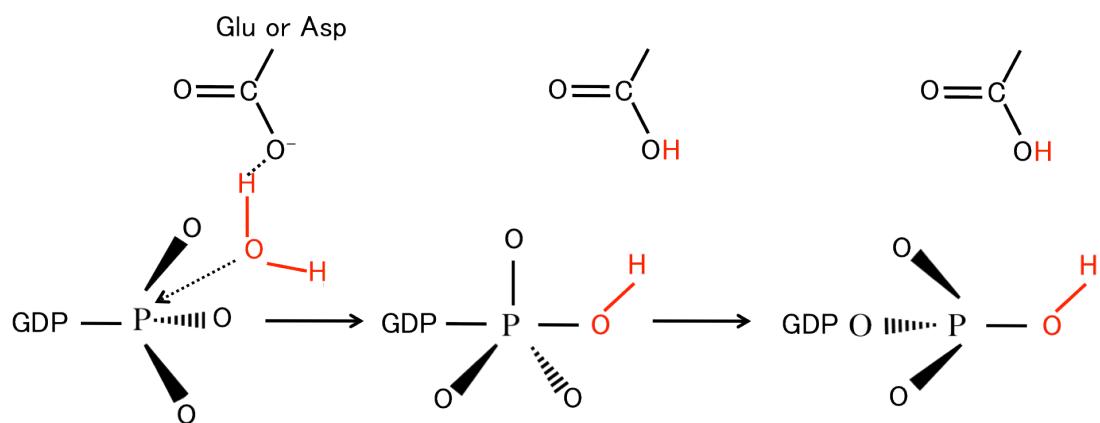


**Figure 1-13. The Glu and Asp of amino acid acts as a catalytic base**
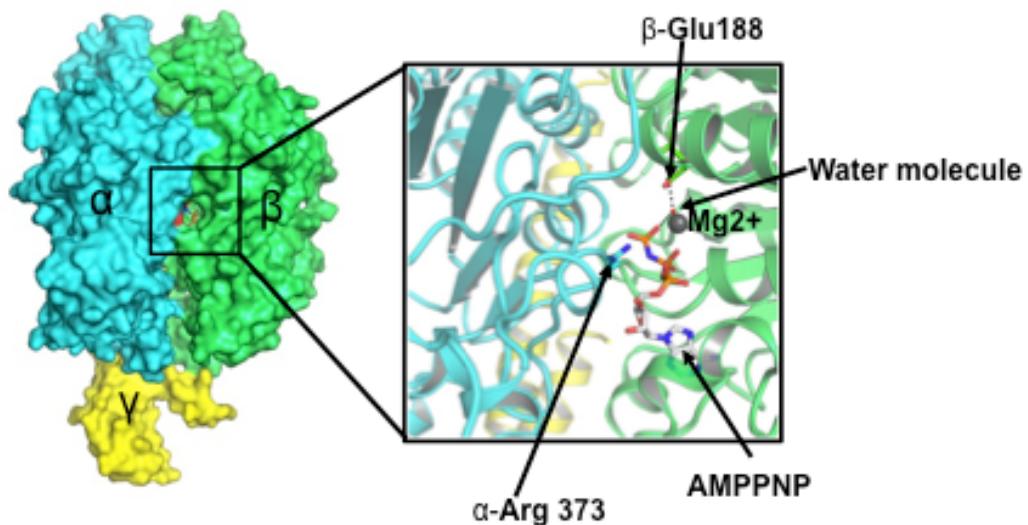
**Figure 1-14. Catalytic Nucleotide Binding Site of F1.** β-Glu188 makes H-bonds to a water molecule and has it ready to attack the$Mg^{2+}$ γ-phosphate of ATP. α-Arg 373 helps stabilize the negative charge. The nucleotide analog is shown in stick representation and colored according to atom types. The magnesium ion is shown as grey sphere. Water molecule is shown as red sphere.
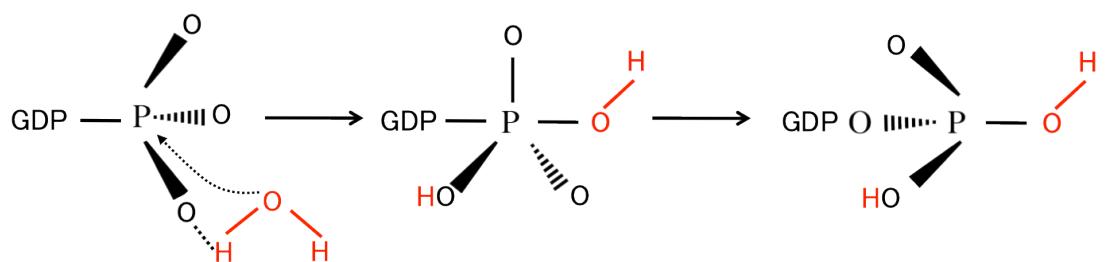
**Figure 1-15. The γ-phosphate acid of GTP acts as a catalytic base.**
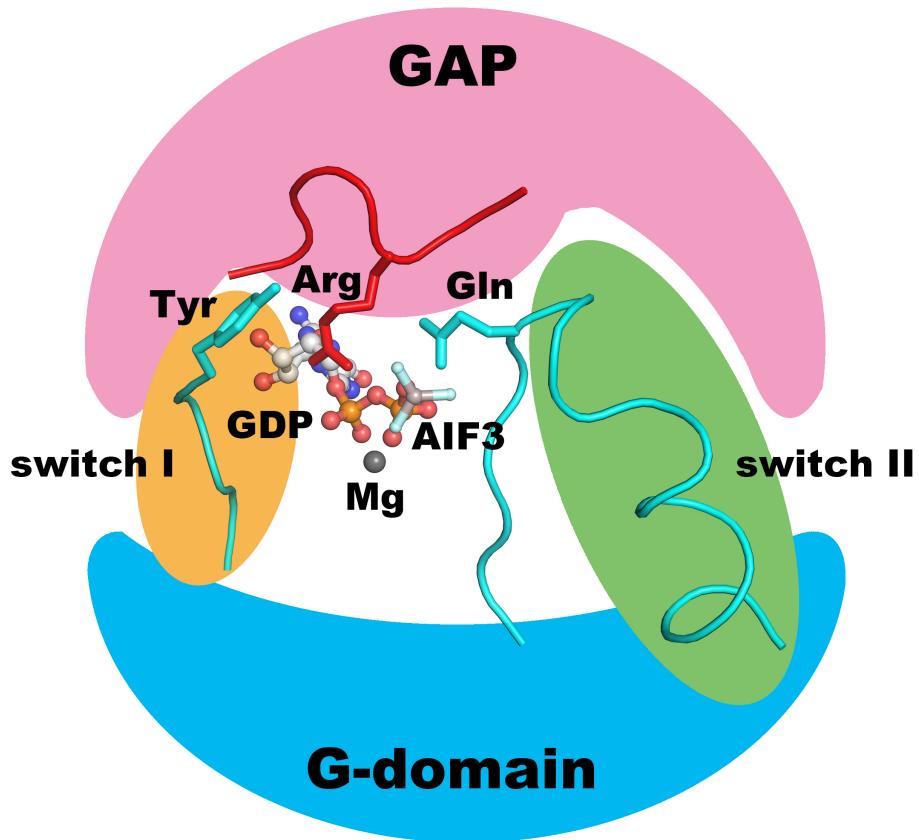
**Figure 1-16. The mechanism of GTPase-activation for Ras.** Only the P-loop, switch I and switch II of the GTPase is shown in cartoon, as well as the GAP loops which provide the arginine fingers. The remainder of the proteins is indicated schematically. Ras is colored cyan, RasGAP red. Structure has been solved in the presence of GDP, magnesium and aluminum fluoride, which is a mimic of the transition state during GTP hydrolysis (indicated as AlF3). The catalytic water is indicated as W. The arginine fingers and catalytic glutamines are indicated as Arg and Gln, respectively. Figure is adapted from (21).
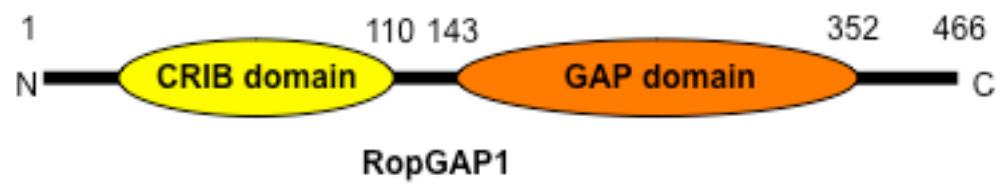
**Figure 1-17. Domain architecture of RopGAP1 containing the CRIB domain (yellow) and GAP domain (orange).**
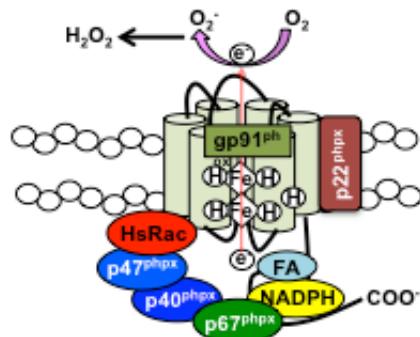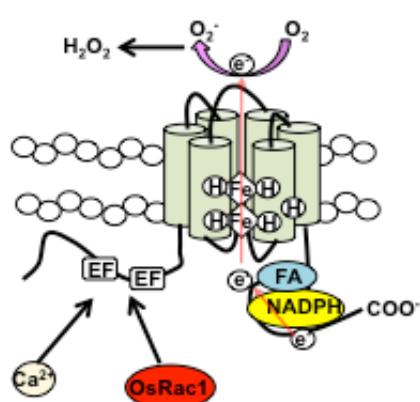
**Figure 1-18. Small GTPases control NADPH oxidase.** (A) NADPH oxidase activity requires p22[phox], p47[phox] and the small GTPase Rac. Activation of the enzyme occurs after translocation of HsRac and p47[phox] to the membrane-bound the gp91[phox]. (B) NADPH oxidase activity requires the small GTPase OsRac1. Activation of the enzyme occurs after interaction of OsRac1 with N-terminal of OsRbohB.
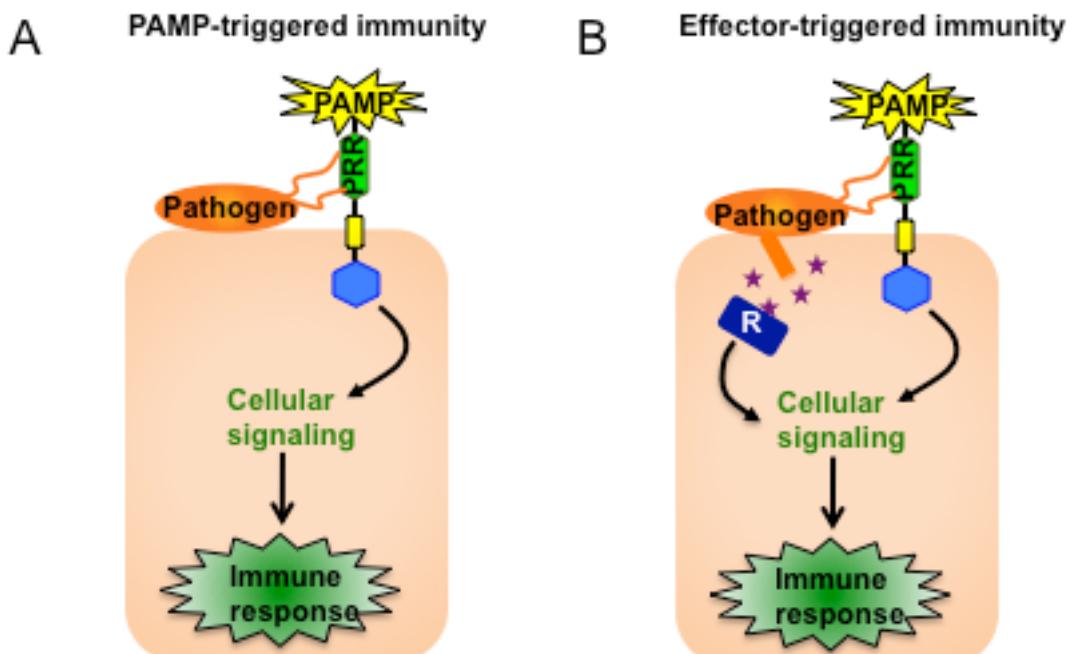
**Figure 1-19.** (A) On pathogen attack, pathogen-associated molecular patterns (PAMPs) are recognized by pattern recognition receptors (PRRs) on their plasma membranes and this detection leads to PAMP-triggered immunity (PTI). (B) When Resistance (R) proteins recognize specific effectors in intracellular, a secondary immune response called effector-triggered immunity (ETI) is induced in plants. Figure is adapted from (74).

**References**

1. Olsen, J. V., Vermeulen, M., Santamaria, A., Kumar, C., Miller, M. L., Jensen, L. J., Gnad, F., Cox, J., Jensen, T. S., Nigg, E. A., Brunak, S., and Mann, M. (2010) Quantitative phosphoproteomics reveals widespread full phosphorylation site occupancy during mitosis. *Sci Signal* **3**, ra3

2. Johnson, L. N. (2009) The regulation of protein phosphorylation. *Biochem. Soc. Trans.* **37**, 627-641

3. Johnson, L. N., and Lewis, R. J. (2001) Structural basis for control by phosphorylation. *Chem. Rev.* **101**, 2209-2242

4. Mandell, D. J., Chorny, I., Groban, E. S., Wong, S. E., Levine, E., Rapp, C. S., and Jacobson, M. P. (2007) Strengths of hydrogen bonds involving phosphorylated amino acid side chains. *J. Am. Chem. Soc.* **129**, 820-827

5. Milner-White, E. J., Coggins, J. R., and Anton, I. A. (1991) Evidence for an ancestral core structure in nucleotide-binding proteins with the type A motif. *J. Mol. Biol.* **221**, 751-754

6. Neuwald, A. F., Aravind, L., Spouge, J. L., and Koonin, E. V. (1999) AAA+: A class of chaperone-like ATPases associated with the assembly, operation, and disassembly of protein complexes. *Genome Res* **9**, 27-43

7. Preininger, A. M., and Hamm, H. E. (2004) G protein signaling: insights from new structures. *Sci STKE* 2004, re3

8. Takai, Y., Sasaki, T., and Matozaki, T. (2001) Small GTP-binding proteins. *Physiol. Rev.* **81**, 153-208

9. Avruch, J., Khokhlatchev, A., Kyriakis, J. M., Luo, Z., Tzivion, G., Vavvas, D., and Zhang, X. F. (2001) Ras activation of the Raf kinase: tyrosine kinase recruitment of the MAP kinase cascade. *Recent. Prog. Horm. Res.* **56**, 127-155

10. Iden, S., and Collard, J. G. (2008) Crosstalk between small GTPases and polarity proteins in cell polarization. *Nat. Rev. Mol. Cell. Biol.* **9**, 846-859

11. Yang, Z., and Watson, J. C. (1993) Molecular cloning and characterization of rho, a ras-related small GTP-binding protein from the garden pea. *Proc. Natl. Acad. Sci. U. S. A.* **90**, 8732-8736

12. Li, H., Wu, G., Ware, D., Davis, K. R., and Yang, Z. (1998) Arabidopsis Rho-related GTPases: differential gene expression in pollen and polar localization in fission yeast. *Plant Physiol* **118**, 407-417

13. Winge, P., Brembu, T., and Bones, A. M. (1997) Cloning and characterization of rac-like cDNAs from Arabidopsis thaliana. *Plant Mol. Biol.* **35**, 483-495

14. Yang, Z. (2002) Small GTPases: versatile signaling switches in plants. *Plant Cell* **14 Suppl**, S375-388

15. Wittinghofer, A. and Waldmann, H. (2000) Ras, a molecular switch involved in tumor formation. *Angew. Chem. Int. Ed* **39**, 4192–4214

16. Schweins, T., Langen, R., and Warshel, A. (1994) Why have mutagenesis studies not located the general base in ras p21. *Nat. Struct. Biol.* **1**, 476-484

17. Pai, E. F., Krengel, U., Petsko, G. A., Goody, R. S., Kabsch, W., and Wittinghofer, A. (1990) Refined crystal structure of the triphosphate conformation of H-ras p21 at 1.35 A resolution: implications for the mechanism of GTP hydrolysis. *EMBO J.* **9**, 2351-2359

18. Tong, L. A., de Vos, A. M., Milburn, M. V., and Kim, S. H. (1991) Crystal structures at 2.2 A resolution of the catalytic domains of normal ras protein and an oncogenic mutant complexed with GDP. *J. Mol. Biol.* **217**, 503-516

19. Bourne, H. R., Sanders, D. A., and McCormick, F. (1991) The GTPase superfamily: conserved structure and molecular mechanism. *Nature* **349**, 117-127

20. Sprang, S. R. (1997) G protein mechanisms: insights from structural analysis. *Annu. Rev. Biochem.* **66**, 639-678

21. Vetter, I. R., and Wittinghofer, A. (2001) The guanine nucleotide-binding switch in three dimensions. *Science* **294**, 1299-1304

22. Pasqualato, S., and Cherfils, J. (2005) Crystallographic evidence for substrate-assisted GTP hydrolysis by a small GTP binding protein. *Structure* **13**, 533-54

23. Feuerstein, J., Goody, R. S., and Webb, M. R. (1989) The mechanism of guanosine nucleotide hydrolysis by p21 c-Ha-ras. The stereochemical course of the GTPase reaction. *J. Biol. Chem.* **264**, 6188-6190

24. Abrahams, J. P., Leslie, A. G., Lutter, R., and Walker, J. E. (1994) Structure at 2.8 A resolution of F1-ATPase from bovine heart mitochondria. *Nature* **370**, 621-628

25. Weber, J., and Senior, A. E. (1997) Catalytic mechanism of F1-ATPase. *Biochim. Biophys. Acta.* **1319**, 19-58

26. Gibbons, C., Montgomery, M. G., Leslie, A. G., and Walker, J. E. (2000) The structure of the central stalk in bovine F(1)-ATPase at 2.4 A resolution. *Nat. Struct. Biol.* **7**, 1055-1061

27. Menz, R. I., Walker, J. E., and Leslie, A. G. (2001) Structure of bovine mitochondrial F(1)-ATPase with nucleotide bound to all three catalytic sites:

implications for the mechanism of rotary catalysis. *Cell* **106**, 331-341

28. Bos, J. L. (1988) The ras gene family and human carcinogenesis. *Mutat. Res.* **195**, 255-271

29. Transformation efficiency of RasQ61 mutants linked to structural features of the switch regions in the presence of Raf. *Structure* **15**, 1618-1629

30. Schmidt, A., and Hall, A. (2002) Guanine nucleotide exchange factors for Rho GTPases: turning on the switch. *Genes Dev.* **16**, 1587-1609

31. Gideon, P., John, J., Frech, M., Lautwein, A., Clark, R., Scheffler, J. E., and Wittinghofer, A. (1992) Mutational and kinetic analyses of the GTPase-activating protein (GAP)-p21 interaction: the C-terminal domain of GAP is not sufficient for full activity. *Mol. Cell. Biol.* **12**, 2050-2056

32. Scheffzek, K., Ahmadian, M. R., Kabsch, W., Wiesmüller, L., Lautwein, A., Schmitz, F., and Wittinghofer, A. (1997) The Ras-RasGAP complex: structural basis for GTPase activation and its loss in oncogenic Ras mutants. *Science* **277**, 333-338

33. Rittinger, K., Walker, P. A., Eccleston, J. F., Smerdon, S. J., and Gamblin, S. J. (1997) Structure at 1.65 A of RhoA and its GTPase-activating protein in complex with a transition-state analogue. *Nature* **389**, 758-762

34. Scheffzek, K., Ahmadian, M. R., and Wittinghofer, A. (1998) GTPase-activating proteins: helping hands to complement an active site. *Trends Biochem. Sci.* **23**, 257-262

35. Schweins, T., Geyer, M., Scheffzek, K., Warshel, A., Kalbitzer, H. R., and Wittinghofer, A. (1995) Substrate-assisted catalysis as a mechanism for GTP hydrolysis of p21ras and other GTP-binding proteins. *Nat. Struct. Biol.* **2**, 36-44

36. Berken, A., Thomas, C., and Wittinghofer, A. (2005) A new family of RhoGEFs

activates the Rop molecular switch in plants. *Nature* **436**, 1176-1180

37. Gu, Y., Li, S., Lord, E. M., and Yang, Z. (2006) Members of a novel class of Arabidopsis Rho guanine nucleotide exchange factors control Rho GTPase-dependent polar growth. *Plant Cell* **18**, 366-381

38. Duan, Q., Kita, D., Li, C., Cheung, A. Y., and Wu, H. M. (2010) FERONIA receptor-like kinase regulates RHO GTPase signaling of root hair development. *Proc. Natl. Acad. Sci. U. S. A.* **107**, 17821-17826

39. Chen, M., Liu, H., Kong, J., Yang, Y., Zhang, N., Li, R., Yue, J., Huang, J., Li, C., Cheung, A. Y., and Tao, L. Z. (2011) RopGEF7 regulates PLETHORA-dependent maintenance of the root stem cell niche in Arabidopsis. *Plant Cell* **23**, 2880-2894

40. Zhang, Y., and McCormick, S. (2007) A distinct mechanism regulating a pollen-specific guanine nucleotide exchange factor for the small GTPase Rop in Arabidopsis thaliana. *Proc. Natl. Acad. Sci. U. S. A.* **104**, 18830-18835

41. Gu, Y., Li, S., Lord, E. M., and Yang, Z. (2006) Members of a novel class of Arabidopsis Rho guanine nucleotide exchange factors control Rho GTPase-dependent polar growth. *Plant Cell* **18**, 366-381

42. Wu, G., Li, H., and Yang, Z. (2000) Arabidopsis RopGAPs are a novel family of rho GTPase-activating proteins that require the Cdc42/Rac-interactive binding motif for rop-specific GTPase stimulation. *Plant Physiol.* **124**, 1625-1636

43. Lamb, C., and Dixon, R. A. (1997) THE OXIDATIVE BURST IN PLANT DISEASE RESISTANCE. *Annu. Rev. Plant Physiol. Plant Mol. Biol.* **48**, 251-275

44. Levine, A., Tenhaken, R., Dixon, R., and Lamb, C. (1994) $H_2O_2$ from the oxidative burst orchestrates the plant hypersensitive disease resistance response. *Cell*

**79**, 583-593

45. Alvarez, M. E., Pennell, R. I., Meijer, P. J., Ishikawa, A., Dixon, R. A., and Lamb, C. (1998) Reactive oxygen intermediates mediate a systemic signal network in the establishment of plant immunity. *Cell* **92**, 773-784

46. Keller, T., Damude, H. G., Werner, D., Doerner, P., Dixon, R. A., and Lamb, C. (1998) A plant homolog of the neutrophil NADPH oxidase gp91phox subunit gene encodes a plasma membrane protein with $Ca^{2+}$ binding motifs. *Plant Cell* **10**, 255-266

47. Sumimoto, H., Hata, K., Mizuki, K., Ito, T., Kage, Y., Sakaki, Y., Fukumaki, Y., Nakamura, M., and Takeshige, K. (1996) Assembly and activation of the phagocyte NADPH oxidase. Specific interaction of the N-terminal Src homology 3 domain of p47phox with p22phox is required for activation of the NADPH oxidase. *J. Biol. Chem.* **271**, 22152-22158

48. Takeya, R., Ueno, N., Kami, K., Taura, M., Kohjima, M., Izaki, T., Nunoi, H., and Sumimoto, H. (2003) Novel human homologues of p47phox and p67phox participate in activation of superoxide-producing NADPH oxidases. *J. Biol. Chem.* **278**, 25234-25246

49. Miyano, K., Koga, H., Minakami, R., and Sumimoto, H. (2009) The insert region of the Rac GTPases is dispensable for activation of superoxide-producing NADPH oxidases. *Biochem J.* **422**, 373-382

50. Groom, Q. J., Torres, M. A., Fordham-Skelton, A. P., Hammond-Kosack, K. E., Robinson, N. J., and Jones, J. D. (1996) rbohA, a rice homologue of the mammalian gp91phox respiratory burst oxidase gene. *Plant J.* **10**, 515-522

51. Torres, M. A., Onouchi, H., Hamada, S., Machida, C., Hammond-Kosack, K. E.,

and Jones, J. D. (1998) Six Arabidopsis thaliana homologues of the human respiratory burst oxidase (gp91phox). *Plant J.* **14**, 365-370

52. Yoshioka, H., Sugie, K., Park, H. J., Maeda, H., Tsuda, N., Kawakita, K., and Doke, N. (2001) Induction of plant gp91 phox homolog by fungal cell wall, arachidonic acid, and salicylic acid in potato. *Mol. Plant-Microbe Interact.* **14**, 725-736

53. Yoshioka, H., Numata, N., Nakajima, K., Katou, S., Kawakita, K., Rowland, O., Jones, J. D., and Doke, N. (2003) Nicotiana benthamiana gp91phox homologs NbrbohA and NbrbohB participate in $H_2O_2$ accumulation and resistance to Phytophthora infestans. *Plant Cell* **15**, 706-718

54. Sagi, M., and Fluhr, R. (2006) Production of reactive oxygen species by plant NADPH oxidases. *Plant Physiol.* **141**, 336-340 (end) Lieberherr, D., Thao, N. P., Nakashima, A., Umemura, K., Kawasaki, T., and Shimamoto, K. (2005) A sphingolipid elicitor-inducible mitogen-activated protein kinase is regulated by the small GTPase OsRac1 and heterotrimeric G-protein in rice 1. *Plant Physiol.* **138**, 1644-1652

55. Torres, M. A., and Dangl, J. L. (2005) Functions of the respiratory burst oxidase in biotic interactions, abiotic stress and development. *Curr. Opin. Plant Biol.* **8**, 397-403

56. Wong, H. L., Pinontoan, R., Hayashi, K., Tabata, R., Yaeno, T., Hasegawa, K., Kojima, C., Yoshioka, H., Iba, K., Kawasaki, T., and Shimamoto, K. (2007) Regulation of rice NADPH oxidase by binding of Rac GTPase to its N-terminal extension. *Plant Cell* **19**, 4022-4034

57. Jones, J. D., and Dangl, J. L. (2006) The plant immune system. *Nature* **444**,

323-329

58. Dodds, P. N., and Rathjen, J. P. (2010) Plant immunity: towards an integrated view of plant-pathogen interactions. *Nat. Rev. Genet.* **11**, 539-548

59. Medzhitov, R., and Janeway, C. A. (1997) Innate immunity: the virtues of a nonclonal system of recognition. *Cell* **91**, 295-298

60. Dangl, J. L., Horvath, D. M., and Staskawicz, B. J. (2013) Pivoting the plant immune system from dissection to deployment. *Science* **341**, 746-751

61. Chisholm, S. T., Coaker, G., Day, B., and Staskawicz, B. J. (2006) Host-microbe interactions: shaping the evolution of the plant immune response. *Cell* **124**, 803-814

62. Physiological and Molecular *Plant Pathology.* **78** (2012) 51-65

63. Apel, K., and Hirt, H. (2004) Reactive oxygen species: metabolism, oxidative stress, and signal transduction. *Annu. Rev. Plant Biol.* **55**, 373-399

64. Ono, E., Wong, H. L., Kawasaki, T., Hasegawa, M., Kodama, O., and Shimamoto, K. (2001) Essential role of the small GTPase Rac in disease resistance of rice. *Proc. Natl. Acad. Sci. U. S. A.* **98**, 759-764

65. Lieberherr, D., Thao, N. P., Nakashima, A., Umemura, K., Kawasaki, T., and Shimamoto, K. (2005) A sphingolipid elicitor-inducible mitogen-activated protein kinase is regulated by the small GTPase OsRac1 and heterotrimeric G-protein in rice 1. *Plant Physiol.* **138**, 1644-1652

66. Kawasaki, T., Henmi, K., Ono, E., Hatakeyama, S., Iwano, M., Satoh, H., and Shimamoto, K. (1999) The small GTP-binding protein rac is a regulator of cell death in plants. *Proc. Natl. Acad. Sci. U. S. A.* **96**, 10922-10926.

67. Thao, N. P., Chen, L., Nakashima, A., Hara, S., Umemura, K., Takahashi, A.,

Shirasu, K., Kawasaki, T., and Shimamoto, K. (2007) RAR1 and HSP90 form a complex with Rac/Rop GTPase and function in innate-immune responses in rice. *Plant Cell* **19**, 4035-4045

68. Nakashima, A., Chen, L., Thao, N. P., Fujiwara, M., Wong, H. L., Kuwano, M., Umemura, K., Shirasu, K., Kawasaki, T., and Shimamoto, K. (2008) RACK1 functions in rice innate immunity by interacting with the Rac1 immune complex. *Plant Cell* **20**, 2265-2279

69. Chen, L., Shiotani, K., Togashi, T., Miki, D., Aoyama, M., Wong, H. L., Kawasaki, T., and Shimamoto, K. (2010) Analysis of the Rac/Rop small GTPase family in rice: expression, subcellular localization and role in disease resistance. *Plant Cell Physiol.* **51**, 585-595

70. Kim, S. H., Oikawa, T., Kyozuka, J., Wong, H. L., Umemura, K., Kishi-Kaboshi, M., Takahashi, A., Kawano, Y., Kawasaki, T., and Shimamoto, K. (2012) The bHLH Rac Immunity1 (RAI1) Is Activated by OsRac1 via OsMAPK3 and OsMAPK6 in Rice Immunity. *Plant Cell Physiol.* **53**, 740-754

71. Kawasaki, T., Henmi, K., Ono, E., Hatakeyama, S., Iwano, M., Satoh, H., and Shimamoto, K. (1999) The small GTP-binding protein rac is a regulator of cell death in plants. *Proc. Natl. Acad. Sci. U. S. A.* **96**, 10922-10926

72. Oda, T., Hashimoto, H., Kuwabara, N., Akashi, S., Hayashi, K., Kojima, C., Wong, H. L., Kawasaki, T., Shimamoto, K., Sato, M., and Shimizu, T. (2010) Structure of the N-terminal regulatory domain of a plant NADPH oxidase and its functional implications. *J. Biol. Chem.* **285**, 1435-1445

73. Alberts, B., Johnson, A., Lewis, J., Raff, M., Roberts, K., and Walter, P. (2002) *Molecular Biology of the Cell*;. 4th ed; Garland Science: New York

74. Pieterse, C.M., Leon-Reyes, A., Van der Ent, S., and Van Wees, S.C. (2009). Networking by small-molecule hormones in plant immunity. *Nature. chemical. Biology.* **5**, 308-316.

# CHAPTER 2

**Purification, crystallization and preliminary X-ray crystallographic analysis of a rice Rac/Rop GTPase, OsRac1**

## 2.1 Introduction

The Ras superfamily of small GTPases (20–30 kDa) comprises five functional families of GTPases referred to as Ras, Ran, Rab, Arf and Rho/Rac. The interconversion between GDP-bound (inactive) and GTP-bound (active) forms allows Ras superfamily members to regulate a number of cellular processes by means of a molecular switch mechanism for extracellular signals in eukaryotes. Although plants lack Ras family and typical animal Rho family members, they contain the Rho-related Rac/Rop GTPases (1, 2). Like other small GTPases, Rac/Rop family members function as molecular switches by interconversion between inactive GDP-bound and active GTP-bound forms in cells, and are an important regulator of signal transduction (1, 3, 4).

In rice, OsRac1 (Rop of Oryza sativa) initiates defence responses through activation of the NADPH-mediated production of reactive oxygen species (ROS) by direct binding to the plant NADPH oxidase OsRbohB (Rboh; respiratory burst oxidase homologue; 5, 6, 7). OsRac1-induced immune responses result in cell death as well as disease resistance against riceblast fungus, rice bacterial blight and Tobacco mosaic virus (5, 8, 9). Moreover, the constitutively active form of OsRac1 interacts strongly with the nucleotide-binding (NB) domain of the rice intracellular immune receptor Pit, and OsRac1 regulates downstream of Pit in the signaling pathways (10). Although it is known that OsRac1 plays important roles as a molecular switch in the innate immunity of rice, details concerning the molecular-switch mechanism involved remain largely unknown.

Here, the purification, crystallization and preliminary crystallographic study of activated OsRac1 are reported. A specific mutation (Gln68 to Leu) of the protein was

48

employed and this mutant was co-crystallized with the GTP analogue Guanosine-5'-[β,γ-imido]triphosphate (GMPPNP) in order to maintain OsRac1 in the active form.

**2.2 Materials and Methods**

*2.2.1 Protein expression*

The *O. sativa Rac1* gene (OsRac1; residues 8–183) was cloned into the pGEX6P-3 vector (GE Health-care) using *BamHI* and *XhoI* restriction-enzyme sites. Point mutations (C32S, G19Vand Q68L) were performed using the QuikChange site-directed mutagenesis kit (Stratagene). The nonconserved surface cysteine residue (Cys32) was substituted to serine to increase the protein stability. The OsRac1(8–183) C32S/Q68L (referred to as OsRac1-Q68L) or C32S/G19V (referred to as OsRac1-G19V) proteins were expressed in Escherichia coli Rosetta (DE3) cells (Novagen) using M9 minimal medium and were induced with 1 m$M$ isopropyl -d-1-thiogalactopyranoside (IPTG) at an optical density (OD600) of 0.5. Following incubation at 288 K for 12 h, the cells were harvested by centrifugation at 4000g for 20 min at 277 K.

*2.2.2 Purification*

The cells were suspended in lysis buffer (50 mM Tris–HCl pH 7.5, 400 mM NaCl, 5 mM $MgCl_2$, 2mM DTT) and lysed by sonication on ice. The supernatant was collected by ultracentrifugation (110 000g for 30 min at 277 K) and then applied onto a Glutathione Sepharose 4B column (GE Healthcare). The column was washed with lysis buffer and the glutathione S-transferase tag was removed by on-column digestion at 277 K overnight with HRV3C protease. The cleaved protein was eluted and purified by gel-filtration chromatography using a HiLoad 26/600 Superdex 75 column (GE Healthcare) pre-equilibrated with buffer A (50 mM Tris–HCl pH 7.5, 150 mM NaCl, 10 mM EDTA, 2 mM DTT). Under denaturing and reducing conditions, the SDS–PAGE showed a single band at about 20 kDa for OsRac1-Q68L.

## 2.2.3 Crystalization

For nucleotide exchange, purified OsRac1 (1–2 mg ml$^{-1}$) was incubated with a 25-fold excess of GMPPNP (Sigma) in buffer A for 12 h at 277 K. Following the addition of 10 mM MgCl$_2$, excess GMPPNP was removed by passage through a HiLoad 26/600 Superdex 75 column (GE Healthcare) using buffer B (10 m$M$ Tris– HCl pH 7.5, 50 mM NaCl, 5 mM MgCl$_2$, 2mM DTT). The protein was then concentrated to 4 mg ml$^{-1}$ by ultrafiltration (10 kDa molecular-weight cutoff; Amicon Ultra, Millipore) in buffer B. The homogeneity of the purified protein was confirmed by AutoFlex MALDI–TOF MS (Bruker Daltonics) or SDS–PAGE using buffer consisting of 40 mM Tris–HCl pH 6.8, 0.4% SDS, 0.4% -mercaptoethanol, 0.2% bromophenol blue, 20% glycerol, 9 M urea, 50 mM DTT, 10 mM EDTA.

Initial crystallization screening was carried out at 277 K by the sitting-drop vapour-diffusion method in a 96-well crystallization plate (Hampton) using commercial screening kits including Crystal Screen, Crystal Screen 2, PEG/Ion, Index, Grid Screen PEG 6000, Grid Screen Ammonium Sulfate (Hampton Research) and The JCSG Core Suites (Qiagen). Crystals of OsRac1-Q68L in complex with GMPPNP were grown at 293 K by the sitting-drop vapour-diffusion method by mixing 0.7 ml of a 4mgml$^{-1}$ protein solution in buffer B with 0.7 ml reservoir solution consisting of 100 mM MES buffer pH 6.0, 10–30% PEG 6000.

## 2.2.4 Data collection and processing

For the X-ray diffraction experiments, crystals were flash-cooled in a 100 K dry nitrogen stream using reservoir solution supplemented with 25%(v/v) glycerol as a

cryoprotectant. Diffraction data were collected from native crystals of OsRac1 using a Rayonix MX225HE CCD detector installed on the BL44 beam-line at SPring-8, Harima, Japan. The oscillation width was 1.5° per image and 160 images were collected. All data were processed and scaled using the HKL-2000 program suite (11). Data-collection and scaling statistics are given in Table 2-1.

## 2.3 Results and discussion

### 2.3.1 Preparation

In order to characterize the structure of OsRac1 in the GTP-bound active state, we introduced a specific mutation (Gln68 to Leu) as reported for the human small GTPase RhoA (12). In the RhoA protein, the single mutation Q63L (Q68 in OsRac1) results in a marked decrease in GTP hydrolysis activity, thereby maintaining the protein in a constitutively active form (12). The OsRac1-Q68L protein was prepared from bacterial cultures and purified chromatographically (Figure 2-1A). The nucleotide bound to the purified protein was exchanged for the nonhydrolyzable GTP analogue GMPPNP. In the gel-filtration analysis, OsRac1-Q68L containing GMPPNP eluted at a similar volume as myoglobin (~17 kDa; Figure 2-1b, marked D), suggesting that OsRac1-Q68L is a monomer in solution.

OsRac1-G19V and wild-type OsRac1 proteins were also prepared to compare these with OsRac1-Q68L. The G19V (Gly19 to Val) mutation was introduced into OsRac1 since it has been shown that a G14V (Gly19 in OsRac1) mutation in RhoA results in a marked decrease in GTP hydrolysis activity (12), thereby maintaining the protein in a constitutively active form in rice (5). Although both OsRac1-G19V and wild-type OsRac1 proteins were successfully purified and converted to GMPPNP-bound forms, crystals of these proteins have yet to be obtained.

### 2.3.2 Data collection and phase determination

The asymmetric unit of the crystal (Figure 2-2) contained one OsRac1 molecule, corresponding to a Matthews coefficient VM of 1.75 $\mathring{A}^3$ $Da^{-1}$ (13). Since OsRac1 shows 76% sequence identity to *Arabidopsis thaliana* Rac7 (AtRac7), the structure of

AtRac7-GDP (PDB entry 2j0v; 14) is considered to be a suitable search model for use in the molecular-replacement approach. Our study should be helpful in obtaining the structure of the active form of OsRac1, thereby contributing towards efforts to delineate the mechanism of immunity responses facilitated by OsRac1 activation.

**Table 2-1.** Data-collection statistics.

---------------------------------------------------------------------------------------------

| | |
|---|---|
| Wavelength (Å) | 0.9000 |
| Space group | $P2_12_12_1$ |
| Unit-cell parameters a, b, c (Å) | 36.8, 59.1, 64.4 |
| Resolution range (Å) | 50.0 - 1.9 (1.97-1.90) |
| No. of observed reflections | 93,928 |
| No. of unique reflections | 11,521 |
| Completeness (%) | 99.8 (100.0) |
| Redundancy | 8.2 (8.3) |
| $I/\sigma(I)$ | 19.7 (7.7) |
| $R_{merge}$ [a] | 0.095 (0.284) |

---------------------------------------------------------------------------------------------

Values in parentheses refer to data in the highest resolution shell in each data set.

[a] $R_{merge} = \Sigma_{hkl} \Sigma_i |I_i(hkl) - <I_i(hkl)>| / \Sigma_{hkl} \Sigma_i I_i(hkl)$, where $I_i(hkl)$ is the observed intensity and $<I_i(hkl)>$ is the average intensity obtained from multiple observations of symmetry-related reflections.
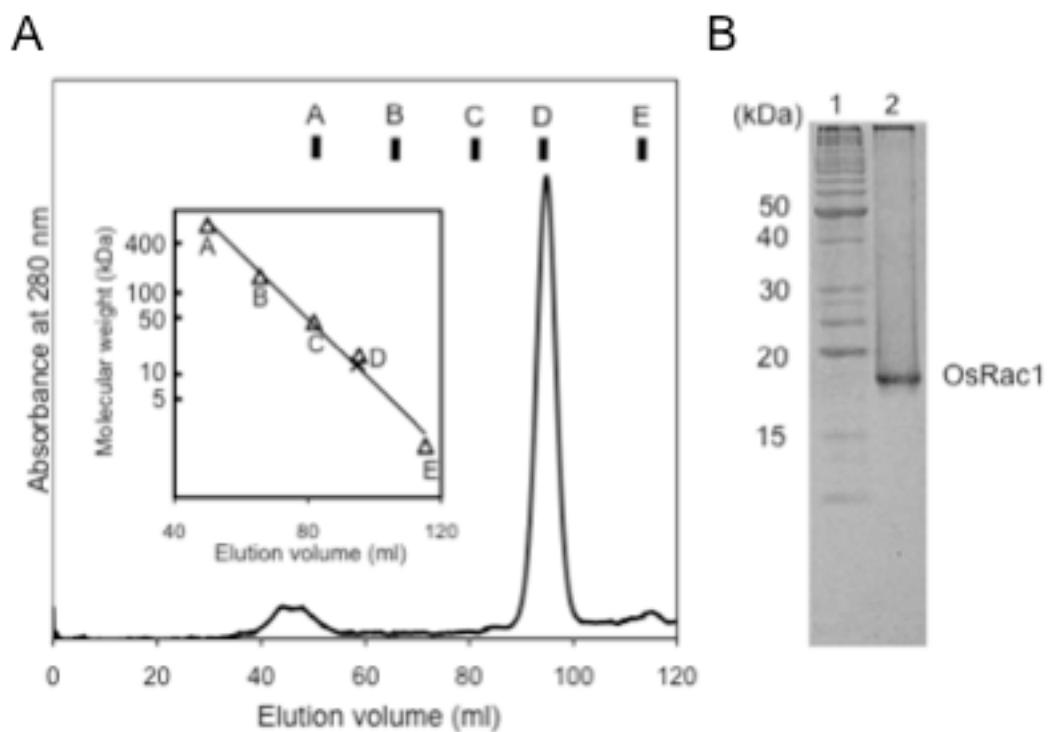
**Figure 2-1.** (A) 15% SDS–PAGE stained with Coomassie Brilliant Blue. Lanes 1 and 2 contain molecular-weight marker (labelled in kDa) and purified OsRac1[Q68L], respectively. (B) Elution profile of gel filtration of OsRac1[Q68L]. The inset shows the calibration curve. The open rectangles correspond to the following marker proteins: A, thyroglobulin, 670.0 kDa; B, γ-globulin, 158.0 kDa; C, ovalbumin, 44.0 kDa; D, myoglobin, 17.0 kDa; E, vitamin $B_{12}$, 1.4 kDa. The cross represents the peak-top position of OsRac1, assuming the molecular weight of the monomeric form containing GMPPNP and $Mg^{2+}$ ion. MALDI–TOF MS analysis gave a single peak at 19 905.8 Da corresponding to the calculated molecular mass of OsRac1[Q68L] (19 963.9 Da).
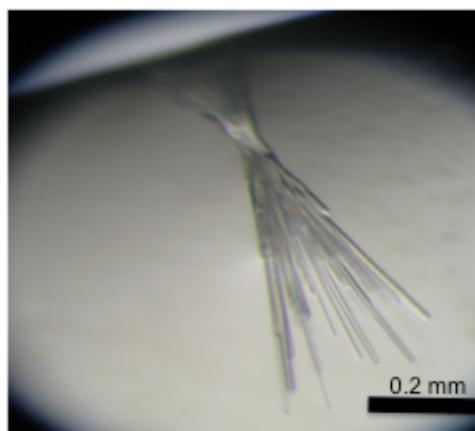
**Figure 2-2. Crystals of OsRac1$^{Q68L}$ in complex with GMPPNP.** The scale bar represents 0.2 mm.

## References

1. Nibau, C., Wu, H.-M. & Cheung, A. Y. (2006). *Trends Plant Sci*. **11**, 309–315.

2. Nagawa, S., Xu, T. & Yang, Z. (2010). *Small GTPase*, **1**, 78–88.

3. Mucha, E., Fricke, I., Schaefer, A.,Wittinghofer, A. & Berken, A. (2011). *Eur. J. Cell Biol*. **90**, 934–943.

4. Craddock, C., Lavagi, I. & Yang, Z. (2012). *Trends Cell Biol*. **22**, 492–501.

5. Kawasaki, T., Henmi, K., Ono, E., Hatakeyama, S., Iwano, M., Satoh, H. & Shimamoto, K. (1999). *Proc. Natl. Acad. Sci. U. S. A.*, **96**, 10922–10926.

6. Wong, H. L., Pinontoan, R., Hayashi, K., Tabata, R., Yaeno, T., Hasegawa, K., Kojima, C., Yoshioka, H., Iba, K., Kawasaki, T. & Shimamoto, K. (2007). *Plant Cell* **19**, 4022–4034.

7. Oda, T., Hashimoto, H., Kuwabara, N., Akashi, S., Hayashi, K., Kojima, C., Wong, H. L., Kawasaki, T., Shimamoto, K., Sato, M. & Shimizu, T. (2010). *J. Biol. Chem*. **285**, 1435–1445.

8. Ono, E.,Wong, H. L., Kawasaki, T., Hasegawa, M., Kodama, O. & Shimamoto, K. (2001). *Proc. Natl. Acad. Sci. U. S. A.*, **98**, 759–764.

9. Moeder, W., Yoshioka, K. & Klessig, D. F. (2005). *Mol. Plant Microbe Interact*. **18**, 116–124.

10. Kawano, Y., Akamatsu, A., Hayashi, K., Housen, Y., Okuda, J., Yao, A., Nakashima, A., Takahashi, H., Yoshida, H., Wong, H. L., Kawasaki, T. & Shimamoto, K. (2010). *Cell Host Microbe* **7**, 362–375.

11. Otwinowski, Z. & Minor, W. (1997). *Methods Enzymol*. **276**, 307–326.

12. Longenecker, K., Read, P., Lin, S.-K., Somlyo, A. P., Nakamoto, R. K. & Derewenda, Z. S. (2003). *Acta Crystallogr. Sect. D Biol. Crystallogr.* **59**, 876–880.

13. Matthews, B. W. (1968). *J. Mol. Biol*. **33**, 491–497.

14. Sørmo, C. G., Leiros, I., Brembu, T., Winge, P., Os, V. & Bones, A. M. (2006). *Phytochemistry*, **67**, 2332–2340.

# CHAPTER 3

**The crystal structure of the plant small GTPase OsRac1 reveals its mode of binding to NADPH oxidase**

## 3.1 Introduction

Small GTP-binding proteins (small G proteins or small GTPase) act as molecular switches and regulate a wide variety of important physiological functions in cells. Plants possess a specific subfamily of small GTPase, called Rac/Rop (Rho-related GTPases from plants) (1, 2), which have attracted recent interest due to their function as molecular switches in the regulation of various cellular responses (3-6). For example, OsRac1, a Rac/Rop of *Oryza sativa*, plays an important role in the regulation of rice immunity (7-15), and *Nicotiana tabacum* NtRac5 regulates ROS production in pollen tubes (16). The AtRop members AtRop1, AtRop3 and AtRop5 redundantly regulate pollen tube growth in *Arabidopsis thaliana* (17), while AtRop2, AtRop4 and AtRop6 regulate root hair development (17). Recently, the activation of AtRop2 and AtRop6 by auxin has been reported to regulate the subcellular distribution of auxin transporters PIN1 and PIN2, which control PIN-mediated pattern formation and morphogenesis in leaves and roots (18-20). AtRop10 and AtRop11, meanwhile, are specific negative regulators of abscisic acid (ABA) responses (21, 22). In addition, AtRop9 functions as a signal integrator of auxin and ABA signaling and plays an important role in embryo development and lateral root formation in *A. thaliana* (23).

Rac/Rops are composed of about 200 amino acids and have masses of 20 - 24 kDa, similar to the animal small GTPases. They are inactive in the GDP-bound form, and are activated by the binding of GTP. Several Rac/Rop structures have been reported, including AtRop5 (GDP-bound form), AtRop9 (GDP-bound form) (24), the AtRop4 (GDP-bound form)-GEF complex (25) and the AtRop7 (apo)-GEF complex (26), but all of these structures are of inactive forms. Structural analysis of active-form animal small GTPases has revealed the biological processes associated with carcinogenic mutations

61

and the biochemical mechanisms of carcinogenesis (27). Hence, the structural determination of plant Rac/Rops in their active form should be an important step in clarifying the mechanism of activation of target effectors.

A constitutively activated mutant of OsRac1 (OsRac1 G19V, denoted as CA-OsRac1) has been reported to increase resistance to rice bacterial blight disease and subsequent cell death (7, 8). Conversely, a dominant-negative mutant (OsRac1 T24N, denoted as DN-OsRac1) was found to decrease the resistance reaction. Transgenic rice lines expressing CA-OsRac1, but not DN-OsRac1, displayed increased production of a phytoalexin, and altered expression of defense-related genes (8). Furthermore, overexpression of CA-OsRac1 induced ROS production in cultured rice cells (7). These data clearly show that OsRac1 acts as a molecular switch during plant innate immunity. CA-OsRac1, but not DN-OsRac1, was also shown to interact directly with an NADPH oxidase, *O. sativa* respiratory burst oxidase homolog (OsRboh) B (11). Transient co-expression of OsRac1 and OsRbohB in leaves of *N. benthamiana* enhanced ROS production, supporting the notion that direct OsRac1-OsRbohB interactions activate NADPH oxidase in plants (11). Although the crystal structure of the N-terminal domain of OsRbohB has been reported (28, 29), the molecular mechanism by which OsRac1 activates OsRbohB for ROS production remains largely unknown.

In this report, the crystal structure of OsRac1 in the active form (GMPPNP-bound form) was determined in an effort to elucidate the molecular mechanism of ROS production in rice. Based on the structural information obtained, the OsRbohB binding site on OsRac1 was predicted, and OsRbohB-binding-deficient mutants of OsRac1 were designed. The OsRbohB binding activity of these mutants was evaluated by *in vitro* pull-down assays and NMR measurements, and the mutants also underwent ROS

production assays using rice cells. This study, together with our previous reports (11, 29), demonstrates that OsRac1 regulates ROS production through direct interactions with OsRbohB.

## 3.2 Materials and Methods

### 3.2.1 *Expression and purification of recombinant OsRac1*

cDNA encoding OsRac1$^{8-183}$, C32S/Q68L (denoted as OsRac1; see Results and Discussion) was cloned into the multiple cloning site of pGEX-6P3 vector (GE Healthcare), and several mutations were introduced using the QuikChange site-directed mutagenesis kit (Stratagene). The resulting plasmids were used to transform *Escherichia coli* Rosetta (DE3) cells (Novagen), which were then grown in M9 medium until the cell suspension reached the appropriate turbidity. Chimeric proteins comprising glutathione S-transferase (GST) fused to the N-terminus of OsRac1 or its mutants were then overexpressed by the addition of 1 mM isopropyl 1-thio-β-D-galactopyranoside for 12 h at 15 °C, after which the cells were harvested by centrifugation. To obtain target proteins for NMR measurements, 0.5 g /l $^{15}$N-ammonium chloride (99 atom % of $^{15}$N) was used as the sole nitrogen source in M9 medium. The overexpressed GST-fused OsRac1 proteins were initially purified by affinity chromatography using Glutathione Sepharose 4B resin (GE Healthcare). After enzymatic cleavage of the GST tag from target proteins using GST-HRV 3C protease, digestion products were passed through Glutathione Sepharose 4B resin, and the OsRac1 and mutant proteins were further purified by size exclusion column chromatography using Superdex 75 (GE Healthcare).

To exchange nucleotide, OsRac1 proteins were incubated with a 25-fold molar excess of GMPPNP (Sigma) in buffer A (50 mM Tris-HCl (pH 7.5), 150 mM NaCl, 10 mM EDTA, 2 mM DTT) for 12 h at 4 °C. After the addition of 10 mM MgCl$_2$, excess unbound nucleotides were removed using Superdex 75 column.

For crystallization and NMR measurements, purified proteins were concentrated by ultrafiltration using Amicon Ultra-10 (Amicon) to 4 mg/ml with buffer B (10 mM

Tris-HCl (pH 7.5), 50 mM NaCl, 5 mM MgCl$_2$, 2 mM DTT) and to 0.1 mg/ml with buffer C (50 mM Bis-Tris (pH 6.8), 50 mM NaCl, 5 mM MgCl$_2$, 2 mM CaCl$_2$, 2 mM DTT), respectively.

For the prey protein in a GST pull-down assay, cDNA encoding OsRbohB (amino acids 138 to 313, denoted as OsRbohB[138-313]) was cloned into pET32c (Novagen). Following overexpression of the chimeric thioredoxin (Trx)-His6-OsRbohB[138-313] in *E. coli* Rosetta (DE3), protein was purified by affinity chromatography using Ni-NTA agarose resin (QIAGEN). After enzymatic cleavage of the Trx-His6 tag from the target protein using recombinant enterokinase (Novagen), OsRbohB[138-313] was further purified by anion exchange and size exclusion chromatography using Superdex 75 in buffer C. For GST pull-down assays, purified OsRbohB[138-313] was concentrated to 0.6 mM by ultrafiltration using Ultra-10 with buffer C.

### 3.2.2 *Crystallization and X-ray data collection*

OsRac1 complexed with the GTP analog GMPPNP was crystallized as described (30). In brief, OsRac1 crystals were obtained at 20 °C using the sitting-drop vapor-diffusion method by mixing 0.7 μl of 4 mg/ml purified protein with 0.7 μl of reservoir solution consisting of 100 mM MES buffer (pH 6.0), 10-30% PEG 6000. For the X-ray diffraction experiments, crystals in a reservoir solution supplemented with 25% (v/v) glycerol as a cryoprotectant were mounted in nylon loops (Hampton Research), flash-cooled using a 100 K dry nitrogen stream, and then kept under the nitrogen stream during data collection. X-ray diffraction data were collected from OsRac1(GMPPNP) crystals using a Rayonix MX225HE CCD detector installed on the BL44XU beamline at SPring-8 (Harima, Japan). The camera was fixed at a distance of

260 mm from the crystal sample using an X-ray wavelength of 0.9000 Å. Data collection for native crystals was performed using an angular range of 240°, an oscillation step of 1.5° and an exposure time of 1.0 s for each image. All data were integrated and scaled using HKL-2000 (31). Diffraction and intensity data-collection statistics are summarized in Table 3-1.

### 3.2.3 *Structure determination and refinement*

The crystal structure was solved by the molecular replacement method using PHASER (32). The tertiary structure coordinates of *A. thaliana* RAC7/ROP9 (PDB code: 2J0V) (24) were used as a search model for OsRac1. Crystal structures of OsRac1 were rebuilt using COOT (33), and refined using REFMAC5 (34) and CNS (35). Ramachandran plot analysis was performed using Rampage (36). Final refinement statistics are summarized in Table 3-1. The solvent accessibility of each amino acid was analyzed using NACCESS (S. Hubbard, J. M. Thornton, NACCESS, University College London, 1993). Coordinates of the final model and structure factors of OsRac1 have been deposited in the Protein Data Bank (PDB code: 4U5X). All structures in the figures were generated using PyMOL (http://www.pymol.org/).

### 3.2.4 *GST pull-down assays*

Following immobilization of each GST-tagged protein onto 50 μl gel volume of Glutathione Sepharose 4B resin, 20 μl of solution containing 0.6 mM purified OsRbohB[138-313] was added and the mixture incubated at 4 °C for 12 h. After washing the resin several times with fresh buffer solution (50 mM Bis-Tris (pH 6.8), 50 mM KCl, 5 mM MgCl$_2$, 2 mM CaCl$_2$, 1 mM phenylmethylsulfonyl fluoride, 3% [v/v] dimethyl

sulfoxide), bound proteins were eluted and analyzed by SDS-PAGE. The SDS-PAGE gels were stained with Coomassie Brilliant Blue.

### 3.2.5 *NMR measurements*

All NMR spectra were measured using a Bruker AVANCE 800 spectrometer equipped with a TXI cryogenic probe at 303 K, and the collected data were processed and analyzed using NMRPipe (37) and Sparky (Goddard & Kneller, SPARKY 3-NMR Assignment and Integration Software, University of California, San Francisco), respectively. All of the 2D $^1$H-$^{15}$N HSQC experiments were performed using 0.1 mM of uniformly $^{15}$N-labeled OsRac1 in 50 mM Bis-Tris (pH 6.8), 50 mM KCl, 5 mM MgCl$_2$, 1 mM DTT, in 90%/10% H$_2$O/D$_2$O.

### 3.2.6 *Rice cell cultures*

To generate rice suspension cells (Kinmaze) expressing CA-OsRac1, CA-OsRac1 Y39A, or CA-OsRac1 D45A, the coding regions of mutated *OsRac1* were introduced into the p2K-GW binary vector (for transgenic plants expressing genes under the maize *ubiquitin* promoter) using the Gateway system (Invitrogen). *Agrobacterium tumefaciens*-mediated transformation of rice calli was performed according to Hiei *et al.* (38). Transformants selected by hygromycin resistance were subcultured in 22 ml R2S medium every week and incubated on a rotary shaker (90 rpm) at 30 °C.

### 3.2.7 *RT-PCR*

Total RNA was extracted from rice suspension cultures using the RNeasy Plant Mini Kit (QIAGEN) and 1 μg was used as a template for reverse transcription using an

oligo dT primer and SuperScript II (Invitrogen). PCR analyses used specific primers for

*OsRac1* (5'- AGATAGGGCCTATCTTGCTGATCATC-3' and 5'-

CTAGAAGTTTCCTCCTAGCTGCAAGC-3'), *HPT* (5'-

GAGCCTGACCTATTGCATCTCC-3' and 5'-

GGCCTCCAGAAGAAGATGTTGG-3') and *ACT1*

(5'-CAATCGTGAGAAGATGACCC -3' and

5'-GTCCATCAGGAAGCTCGTAGC-3').

### 3.2.8 *Measurement of ROS production*

Rice suspension cells were subcultured for 4 days in fresh medium, and approximately 20 mg of cells was placed into each well of white 96-well plates (Greiner Bio-One). Two hundred microliters of 500 µM L-012 (Wako Chemicals) dissolved in medium was added to each well and chemiluminescence was detected using an LAS-4000 mini luminescent image analyzer (FUJIFILM) at 180 min. Emission intensity from each well was measured using ImageJ (http://rsbweb.nih.gov/ij/) and the following formula: (intensity of each well − intensity of background) / weight of suspension cells in each well.

## 3.3 Results and discussion

### 3.3.1 *Structure determination of OsRac1 in active form*

For the crystallization of active-form OsRac1, an OsRac1 mutant and the GTP analog GMPPNP were used to prevent GTP hydrolysis. GTPase activity of the human small GTPase HsRhoA is significantly attenuated by substitution of glutamine to leucine at position 63 (39). In this study, the corresponding OsRac1 mutant comprising the substitution Q68L was used. To increase the stability of the OsRac1 protein, Cys32 was substituted to serine and the N and C termini were truncated. Hereafter, 'OsRac1' refers to this truncated mutant OsRac1$^{8-183}$, C32S/Q68L.

The OsRac1-GMPPNP-Mg$^{2+}$ complex, designated as OsRac1(GMPPNP), was crystallized as previously described (30). The crystals gave strong and high-resolution X-ray diffraction. The diffraction data were collected to 1.9 Å resolution from one crystal (Table 3-1), and displayed orthorhombic $P2_12_12_1$ symmetry with an estimated mosaicity of 0.41-0.62° and a Wilson B factor of 12.7 Å$^2$. The unit cell ($a = 36.8$, $b = 59.1$, $c = 64.4$ Å) contains one molecule of OsRac1(GMPPNP) per asymmetric unit. The crystal structure of OsRac1(GMPPNP) was determined at 1.9 Å resolution with clear electron density for all atoms with $R_{work}$ 15.7% and $R_{free}$ 20.3% (Figure 3-1A). OsRac1(GMPPNP) comprised a half-β-barrel-shaped structure formed by six β-strands (β1-β6). These β-strands were sandwiched between five α-helices (α1-α5), where two α-helices (α1, α5) were wrapped inside and three α-helices (α2-α4) were located outside.

### 3.3.2 *Structural comparison of OsRac1 with HsRac1 and HsRhoA - Rac/Rop proteins in GTP form*

OsRac1 belongs to the Rho family of proteins, which includes HsRac1 and HsRhoA. OsRac1 shares 62% amino acid identity with HsRac1 and 49% identity with HsRhoA. Since the active-form structures of HsRac1 and HsRhoA have been determined (40, 41), these three Rho family protein structures were compared. The overall structures of OsRac1(GMPPNP) and the HsRac1-GMPPNP, $Mg^{2+}$ complex, designated as HsRac1(GMPPNP) (PDB code: 1MH1), were similar (Figure 3-1B). The root mean square deviation (RMSD) of 141 Cα atoms was approximately 1.4 Å. The overall structures of OsRac1(GMPPNP) and the HsRhoA-GTPγS, $Mg^{2+}$ complex, designated as HsRhoA(GTPγS) (PDB code: 1A2B), were also similar (Figure 3-1B), and the RMSD value of 140 Cα atoms was approximately 1.6 Å. The geometry of the nucleotide- and $Mg^{2+}$ ion-binding pocket and the hydrogen-bond network pattern are essentially the same among these three Rho family proteins. Major structural differences between OsRac1(GMPPNP), HsRac1(GMPPNP) and HsRhoA(GTPγS) were found in Switch I (35FPTDYIPTVFD45 in OsRac1) and the Insert (129DRAYLADHPASSII141 in OsRac1) region.

Switch I in OsRac1(GMPPNP) forms a loop structure, as it does in HsRac1(GMPPNP) and HsRhoA(GTPγS); however, the Switch I structures were not superimposed (Figure 3-1B). The RMSD value of OsRac1(GMPPNP) and HsRac1 (GMPPNP) was approximately 2.5 Å for the 11 Cα atoms located in Switch I, and that of OsRac1(GMPPNP) and HsRhoA(GTPγS) was 2.2 Å. Switch I in OsRac1(GMPPNP) was located further away from the guanine nucleotide than it was in the other two proteins (Figure 3-1B).

The Insert region is conserved in the Rho family, but not in other small GTPase families. HsRac1(GMPPNP) and HsRhoA(GTPγS) contain one α-helix (αi) followed by

70

an extended short loop, while OsRac1(GMPPNP) contains two helices (αi and αi2) in this region (Figures 3-1B and 3-2). The Insert region of OsRac1 is relatively short due to the absence of two amino acids, and the αi helix is significantly shorter (Figure 3-2). The $3_{10}$-helix αi2 (Ala138-Ser140) is absent in other Rho family proteins, and seems to represent unique structural features of OsRac1(GMPPNP) (Figures 3-1 and 3-2).

### 3.3.3 *Structural comparison of OsRac1 with plant Rac/Rop proteins*

In an effort to determine whether unique structural features of OsRac1(GMPPNP) are conserved in the plant Rac/Rop protein family, the structure of OsRac1(GMPPNP) was compared with the reported structures of Rac/Rop proteins, such as AtRop5(GDP), AtRop9(GDP) (24), and the AtRop4(GDP)-GEF (25) and AtRop7(apo)-GEF complexes (26). Of these plant Rac/Rop proteins, only OsRac1 is the GTP-bound form. The overall structure of OsRac1 was similar to those of the AtRop proteins. However, structural differences were observed in the Switch I and Switch II regions of GTP (GMPPNP)-bound OsRac1 and the GDP-bound AtRop proteins (Figures 3-3 and 3-4). In animal, extensive structural analysis revealed that large conformational changes occur between the GDP- and GTP-bound states in two regions, Switch I and Switch II. These regions play important roles in interactions with downstream targets to transduce signals (41).

The Switch I region in OsRac1(GMPPNP) and AtRop9(GDP) were well ordered and formed similar loop structures. In contrast, in other AtRop proteins, this region was partially disordered (Figures 3-3, 3-4 and 3-5). The Switch II region of OsRac1(GMPPNP) adopted a long helical conformation (Figures 3-3, 3-4 and 3-5). A similar long helical conformation was observed in AtRop5(GDP) and the animal Rho

71

family. However, most AtRop proteins adopted a loop-like structure without a long helix. These structural differences in the Switch I and Switch II regions were not unexpected, since all of the AtRop protein structures reported were of the inactive form. A notable structural difference also occurred in the Insert region. As mentioned above, the Insert region of OsRac1 comprised an insert α-helix (αi) and the short $3_{10}$-helix (αi2) (Figures 3-3, 3-4 and 3-5). The αi helix was present in all AtRop proteins, but the αi2 helix was unique to OsRac1. These structural differences in the Insert region may affect the interaction with GEF proteins, since the αi helix within the Insert region of AtRop4 is known to be involved in the interaction with the plant-specific Rop nucleotide exchanger (PRONE) domain of PRONE8 (25, 26).

### 3.3.4 *Interaction of OsRac1 with OsRbohB$^{138-313}$*

CA-OsRac1, but not DN-OsRac1, interacts directly with OsRbohB$^{138-313}$ (11). From structural comparisons of OsRac1(GMPPNP) with inactive-form AtRop proteins, Switch I, Switch II and the Insert region were found to differ. Therefore, the OsRbohB$^{138-313}$-binding site of OsRac1(GMPPNP) is expected to involve Switch I, Switch II or the Insert region. Acidic residues in Switch I (Asp38, Tyr39 and Asp45), Switch II (Glu69 and Asp70) and the Insert (Asp135) region were found to be located on the molecular surface of OsRac1(GMPPNP) (Figures 3-6A and 3-7). The crystal structure of OsRbohB$^{138-313}$ has been solved and it was suggested that Arg273 and Tyr277 of OsRbohB$^{138-313}$ play an essential role in binding to OsRac1 (29). Interestingly, Arg273 and Tyr277 and surrounding residues form a positively-charged cluster on the molecular surface of OsRbohB$^{138-313}$ (Figure 3-6B). In view of these features, we

anticipated that an electrostatic contribution would be important in the interaction between OsRac1(GMPPNP) and OsRbohB[138-313].

To test the importance of the charge interaction, we performed *in vitro* pull-down assays using OsRbohB[138-313] and CA-OsRac1 as prey and bait proteins, respectively (Figure 3-6C). The acidic residues located on the molecular surface of OsRac1 were replaced with alanine. Among the mutants generated, Switch I mutants Y39A and D45A showed markedly attenuated binding with OsRbohB[138-313] (Figure 3-6C). To determine whether the tertiary structures of the Y39A and D45A mutants are disrupted, 2D $^1$H-$^{15}$N heteronuclear single quantum coherence (HSQC) NMR spectra were measured. The $^1$H-$^{15}$N HSQC spectra of the Y39A and D45A mutants were well resolved (Figure 3-6D), and no marked chemical shift changes were observed in comparison with the wild-type (11). These NMR data indicated that the tertiary structures of the Y39A and D45A mutants are folded and are not substantially altered by the mutations. All of these data indicated that the Switch I Tyr39 and Asp45 residues of OsRac1 are critical for the direct interaction with OsRbohB[138-313].

### 3.3.5 *Disruption of the interaction between OsRac1 and OsRbohB compromises ROS production in rice cells*

To establish whether the interaction of OsRac1 Tyr39 and Asp45 residues with OsRbohB affects the activation of NADPH oxidase, we examined ROS production in transgenic rice suspension cells overexpressing CA-OsRac1 Y39A and D45A under the maize *ubiquitin* promoter. RT-PCR analysis confirmed that the *OsRac1* mutants were highly expressed in transgenic cells (Figure 3-8A). In these experiments, we used L-012, a luminol derivative, to detect ROS (42). When suspension cells were treated with 0.5

mM L-012 and the chemifluorescence examined using an LAS-4000 image analyzer, all CA-OsRac1 lines generated a large amount of ROS, as reported by Kawasaki et al. (7) (Figures 3-8B and 3-8C). In contrast, the levels of ROS in all lines of both CA-OsRac1 Y39A and CA-OsRac1 D45A were markedly lower than that in CA-OsRac1 suspension cells (Figure 3-8B and 3-8C). OsRac1 Tyr39 and Asp45 residues therefore play an important role in the activation of NADPH oxidase in rice suspension cells.

### 3.3.6 *Important residues in Switch I for OsRbohB binding*

OsRac1 Switch I Tyr39 and Asp45 residues are necessary for the direct interaction of OsRac1 with OsRbohB[138-313], which leads to NADPH oxidase activation and ROS production. To identify other residues of Switch I that may also be important, each of the 11 residues in OsRac1 Switch I was replaced with alanine, and the mutants were subjected to *in vitro* pull-down assays (Figure 3-9). F35A, Y39A, T42A and D45A mutants showed markedly reduced binding with OsRbohB[138-313], while V43A and F44A mutants also showed moderately reduced binding (Figures 3-9C and 3-9D). The solvent accessibility of all residues located in Switch I was calculated using the structure of OsRac1(GMPPNP) (Figure 3-9E). The solvent accessibility values for Phe35, Tyr39, Thr42, Val43, Phe44 and Asp45 residues were 16%, 100%, 55%, 54%, 54% and 69%, respectively. The side chains of Phe35 and Thr42 interacted with GMPPNP (Figure 3-10), and substitution to alanine destabilized binding to GMPPNP. The Tyr39, Val43, Phe44 and Asp45 residues were exposed to the solvent, and were not involved in direct binding to GMPPNP or coordination of the $Mg^{2+}$ ion (Figure 3-10B). Accordingly, we conclude that Switch I Tyr39, Val43, Phe44 and Asp45 residues are involved in the OsRbohB[138-313]-binding site (Figure 3-10B).

GTP-bound OsRac1 binds much more strongly than GDP-bound OsRac1 with OsRbohB (11). To elucidate the differences of GTP- and GDP-bound OsRac1, we used AtRop9, which showed the highest sequence similarity to OsRac1 in PDB, as a model of GDP-bound OsRac1. A structural comparison of OsRac1 (GTP form) with AtRop9 (GDP form) showed a difference in their Rboh-binding sites. In OsRac1, the OsRbohB-binding site formed an acidic pocket-like surface centered on Asp45 (Figure 6A), but this feature was not observed in AtRop9 (Figure 3-11B). The acidic surface in OsRac1 was well stabilized by a hydrogen bond network among GMPPNP:$Mg^{2+}$ and residues in $\alpha 1$, $\beta 2$, $\beta 3$ and the C-terminal portion of Switch I. The main chain of the $Mg^{2+}$ ion-coordinating residue Asp64 in $\beta 3$ contacted the side chain of the Switch I residue Asp45, and the side chain of the neighboring residue Asn46 was held by hydrogen bonds from Leu27/Thr31 in $\alpha 1$ (Figure 3-11C). In the AtRop9-GDP complex, these hydrogen bonds did not form, and the position of the Asp41 side chain was largely different from that of Asp45 in OsRac1 (6 Å apart at the C$\gamma$ atom positions in superposed structures) so that the acidic pocket-like surface was covered (Figures 3-11B and 3-11D). We note that all of these important residues in OsRac1 - Leu27, Thr31, Asp45, Asn46 and Asp64 - are conserved in AtRop9. The GDP to GTP exchange in OsRac1 may induce a conformational change and increases the stability of the C-terminal acidic region of Switch I, so that OsRac1 associates more strongly with the basic surface of OsRbohB.

### 3.3.7 Interaction site of HsRac1 with p67$^{phox}$, an essential component of the NADPH oxidase complex

As described above, OsRac1 Switch I Tyr39, Val43, Phe44 and Asp45 residues interact with OsRbohB[138-313], with at least Tyr39 and Asp45 playing a key role in the activation of NADPH oxidase in rice cells (Figure 3-12). Switch I of HsRac1/HsRac2 has been reported to be important for the activation of NADPH oxidase (43, 44). For example, substitutions of Phe28, Thr35, Val36 and Asp38 of HsRac2, which correspond respectively to Phe35, Thr42, Val43 and Asp45 of OsRac1, resulted in a significant reduction in activation ability (43), and alanine substitutions at Thr35 and Asp38 in HsRac2 abolished it completely. In animals, phagocytic NOX2 is the best characterized NADPH oxidase, and its activation process is relatively well understood. Unlike NADPH oxidase of plants (Rboh), NOX2 does not interact directly with HsRac1/HsRac2 (44), and NOX2 activation requires the formation of a multi-component complex (45, 46). One essential component is the direct interaction of p67$^{phox}$ with NOX2 and HsRac1/HsRac2 (45, 47). The crystal structure of the HsRac1-p67$^{phox}$ complex showed that HsRac1 binds to p67$^{phox}$ via α1, Switch I, and the loop connecting β6 to α5 (Figures 3-12 and 3-13) (48). Although the Switch I region is therefore critical for the activation of NADPH oxidase in both plants and animals, molecular details of the interacting regions differ between plants and animals (Figures 3-12 and 3-13).

## 3.4 Conclusion

OsRac1 Switch I was identified as the region that binds OsRbohB[138-313], and four residues in this region (Tyr39, Val43, Phe44 and Asp45), especially Tyr39 and Asp45, were found to be critical for the interaction and for ROS production in rice cells. Previous studies have shown that ROS production by NADPH oxidase is regulated by Rac/Rop proteins (11, 16, 49). Our data, combined with our previous results (11, 13, 16, 29), assist in delineating the mechanism of rice immunity. In particular, OsCERK1, the receptor for pathogen-associated molecular patterns such as chitin, phosphorylates and activates OsRacGEF1, and activated OsRacGEF1 subsequently activates OsRac1 by the guanine nucleotide exchange process. Finally, OsRac1 activates ROS production via direct interaction with the NADPH oxidase OsRbohB (Figures 3-12 and 3-13). Our results have also contributed towards delineation of the molecular mechanisms associated with various plant cellular responses, such as pollen tube growth and root hair development, that are influenced by Rac/Rop proteins.

**Table 3-1**

Data collection and refinement statistics of the OsRac1-GMPPNP-Mg$^{2+}$ complex (OsRac1(GMPPNP)) [a]

| | OsRac1(GMPPNP) |
|---|---|
| **Data Collection** | |
| Space group | $P2_12_12_1$ |
| Cell constants $a$, $b$, $c$ (Å) | 36.8, 59.1, 64.4 |
| Resolution (Å) | 50-1.9 (1.97-1.9) |
| Redundancy | 8.2 (8.3) |
| Completeness (%) | 99.8 (100) |
| $I/\sigma(I)$ | 19.7 (7.7) |
| $R_{merge}$ (%)[b] | 9.5 (28.4) |
| | |
| **Refinement** | |
| Resolution range (Å) | 50-1.9 |
| No. reflections | 10901 |
| $R_{work}$ (%)[c] | 15.7 |
| $R_{free}$ (%)[c] | 20.3 |
| No. atoms | |
| Protein | 1384 |
| Ligand and ion | 51 |
| Solvent | 90 |
| Average B-factor (Å$^2$) | 16.1 |
| R.m.s. deviations | |
| Bond length (Å) | 0.019 |
| Bond angles (°) | 2.2 |
| Ramachandran analysis | |
| Favored (%) | 98.9 |
| Allowed (%) | 1.1 |
| Disallowed (%) | 0 |

[a]Values in parentheses refer to the highest resolution shell.
[b]$R_{merge} = \Sigma_h \Sigma_i |I(h)_i - \langle I(h)\rangle|/\Sigma_h \Sigma_i I(h)_i$, where $I(h)$ is the intensity of reflection $h$, $\Sigma_h$ is the sum of all measured reflections and $\Sigma_i$ is the sum of $i$ measurements of reflection.
[c]$R_{work}$ and $R_{free} = (\Sigma_{hkl} ||F_o| - |F_c||/\Sigma_{hkl} |F_o|)$, where the free reflections (5% of the total used) were held aside for $R_{free}$ throughout refinement.
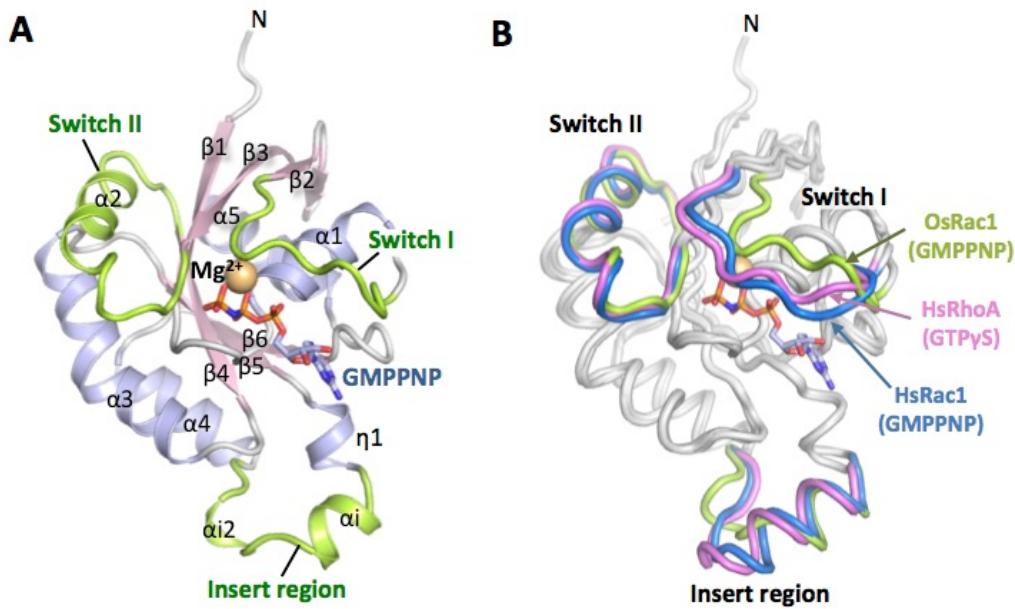
**Figure 3-1. Overall structure of OsRac1.** (A) Ribbon representation of overall structure of OsRac1 in its GMPPNP, $Mg^{2+}$-bound form. Switch I, Switch II and Insert regions are colored in green. GMPPNP is shown in the stick model (red, oxygen; blue, nitrogen; orange, phosphorus). The $Mg^{2+}$ ion is shown as an orange sphere. (B) Superimposition of the crystal structures of OsRac1(GMPPNP), HsRac1(GMPPNP) (PDB code: 1MH1) and HsRhoA(GTPγS) (PDB code: 1A2B). Switch I, II and Insert regions are colored as indicated in the protein labels. Models were generated using PyMOL.
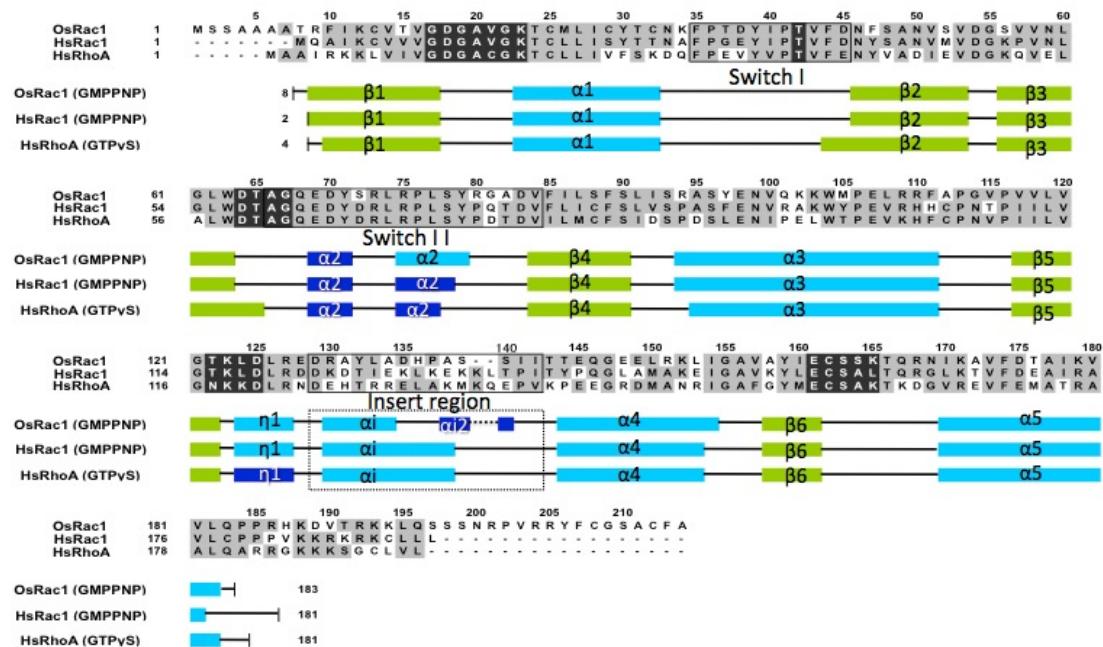
**Figure 3-2. Comparison of primary sequences of OsRac1, HsRac1 and HsRhoA by multiple sequence alignment.** Secondary structural elements are calculated from structures in Protein Data Bank (HsRac1: 1MH1; HsRhoA: 1A2B) and indicated under the amino acid sequences (β-strand: green; α-helix: cyan; $3_{10}$-helix: blue). The sequences of the Switch I, Switch II and Insert regions are boxed by dashed black lines, and secondary structure of the Insert regions are boxed by black dashed-line. Conserved motifs which are important for GTP hydrolysis are highlighted by white letters on a black background. The dotted line indicates disordered region.
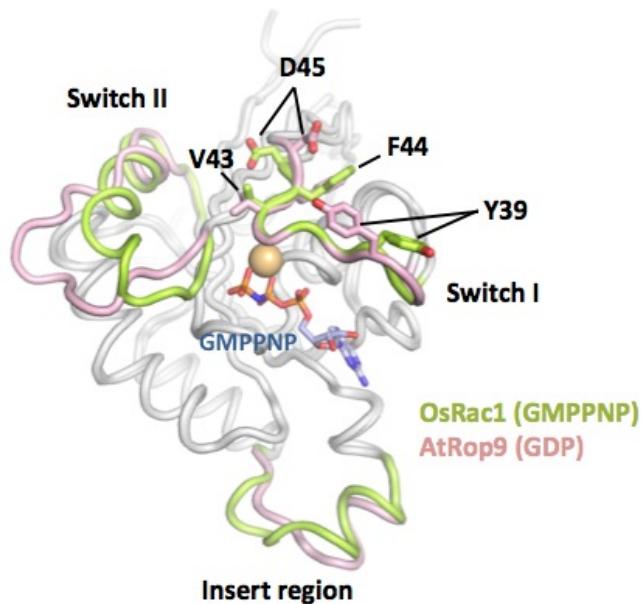
**Figure 3-3. Comparison of the overall structures of OsRac1(GMPPNP) and AtRop9(GDP).** Main chains of OsRac1(GMPPNP) and AtRop9(GDP) (PDB code: 2J0V, chain B) were superimposed using PyMOL. Switch I, Switch II and Insert regions of the OsRac1 and AtRop9 proteins, respectively, are colored in green and pink. Side-chains of four key Switch I residues in OsRac1 (Val43, Phe44, Asp45 and Tyr39) and equivalent residues in AtRop9 (Val39, Phe40, Asp41 and Tyr35) are shown as stick representations.
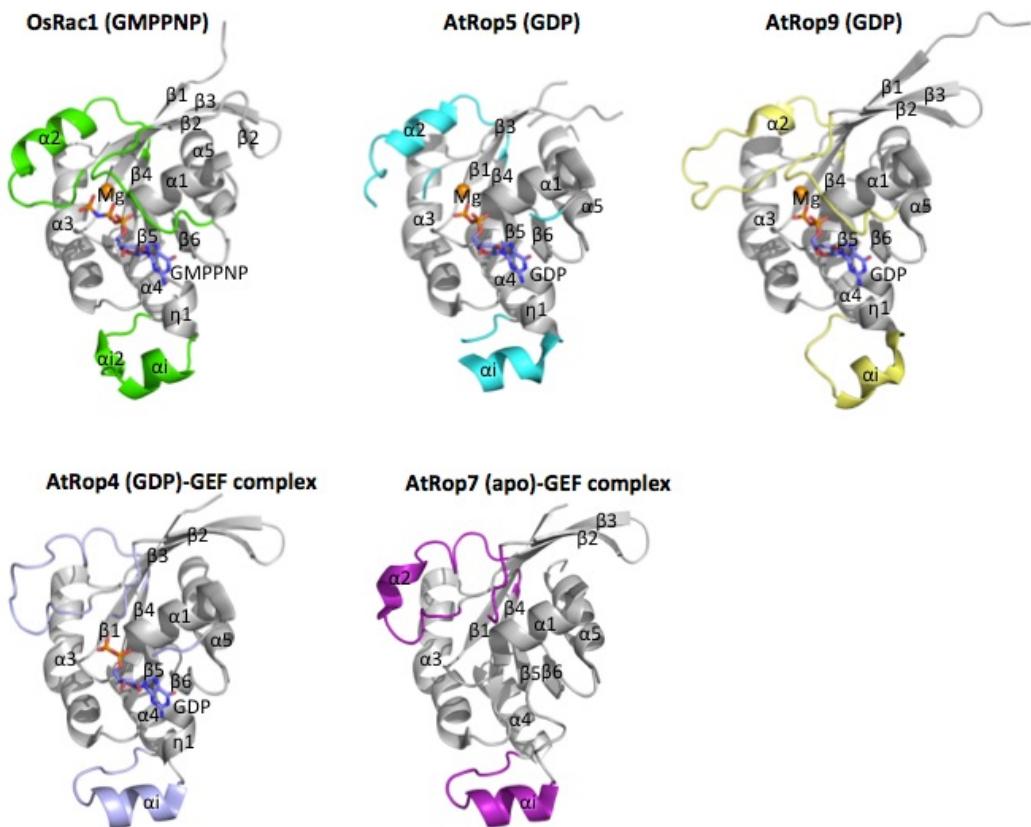
**Figure 3-4. Comparison of the structures of OsRac1(GMPPNP), AtRop5(GDP) (PDB code: 3BWD), AtRop9(GDP) (PDB code: 2J0V, chain B), the AtRop4(GDP)-GEF(PRONE) complex (PDB code: 2NTY, chain B) and the AtRop7(apo)-GEF(PRONE) complex (PDB code: 2WBL, chain C).** Switch I, Switch II and the Insert region are in non-gray colors. GMPPNP and GDP are shown as stick models (red, deep blue, and orange indicate O, N and P atoms, respectively). The Mg$^{2+}$ ion is shown as an orange sphere. Models were generated using PyMOL.
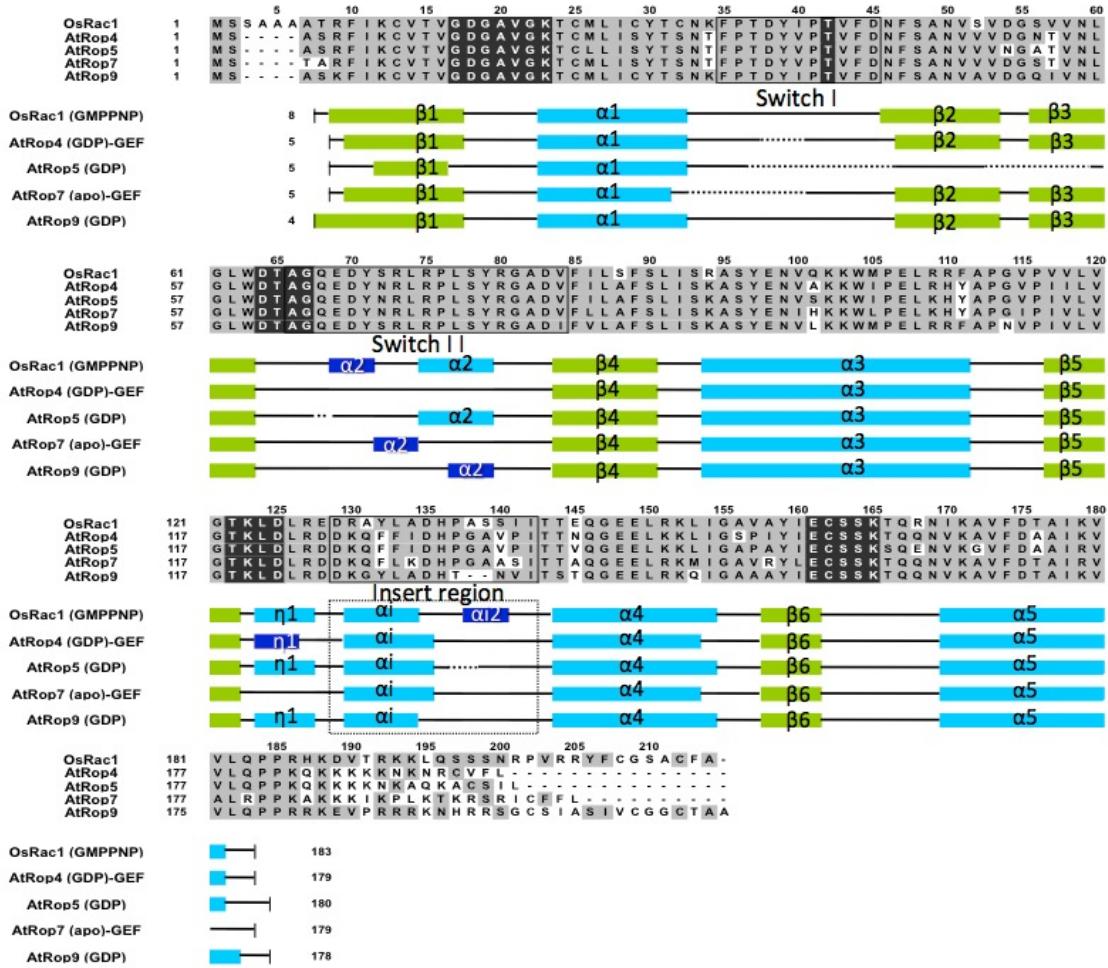
**Figure 3-5. Comparison of primary sequences of plant Rac/Rops by multiple sequence alignment.** Secondary structural elements calculated from structures of OsRac1, AtRop4(PDB code: 2NTY), AtRop5(PDB code: 3BWD), AtRop7(PDB code: 2WBL) and AtRop9(PDB code: 2J0V) are drawn under the amino acid sequences (β-strand: green; α-helix: cyan; $3_{10}$-helix: blue). The sequence of the Switch I, Switch II and Insert regions are boxed by thin black lines, and secondary structures of the Insert regions are indicated by dashed black lines. Conserved motifs which are important for GTP hydrolysis are highlighted by white letters on a black background. The dotted lines indicate disordered regions.
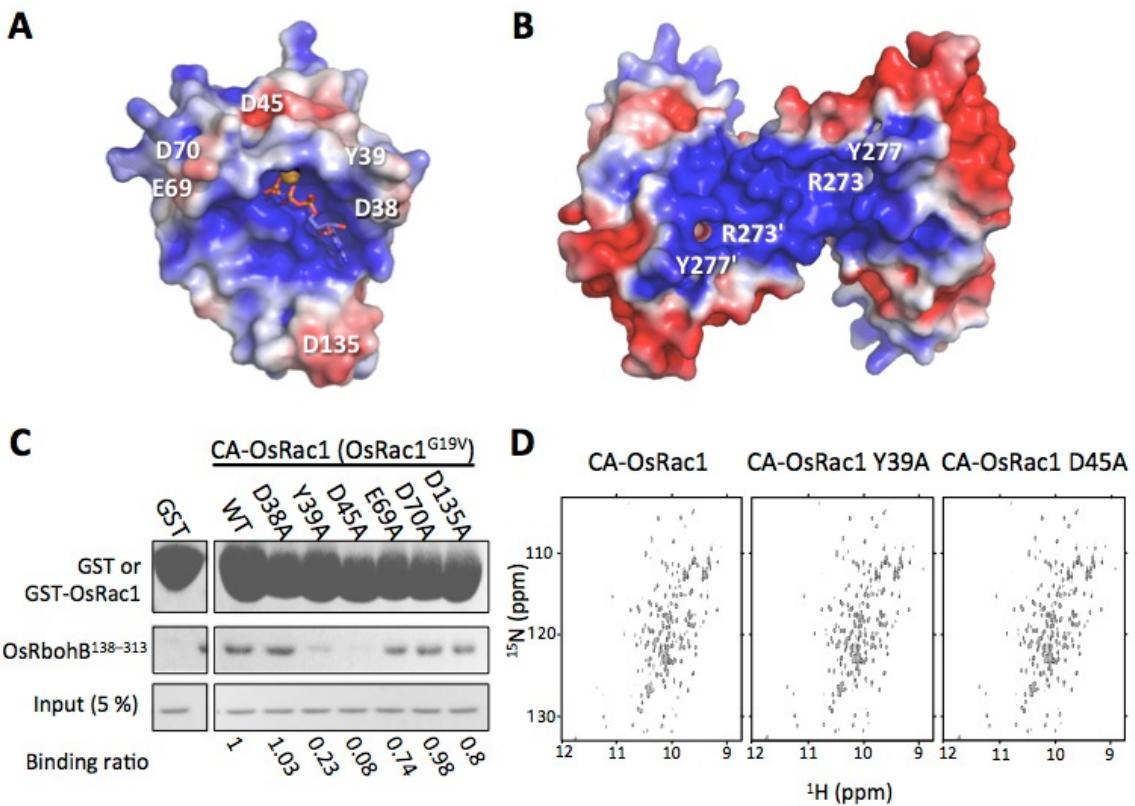
**Figure 3-6. Mode of binding between OsRac1 and OsRbohB$^{138-313}$.** Electrostatic potential of the molecular surface of OsRac1(GMPPNP) (A) and OsRbohB$^{138-313}$ (PDB code: 3A8R) (B) Amino acid residues labeled with the single-letter code are putative key residues involved in the OsRac1-OsRbohB$^{138-313}$ interaction. Positively and negatively charged sites are colored in blue and red, respectively. The surface potential was generated using PyMOL with APBS tools (±3 *kT*). (C) GST pull-down binding assay between the full-length CA-OsRac1 and OsRbohB$^{138-313}$. Alanine substitutions were introduced in place of Asp38, Tyr39, Asp45 (in Switch I), Glu69, Asp70 (in Switch II), and Asp135 (in the Insert region) of GST-fused full-length CA-OsRac1. Each mutant was overexpressed in *E. coli*, purified, and equal amounts of each GST-fused protein were used as bait for the OsRbohB$^{138-313}$ pull-down. The amount of OsRbohB$^{138-313}$ pulled down was quantitated by densitometric analysis. Numerical values below the panel indicate the ratio of OsRbohB$^{138-313}$ binding to OsRac1 mutants compared with wild-type OsRac1(WT). (D) 2D $^1$H-$^{15}$N HSQC spectra of CA-OsRac1wild-type (left),Y39A (center) and D45A (right).
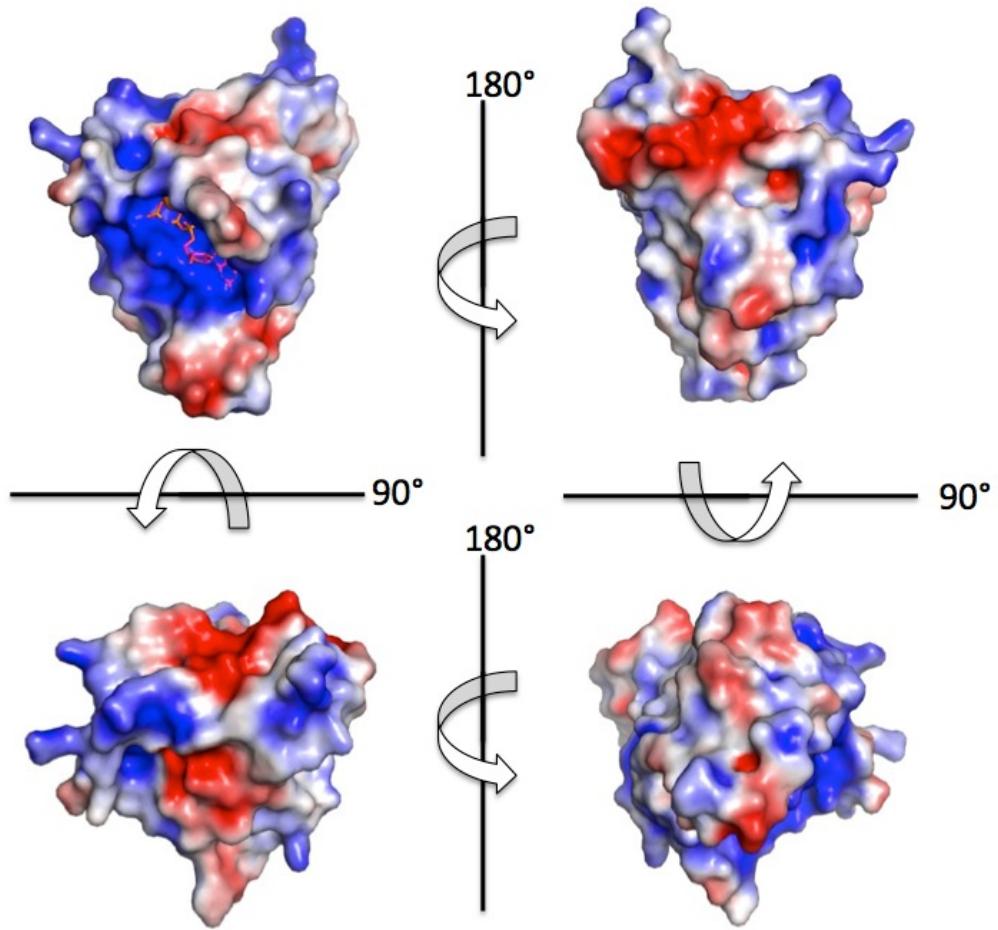
**Figure 3-7. Mapping of electrostatic potential of OsRac1-GMPPNP.** Positive and negative charges on the molecular surface are colored blue and red, respectively. GMPPNP is shown in the stick model and the $Mg^{2+}$ ion is shown as an orange sphere. The surface potential was calculated using APBS tools.
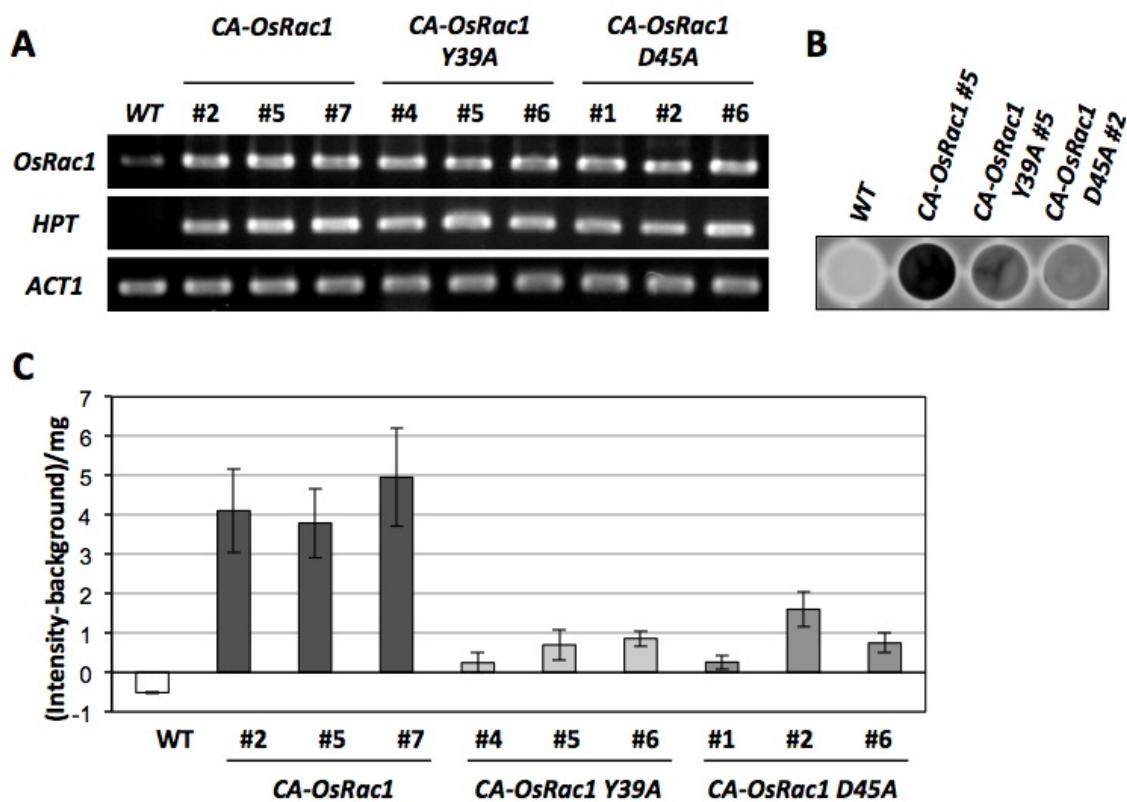
**Figure 3-8. Biological significance of Tyr39 and Asp45 residues in ROS production in rice cells.** *CA-OsRac1 Y39A* and *D45A* mutants were overexpressed in rice cells and their effect on OsRbohB–NADPH oxidase activity was evaluated by quantifying ROS production. (A) Expression of endogenous OsRac1(*WT*) as well as exogenous *CA-OsRac1* and its *Y39A* and *D45A* mutants, *hygromycin phosphotransferase (HPT)* and *Actin1 (ACT1)* in these transgenic rice cells was confirmed by RT-PCR. (B) Example of ROS detection in WT, CA-OsRac1 #5, CA-OsRac1 Y39A #5 and CA-OsRac1 D45A #2 rice suspension cells using the L-012 reagent. (C) Quantification of ROS production in WT, CA-OsRac1, CA-OsRac1 Y39A and CA-OsRac1 D45A lines. The luminescence intensity recorded from each well was measured by ImageJ. Data are mean ± SE of four biological replicates.
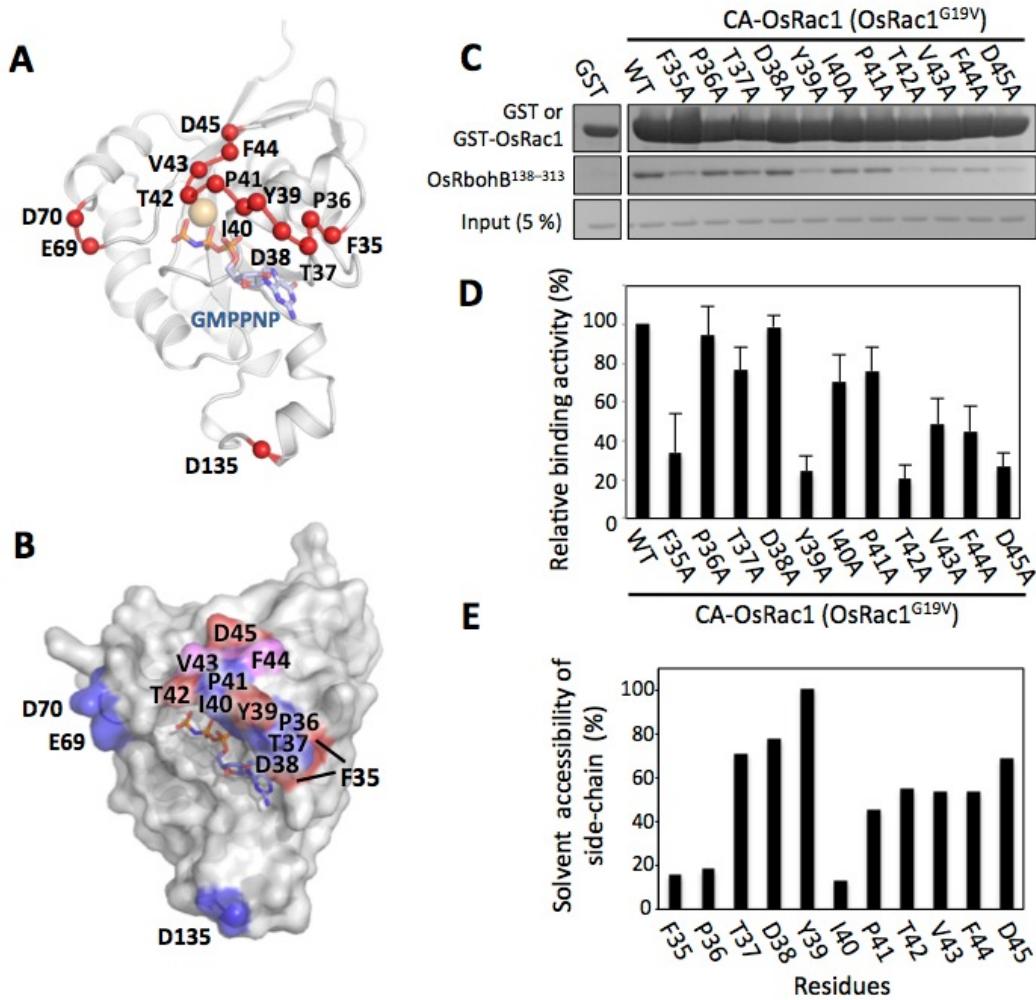
**Figure 3-9. Effects of mutations in OsRac1 Switch I residues on OsRbohB$^{138-313}$ binding.** (A) The alanine-substituted residues in CA-OsRac1 are mapped on the OsRac1 crystal structure as red spheres. (B) Surface representation of the OsRbohB$^{138-313}$-binding interface on OsRac1. OsRac1 mutations that markedly affected (red) or had no effect on binding (blue) are distinguished. Mutation of residues colored pink was shown to moderately affect OsRbohB$^{138-313}$ binding. (C) Pull-down assay using OsRac1 mutants. Single alanine substitutions in Switch I were introduced in the full-length CA-OsRac1 background of the GST fusion construct. Equal amounts of each GST-fused OsRac1 protein were used as bait for OsRbohB$^{138-313}$ (middle panel). (D) Quantification by densitometric analysis of the amount of OsRbohB$^{138-313}$ pulled down in the *in vitro* pull-down assay using CA-OsRac1 mutants and OsRbohB$^{138-313}$. The relative binding activities were assessed by comparison with the value of GST-CA-OsRac1(WT) binding activity to OsRbohB$^{138-313}$, which was set to 100%.

Binding level of each mutant was categorized by the value as markedly reduced (below 40%), moderately reduced (between 40 and 60%) and weak or no effect on binding (above 60%). Average and error values were determined from three independent experiments. (E) Analysis of solvent accessibility for each amino acid of Switch I. The calculation was performed using NACCESS (S. Hubbard, J. M. Thornton, NACCESS, University College London, 1993).
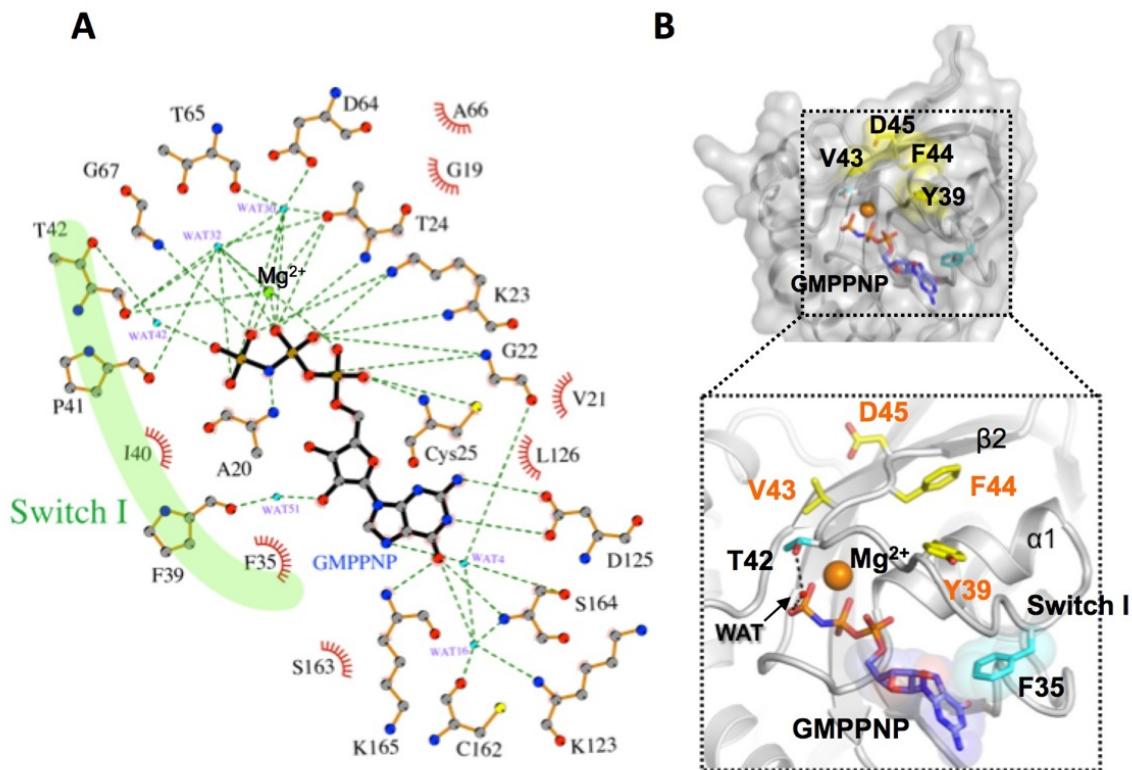
**FIGURE 3-10.** Interaction between OsRac1 and GMPPNP. (A) 2D scheme of interaction between OsRac1 and GMPPNP. OsRac1 residues, which contact with GMPPNP or the $Mg^{2+}$ ion, and the GMPPNP molecule are shown in the ball-and-stick model (red, oxygen; blue, nitrogen; orange, phosphorus; gray, carbon; yellow, sulfur). The $Mg^{2+}$ ion and water molecules (WAT) are shown in sphere colored green and cyan, respectively. Hydrogen bonds are indicated by dashed green lines and the OsRac1 residues which form hydrophobic interactions with GMPPNP are represented by arcs with spokes. The figure was generated by LIGPLOT software (Wallace *et al.*, Protein Eng., 1995). (B) Critical residues in Switch I for OsRbohB[138-313] binding are shown as a stick representation colored with yellow (Tyr39, Val43, Phe44 and Asp45). Other Switch I residues which form direct interactions with GMPPNP are colored cyan (Thr42 (hydrogen bond) and Phe35 (hydrophobic contact)). The $Mg^{2+}$ ion and the water molecule (WAT) are shown as an orange sphere and small red sphere, respectively. The hydrogen bond is indicated by dashed black line.
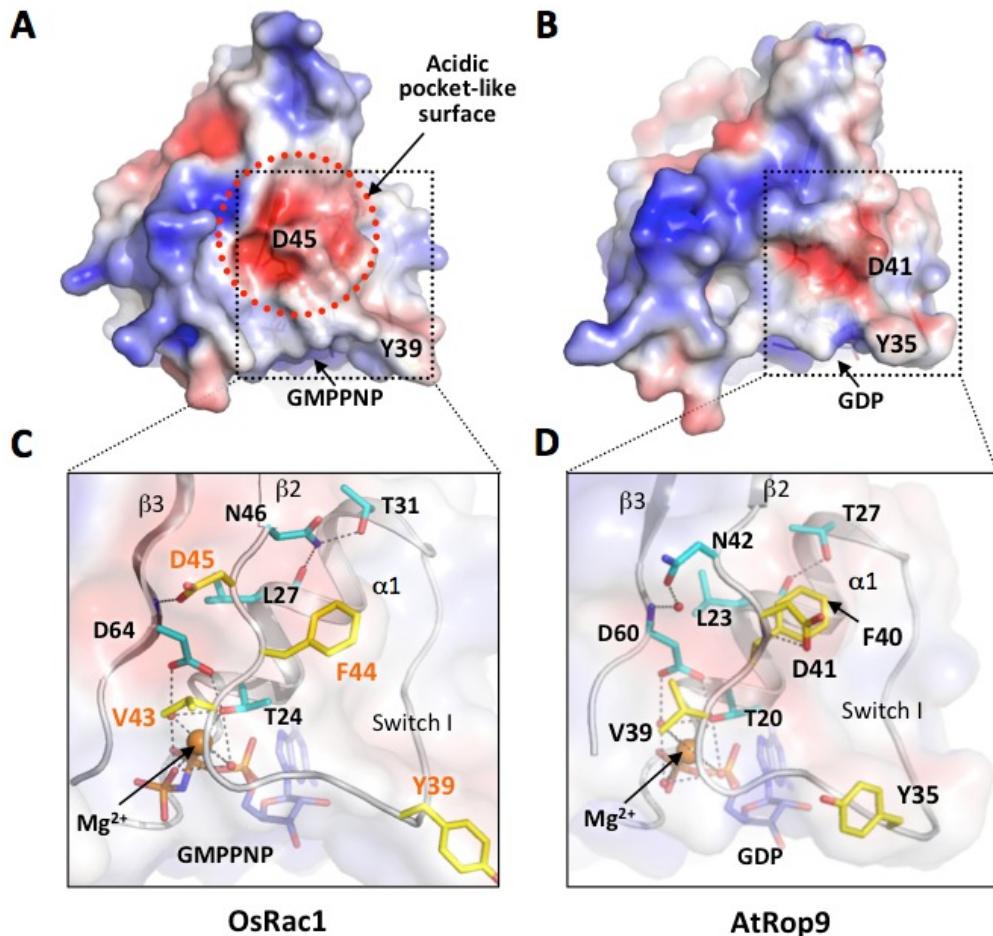
**Figure 3-11. Surface charge difference between OsRac1 (GTP form) and AtRop9 (GDP form).** The surface electrostatic potential ($\pm$ 3 $kT$) and the hydrogen bond network around the C-terminal portions of Switch I of OsRac1(GMPPNP) (A, C) and AtRop9-GDP (B, D) are shown. AtRop9 shows the highest sequence similarity to OsRac1 in PDB. The surface representations and ribbon cartoons are rotated by 50° about the horizontal axis compared with the depiction in Figure 3A. The acidic pocket-like structure of OsRac1 is demarcated by the red dashed circle (A). Critical residues in OsRac1 for OsRbohB[138-313] binding are shown as a stick representation (Tyr39, Val43, Asp45 and Phe44; colored yellow with red label). Other residues which that form the hydrogen bonds with these critical residues, and with GMPPNP/GDP and the $Mg^{2+}$ ions, are colored cyan (C,D).
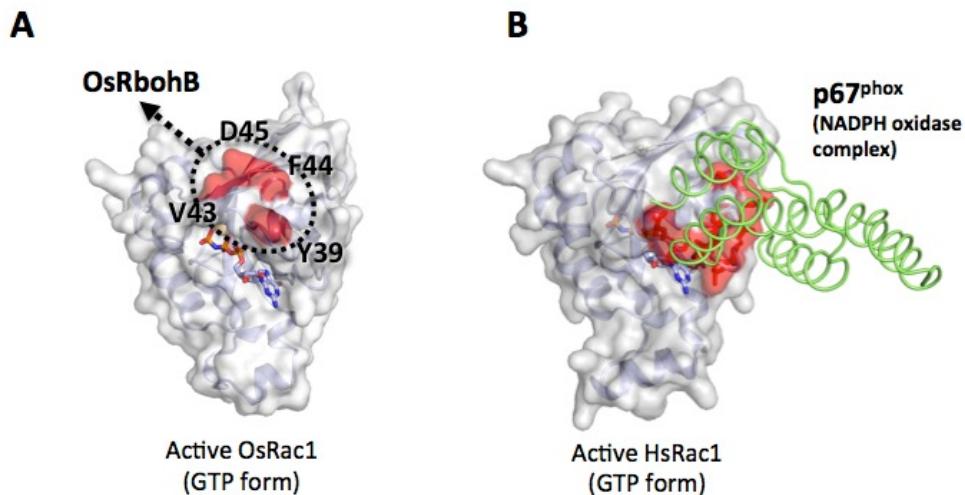
**Figure 3-12. Binding modes of plant and animal Rac/Rop proteins to NADPH oxidase.** (A) Surface representation of OsRac1(GMPPNP). Four residues that are critical for the recognition and activation of the plant NADPH oxidase OsRbohB[138-313], revealed in this study, are shown in red. (B) X-ray structure of the HsRac1-p67[phox] complex (PDB code: 1E96). HsRac1 and p67[phox] are shown in surface (gray) and ribbon (green) representations, respectively. The p67[phox]-binding interface on HsRac1 is colored red. Activated OsRac1 interacts directly with the N-terminal domain of OsRbohB through Tyr39 and Asp45, and induces ROS production by OsRbohB, leading to an immune response in plant cells. Although Switch I is critical for the activation of NADPH oxidase in both plant and animal Rac/Rop proteins, details of their binding regions are different.
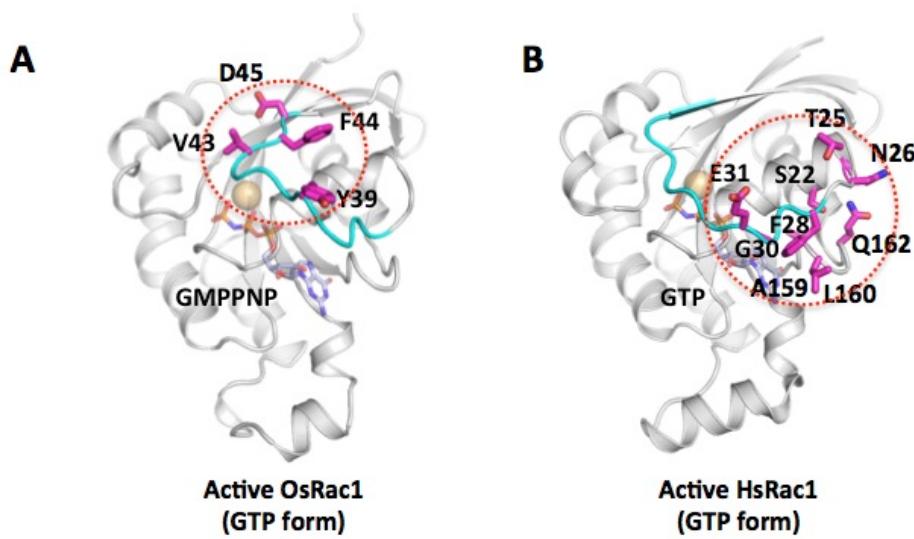
**Figure 3-13. Differences in the NADPH oxidase-binding sites in plant and animal.** OsRac1(GMPPNP) (A) and HsRac1(GTP) (B) are shown in ribbon representation. Side chains of amino acid residues that are important for the interaction with the NADPH oxidases (OsRbohB[138-313] or p67[phox]) are shown in the stick model (magenta) and demarcated by the orange dashed circles. Switch I regions are colored in cyan. Although the Switch I regions are critical for the activation of NADPH oxidase in both plant and animal, molecular details of the interacting regions are slightly different.

**References**

1. Yang, Z. (2002) Small GTPases: versatile signaling switches in plants. *Plant Cell* **14 Suppl**, S375-388.

2. Zheng, Z. L., and Yang, Z. (2000) The Rop GTPase: an emerging signaling switch in plants. *Plant Mol. Biol.* **44**, 1-9.

3. Nibau, C., Wu, H. M., and Cheung, A. Y. (2006) RAC/ROP GTPases: 'hubs' for signal integration and diversification in plants. *Trends Plant Sci.* **11**, 309-315.

4. Yang, Z., and Fu, Y. (2007) ROP/RAC GTPase signaling. *Curr. Opin. Plant Biol.* **10**, 490-494.

5. Xu, T., Wen, M., Nagawa, S., Fu, Y., Chen, J. G., Wu, M. J., Perrot-Rechenmann, C., Friml, J., Jones, A. M., and Yang, Z. (2010) Cell surface- and rho GTPase-based auxin signaling controls cellular interdigitation in *Arabidopsis*. *Cell* **143**, 99-110.

6. Oda, Y., and Fukuda, H. (2012) Initiation of cell wall pattern by a Rho- and microtubule-driven symmetry breaking. *Science* **337**, 1333-1336.

7. Kawasaki, T., Henmi, K., Ono, E., Hatakeyama, S., Iwano, M., Satoh, H., and Shimamoto, K. (1999) The small GTP-binding protein rac is a regulator of cell death in plants. *Proc. Natl. Acad. Sci. U. S. A.* **96**, 10922-10926.

8. Ono, E., Wong, H. L., Kawasaki, T., Hasegawa, M., Kodama, O., and Shimamoto, K. (2001) Essential role of the small GTPase Rac in disease resistance of rice. *Proc. Natl. Acad. Sci. U.S.A.* **98**, 759-764.

9. Suharsono, U., Fujisawa, Y., Kawasaki, T., Iwasaki, Y., Satoh, H., and Shimamoto, K. (2002) The heterotrimeric G protein alpha subunit acts upstream of the small GTPase Rac in disease resistance of rice. *Proc. Natl. Acad. Sci. U.S.A.* **99**, 13307-13312.

10. Fujiwara, M., Umemura, K., Kawasaki, T., and Shimamoto, K. (2006) Proteomics of Rac GTPase signaling reveals its predominant role in elicitor-induced defense response of cultured rice cells. *Plant Physiol.* **140**, 734-745.

11. Wong, H. L., Pinontoan, R., Hayashi, K., Tabata, R., Yaeno, T., Hasegawa, K., Kojima, C., Yoshioka, H., Iba, K., Kawasaki, T., and Shimamoto, K. (2007) Regulation of rice NADPH oxidase by binding of Rac GTPase to its N-terminal extension. *Plant Cell* **19**, 4022-4034.

12. Kawano, Y., Akamatsu, A., Hayashi, K., Housen, Y., Okuda, J., Yao, A., Nakashima, A., Takahashi, H., Yoshida, H., Wong, H. L., Kawasaki, T., and Shimamoto, K. (2010) Activation of a Rac GTPase by the NLR family disease resistance protein Pit plays a critical role in rice innate immunity. *Cell Host Microbe* **7**, 362-375.

13. Akamatsu, A., Wong, H. L., Fujiwara, M., Okuda, J., Nishide, K., Uno, K., Imai, K., Umemura, K., Kawasaki, T., Kawano, Y., and Shimamoto, K. (2013) An OsCEBiP/OsCERK1-OsRacGEF1-OsRac1 module is an essential early component of chitin-induced rice immunity. *Cell Host Microbe* **13**, 465-476.

14. Kawano, Y., Chen, L., and Shimamoto, K. (2010) The function of Rac small GTPase and associated proteins in rice Innate Immunity. *Rice* **3**, 112-121.

15. Kawano, Y., and Shimamoto, K. (2013) Early signaling network in rice PRR-mediated and R-mediated immunity. *Curr. Opin. Plant Biol.* **16**, 496-504.

16. Potocký, M., Pejchar, P., Gutkowska, M., Jiménez-Quesada, M. J., Potocká, A., Alché, J. e. D., Kost, B., and Žárský, V. (2012) NADPH oxidase activity in pollen tubes is affected by calcium ions, signaling phospholipids and Rac/Rop GTPases. *J. Plant Physiol.* **169**, 1654-1663.

17. Craddock, C., Lavagi, I., and Yang, Z. (2012) New insights into Rho signaling from plant ROP/Rac GTPases. *Trends Cell Biol.* **22**, 492-501.

18. Chen, X., Naramoto, S., Robert, S., Tejos, R., Löfke, C., Lin, D., Yang, Z., and Friml, J. (2012) ABP1 and ROP6 GTPase signaling regulate clathrin-mediated endocytosis in *Arabidopsis* roots. *Curr. Biol.* **22**, 1326-1332.

19. Lin, D., Nagawa, S., Chen, J., Cao, L., Chen, X., Xu, T., Li, H., Dhonukshe, P., Yamamuro, C., Friml, J., Scheres, B., Fu, Y., and Yang, Z. (2012) A ROP GTPase-dependent auxin signaling pathway regulates the subcellular distribution of PIN2 in *Arabidopsis* roots. *Curr. Biol.* **22**, 1319-1325.

20. Nagawa, S., Xu, T., Lin, D., Dhonukshe, P., Zhang, X., Friml, J., Scheres, B., Fu, Y., and Yang, Z. (2012) ROP GTPase-dependent actin microfilaments promote PIN1 polarization by localized inhibition of clathrin-dependent endocytosis. *PLoS Biol.* **10**, e1001299.

21. Zheng, Z. L., Nafisi, M., Tam, A., Li, H., Crowell, D. N., Chary, S. N., Schroeder, J. I., Shen, J., and Yang, Z. (2002) Plasma membrane-associated ROP10 small GTPase is a specific negative regulator of abscisic acid responses in *Arabidopsis*. *Plant Cell* **14**, 2787-2797.

22. Li, Z., Gao, X., Chinnusamy, V., Bressan, R., Wang, Z. X., Zhu, J. K., Wu, J. W., and Liu, D. (2012) ROP11 GTPase negatively regulates ABA signaling by protecting ABI1 phosphatase activity from inhibition by the ABA receptor RCAR1/PYL9 in Arabidopsis. *J. Integr. Plant. Biol.* **54**, 180-188.

23. Nibau, C., Tao, L., Levasseur, K., Wu, H. M., and Cheung, A. Y. (2013) The *Arabidopsis* small GTPase AtRAC7/ROP9 is a modulator of auxin and abscisic acid signaling. J Exp Bot 64, 3425-3437.

24. Sørmo, C. G., Leiros, I., Brembu, T., Winge, P., Os, V., and Bones, A. M. (2006) The crystal structure of Arabidopsis thaliana RAC7/ROP9: the first RAS superfamily GTPase from the plant kingdom. *Phytochemistry,* **67**, 2332-2340.

25. Thomas, C., Fricke, I., Scrima, A., Berken, A., and Wittinghofer, A. (2007) Structural evidence for a common intermediate in small G protein-GEF reactions. *Mol. Cell* **25**, 141-149.

26. Thomas, C., Fricke, I., Weyand, M., and Berken, A. (2009) 3D structure of a binary ROP-PRONE complex: the final intermediate for a complete set of molecular snapshots of the RopGEF reaction. *Biol. Chem.* **390**, 427-435.

27. Al-Mulla, F., Milner-White, E. J., Going, J. J., and Birnie, G. D. (1999) Structural differences between valine-12 and aspartate-12 Ras proteins may modify carcinoma aggression. *J. Pathol.* **187**, 433-434.

28. Oda, T., Hashimoto, H., Kuwabara, N., Hayashi, K., Kojima, C., Kawasaki, T., Shimamoto, K., Sato, M., and Shimizu, T. (2008) Crystallographic characterization of the N-terminal domain of a plant NADPH oxidase. *Acta Crystallogr. Sect. F Struct. Biol. Cryst. Commun.* **64**, 867-869.

29. Oda, T., Hashimoto, H., Kuwabara, N., Akashi, S., Hayashi, K., Kojima, C., Wong, H. L., Kawasaki, T., Shimamoto, K., Sato, M., and Shimizu, T. (2010) Structure of the N-terminal regulatory domain of a plant NADPH oxidase and its functional implications. *J. Biol. Chem.* **285**, 1435-1445.

30. Kosami, K., Ohki, I., Hayashi, K., Tabata, R., Usugi, S., Kawasaki, T., Fujiwara, T., Nakagawa, A., Shimamoto, K. and Kojima, C. (2014) Purification, crystallization and preliminary X-ray crystallographic analysis of a rice Rac/Rop GTPase, OsRac1. *Acta Crystallogr. F Struct. Biol. Commun*. **70**, 113-115.

31. Otwinowski Z., and Minor W. (1997) *Methods Enzymol.* **276**, 307–326.

32. McCoy, A. J., Grosse-Kunstleve, R. W., Adams, P. D., Winn, M. D., Storoni, L. C., and Read, R. J. (2007) Phaser crystallographic software. *J. Appl. Crystallogr.* **40**, 658-674.

33. Emsley, P., Lohkamp, B., Scott, W. G., and Cowtan, K. (2010) Features and development of Coot. *Acta Crystallogr. Sect. D Biol. Crystallogr.* **66**, 486-501.

34. Murshudov, G. N., Vagin, A. A., and Dodson, E. J. (1997) Refinement of macromolecular structures by the maximum-likelihood method. *Acta Crystallogr. Sect. D Biol. Crystallogr.* **53**, 240-255.

35. Brünger, A. T., Adams, P. D., Clore, G. M., DeLano, W. L., Gros, P., Grosse-Kunstleve, R. W., Jiang, J. S., Kuszewski, J., Nilges, M., Pannu, N. S., Read, R. J., Rice, L. M., Simonson, T., and Warren, G. L. (1998) Crystallography & NMR system: A new software suite for macromolecular structure determination. *Acta Crystallogr. Sect. D Biol. Crystallogr.* **54**, 905-921.

36. Lovell, S. C., Davis, I. W., Arendall III, W. B., de Bakker, P. I. W., Word, J. M., Prisant, M. G., Richardson, J. S., and Richardson, D. C. (2003) Structure validation by Cα geometry: φ, ψ and Cβ deviation. *Proteins: Struct. Funct. Genet.* **50**, 437-450.

37. Delaglio, F., Grzesiek, S., Vuister, G. W., Zhu, G., Pfeifer, J., and Bax, A. (1995) NMRPipe: a multidimensional spectral processing system based on UNIX pipes. *J. Biomol. NMR* **6**, 277-293.

38. Hiei, Y., Ohta, S., Komari, T., and Kumashiro, T. (1994) Efficient transformation of rice (*Oryza sativa* L.) mediated by Agrobacterium and sequence analysis of the boundaries of the T-DNA. *Plant J.* **6**, 271-282.

39. Longenecker, K., Read, P., Lin, S. K., Somlyo, A. P., Nakamoto, R. K., and Derewenda, Z. S. (2003) Structure of a constitutively activated RhoA mutant (Q63L) at 1.55 A resolution. *Acta Crystallogr. Sect. D Biol. Crystallogr.* **59**, 876-880.

40. Hirshberg, M., Stockley, R. W., Dodson, G., and Webb, M. R. (1997) The crystal structure of human rac1, a member of the rho-family complexed with a GTP analogue. *Nat. Struct. Biol.* **4**, 147-152.

41. Ihara, K., Muraguchi, S., Kato, M., Shimizu, T., Shirakawa, M., Kuroda, S., Kaibuchi, K., and Hakoshima, T. (1998) Crystal structure of human RhoA in a dominantly active form complexed with a GTP analogue. *J. Biol. Chem.* **273**, 9656-9666.

42. Yamaguchi, K., Imai, K., Akamatsu, A., Mihashi, M., Hayashi, N., Shimamoto, K., and Kawasaki, T. (2012) SWAP70 functions as a Rac/Rop guanine nucleotide-exchange factor in rice. *Plant J.* **70**, 389-397.

43. Xu, X., Barry, D. C., Settleman, J., Schwartz, M. A., and Bokoch, G. M. (1994) Differing structural requirements for GTPase-activating protein responsiveness and NADPH oxidase activation by Rac. *J. Biol. Chem.* **269**, 23569-23574.

44. Koga, H., Terasawa, H., Nunoi, H., Takeshige, K., Inagaki, F., and Sumimoto, H. (1999) Tetratricopeptide repeat (TPR) motifs of p67[phox] participate in interaction with the small GTPase Rac and activation of the phagocyte NADPH oxidase. *J. Biol. Chem.* **274**, 25051-25060.

45. Bedard, K., and Krause, K. H. (2007) The NOX family of ROS-generating NADPH oxidases: physiology and pathophysiology. *Physiol. Rev.* **87**, 245-313.

46. Han, C. H., Freeman, J. L., Lee, T., Motalebi, S. A., and Lambeth, J. D. (1998) Regulation of the neutrophil respiratory burst oxidase. Identification of an activation domain in p67[phox]. *J. Biol. Chem.* **273**, 16663-16668.

47. Diekmann, D., Abo, A., Johnston, C., Segal, A. W., and Hall, A. (1994) Interaction of Rac with p67[phox] and regulation of phagocytic NADPH oxidase activity. *Science* **265**, 531-533.

48. Lapouge, K., Smith, S. J., Walker, P. A., Gamblin, S. J., Smerdon, S. J., and Rittinger, K. (2000) Structure of the TPR domain of p67[phox] in complex with Rac-GTP. *Mol. Cell* **6**, 899-907.

49. Jones, M. A., Raymond, M. J., Yang, Z., and Smirnoff, N. (2007) NADPH oxidase-dependent reactive oxygen species formation required for root hair growth depends on ROP GTPase. *J. Exp. Bot.* **58**, 1261-1270.

# CHAPTER  4

**GENERAL DISCUSSION**

## 4. GENERAL DISCUSSION

### 4.1 The conformational change of OsRac1

GDP/GTP exchange induces a conformational change in Small G proteins. As mentioned in Chapter 1, it is thought that this conformational change is leaded by interaction between phosphoryl group of GTP and basic residues of small G proteins. In HsRac1(GMPPNP), γ-phosphate of GTP can form hydrogen bond with main-chains of Thr35 and Gly60 and this interaction leads to conformational change (Figure 4-1 A). In OsRac1, γ-phosphate of GMPNP forms water-mediated hydrogen bond with side-chain of Thr41, instead of main chain of Thr35 in HsRac1(GMPPNP). Furthermore, the main-chain of Gly67 of switch II in OsRac1 direct hydrogen bond to γ-phosphate. These interactions pull switch I and switch II regions to GMPPNP and induce the conformational change of OsRac1 (Figure 4-1 B). Lys22 of p-loop also forms hydrogen bond with γ-phosphate and this Lys residues has also hydrogen bond with main-chains of Gly17 and Asp18. Therefore, the interaction between Lys residues and γ-phosphate may increase the stability of GTP binding-site. In the AtRop9-GDP complex, these hydrogen bonds did not form (Figure 4-1 C).

### 4.2 The open conformation of switch I region of OsRac1

In Chapter 3, compared with RhoA(GTPγS) (PDB code: 1A2B) and HsRac1(GMPPNP) (PDB code: 1MH1), the large deviations are primarily due to differences in switch I region. In the crystal structure of HsRac1(GMPPNP) and RhoA(GTPγS), switch I region is in "closed" conformations, whereas that of in OsRac1(GMPPNP) is in "opened" conformation (Figure 3-1 B). It is surprising that RhoA(GDP) (PDB code: 1FTN) and AtRop9(GDP) (PDB code: 2J0V) also show the

opened conformation in switch I region (Figure 4-2).

The conformational change in switch I region is induced by GDP/GTP exchange but the critical GTP interacting sites of OsRac1(GMPPNP) appear similar to that of RhoA(GTPγS) and HsRac1(GMPPNP) with some unique distinctions. The conformational difference in switch I region may be induced by interaction between Tyr residue in switch I region (Tyr39 in OsRac1, Tyr34 in HsRhoA) and the guanine nucleotide. Tyr residue in switch I region is highly conserved between animal and plants (Figure 3-2, Figure 3-5). Tyr34 of RhoA(GMPPNP) (PDB code: 1KMQ) interacts with O1G atom of γ-phosphate of GMPPNP (Figure 4-2) however these Tyr residues in OsRac1(GMPPNP), HsRhoA (GDP) and AtRop7(GDP) were exposed to the molecular surface (Figure 4-2). Additionally, as mentioned, although Thr resides of switch I in HsRac1 directly interacts with the γ-phosphate of GMPPNP, Thr resides of OsRac1 interacts with the γ-phosphate of GMPPNP through water molecule.

Thereby, the conformation change in switch I region between animals and plants may be induced by interaction between the Tyr/Thr residue in switch I region and the guanine nucleotide.

### 4.3 The long helical conformation of switch II region

The overall structure of OsRac1(GMPPNP) was similar to the structures AtRop proteins. However, structural differences were observed in the switch I, switch II, and Insert region between OsRac1(GMPPNP) and the AtRop proteins. In comparison switch I with switch II region of AtRop proteins(GDP or GEF complex), OsRac1(GMPPNP) adopted a long helical conformation (Figure 4-3 and Figure 4-4A). On the other hand, most AtRop proteins(GDP or GEF complex) adopted a loop

structure (Figure 4-3 and Figure 4-4) (1). In N-terminal of switch II region, Thr65 of OsRac1 has water-mediated hydrogen bonds to β- and γ-phosphates and Gly67 of OsRac1 has direct hydrogen bonds to γ-phosphate and R75 of OsRac1 has hydrogen bonds to E103 of OsRac1 (Figure 4-4 A). These hydrogen bonds were not observed in AtRop proteins except for AtRop5 (Figure 4-4 B-E). These hydrogen bonds probability stabilize the long helical conformation in switch II region.

## 4.4 Effect of Q68L mutation on the GTPase activity

In this thesis, we introduced a specific mutation (Gln68 to Leu) to attenuate the GTPase activity of OsRac1. This glutamine residue, adjacent to DXXG motif in switch II/G3 is a key player in hydrolyzing GTP to GDP. The mutation at this glutamine residue remains in the active GTP-bund state much longer than the wild type in many small GTPases. In this thesis, OsRac1$^{Q68L}$ mutant markedly inhibited intrinsic GTPase activity. What kind of influence does the single mutation have on the structure of OsRac1? To answer this question, the structure of Ras$^{Q61L}$ was compared with the structures of wild type Ras.

The overall structures of Ras(GMPPNP) (PDB code: 3K8Y) and the Ras$^{Q61L}$(GppNHp) (PDB code: 3OIU) were very similar. The root mean square deviation (RMSD) of 133 Cα atoms was approximately 0.07 Å. Thus, it is thought overall structure of small GTPase was not highly influenced by Gln to Lue mutation.

The role of this Gln is to stabilize the transition state by orienting the relative positions of the nucleophilic water and the γ-phosphate. The crystal structure of Ras(GMPPNP) (PDB code: 3K8Y) has two water molecules which can form the hydrogen bond with oxygen atom of γ-phosphate (Figure 4-5 A). The first water

molecule (Wat175 in Ras) is the so-called pre-catalytic water molecule proposed to be the nucleophile in the hydrolysis reaction. It is positioned at a distance of 2.8 Å from oxygen atom (O1G) of γ-phosphate and at a distance of 3.1 Å from main-chain of Q61. The main chain of Q61 forms hydrogen bond with pre-catalytic water molecule (Figure 4-5 A). The second water molecule (Wat189 in Ras) is the so-called bridging water. It is positioned at 2.6 Å from the oxygen atom (O1G) of γ-phosphate atom and at a distance of 2.6 Å from the hydroxyl group of Y32, bridging between the two groups (Figure 4-5 A). The γ-phosphate of GTP abstracts a proton from the bridging water molecule (Wat189 in Ras), which in turn activates the catalytic water molecule (Wat175 in Ras) for nucleophilic attack on the γ-phosphate during the hydrolysis reaction (2).

These two water molecules were found in the same location as in the HsRac1(GMPPNP) (PDB code: 1MH1) (Figure 4-5 B). However, the crystal structure of the the RhoA$^{Q63L}$(GMPPNP) (PDB code: 1KMQ) and OsRac1(GMPPNP) reveal somewhat different water arrangement. First, the bridging water molecule (Wat189 in Ras) is completely absent in theses RhoA$^{Q63}$ and OsRac1$^{Q68L}$ mutant structures (Figure 4-5 C, D). Second, the pre-catalytic water molecules of the RhoA$^{Q63L}$(GMPPNP) are observed in the same location as in Ras(GMPPNP), with nearly ideal hydrogen-bonds to the O1G atom of the γ-phosphate and to the carbonyl oxygen atom of Thr (T35 of Ras and T37 of RhoA) (Figure 4-5 C). The position of water molecule in the OsRac1(GMPPNP) active site is different from RhoA$^{Q63L}$(GMPPNP). In structure of OsRac1(GMPPNP), the water molecule was absent in the same location of active site, however a water molecule was observed around active site with hydrogen-bonds to the O1G atom of the γ-phosphate and to the carbonyl oxygen atom of Thr (T42 of OsRac1) (Figure 4-5 D). We postulate that the pre-catalytic water molecule was shifted by Q68L

104

mutation in OsRac1. Shift of this pre-catalytic water molecule is possible mean of inhibiting GTP hydrolysis by the constitutively active mutation Q68L of OsRac1. The mechanism of constitutively active by Q68L mutation of OsRac1 may be almost the same as that of RhoA$^{Q63L}$(GMPPNP).

## 4.5 GEF binding

Recently, a new type of GEF has been identified in plants (3). The GEF contains highly conserved region, referred to as PRONE (Plant specific Rop nucleotide exchanger). Rops are activated by PRONE domain and OsRac1 is activated by PRONE domain of OsRacGEF1 (4).

In the crystal structure of AtRop4–PRONE8, PRONE domain of RopGEF interactions with switch I region, switch II region and insert region of AtRop4 (5). Therefore, the conformational change of switch I region and switch II region in GTP bound form may influence Rops binding to PRONE domain. However, it could be imagined that the switch I region and switch II region of OsRac1(GMPPNP) fit into binding pocket of PRONE domain of AtRop4-PRONE8 complex (PDB code: 2NTY) (Figure 4-6). This observation is consistent with previous results that PRONE domain of OsGEF1 interacts with GTP- and GDP-bound forms of OsRac1 (4). These results suggest that Rops binding to PRONE domain is not influenced by conformational change of switch I region and switch II region between GTP and GDP GDP-bound forms.

## 4.6 GAP binding

RhoGAPs play the key roles in the control of Rho GTPase activity and cellular processes. Mammalian Rho proteins in complex with the RhoGAP domain are well characterized in structural and biochemical studies. The sequences alignment for the RopGAPs shows conserved structural domains (Figure 4-7 A). The central region containing GAP-like domain shares 70% amino acid identity among RopGAPs and about 27% identity with RhoGAP domains from animals and yeast (Figure 4-7 B).

In crystal structure of Rho-GAP complex (PDB code: 1TX4), RhoGAP domain interacts with switch I region and switch II region of Rho proteins (6). In this thesis, comparison of OsRac1(GMPPNP) structure with AtRop9(GDP) structure showed the significant structural difference in switch I and switch II (Figure 3-3, Figure 3-4), therefore Rops binding to GAP domain of RopGAP may be influenced by conformational change of switch I and switch II region.

In RhoA-GAP complex (PDB code:1TX4), E64 amino acid in Switch II region of RhoA forms hydrogen binds with side chains of T90, T123 and R126 of RhoGAP, D65 amino acid in Switch II region of RhoA form hydrogen binds with side chains of K122, R126 and N202 of RhoGAP and Y66 amino acid in Switch II region of RhoA form hydrogen binds with main chain of V197 and side chains of N220 of RhoGAP. Out of these residues of RhoGAP, K122 and R126 of RhoGAP are highly conserved between plants and animals (Figure 4-7 B). Therefore, K122 and R126 of RhoGAP may be important for binding with Rops.

The overall structures of OsRac1(GMPPNP) and the RhoA-GAP complex, designated as HsRhoA were very similar. It could be imagined that the switch I region and switch II region of OsRac1 fit into binding pocket of GAP domain on the structure of the RhoA-GAP complex superimposed with OsRac1 (GMPPNP) (Figure 4-8 A). E69

of OsRac1 is located at distance of 3.7 Å from the R126 of RhoGAP and are slightly distant to form hydrogen bonding with R126 of RhoGAP. D70 of OsRac1 (D65 of RhoA) are located at distance of 3.2 Å from the R126 of RhoGAP and enable hydrogen bonding (Figure 4-8 C). However, D70 of OsRac1 (D65 of RhoA) are located at distance of 5.3 Å from the K122 of RhoGAP and are distant to form hydrogen bonding with K122 of RhoGAP (Figure 4-8 C).

In case of AtRop7 (GDP), the switch I region and switch II region of AtRop7(GDP) can also fit into binding pocket of GAP domain of RhoGAP. E65 of AtRop9 (E64 of RhoA) are located at distance of 2.9 Å from the R126 of RhoGAP and are enable hydrogen bonding with R126 of RhoGAP (Figure 4-8 D). However D66 of AtRop9 (D65 of RhoA) are located at the distance of 11.5 Å from the R126 of RhoGAP and at the distance of 5.3 Å from the K122 of RhoGAP (Figure 4-8 D). Therefore, D66 of AtRop9 is unable to hydrogen bonds with K122 and R126 of RhoGAP. Conceivably the GDP to GTP exchange in Rops induces a conformational change of Switch II, so that Rops may strongly associate with GAP.

As mentioned in Chapter 1, the GAP inserts the side chain of a positively charged arginine residue into the active site of GTPase. This arginine finger neutralizes the developing negative charges in the transition state of GTP hydrolysis. In the HsRhoA-GAP complex, R85 (arginine finger) of RhoGAP inserts into the active site of HsRhoA (Figure 4-9 A). In case of model of OsRac1(GMPPNP)-GAP complex, the positively charged arginine residue (R85) also inserts into the active site of OsRac1 (Figure 4-9 B). R85 of RhoGAP is highly conserved between plants and animals (Figure 4-7 B). Therefore, the mechanism of GTP hydrolysis by GAP may be similar to plants and animals.

### 4.7 NADPH oxidase activation by small GTPase in animals and plants

In animals, switch I region of HsRac1/2 has been reported to be important for ROS production in the activation of NADPH oxidase (7, 8). Although switch I region is critical in the activation of NADPH oxidase in both plants and the animals, details of the interaction regions differ between plants and animals. In HsRac1, some of N-terminal residues (F28, G30 and E31) of switch I region are involved in HsRac1 docking with p67$^{phox}$ (9), whereas OsRac1 does not involve N-terminal residues of switch I region in interaction with OsRbohB (Figure 3-10 and Figure 3-11). In HsRac1-p67$^{phox}$ complex, the third phosphate of GTP attracts Tyr32 of HsRac1 on the switch I region, twisting the adjacent residues into position. This influences the position of adjacent G30 and E31 so that HsRac1 may associate with p67$^{phox}$. But the Tyr39 of OsRac1 does not attract the third phosphate of GMPPNP (Figure 4-2, Figure 4-10). For this reason, the large conformational change around N-terminal of switch I region may be not caused by GDP/GTP exchange in OsRac1.
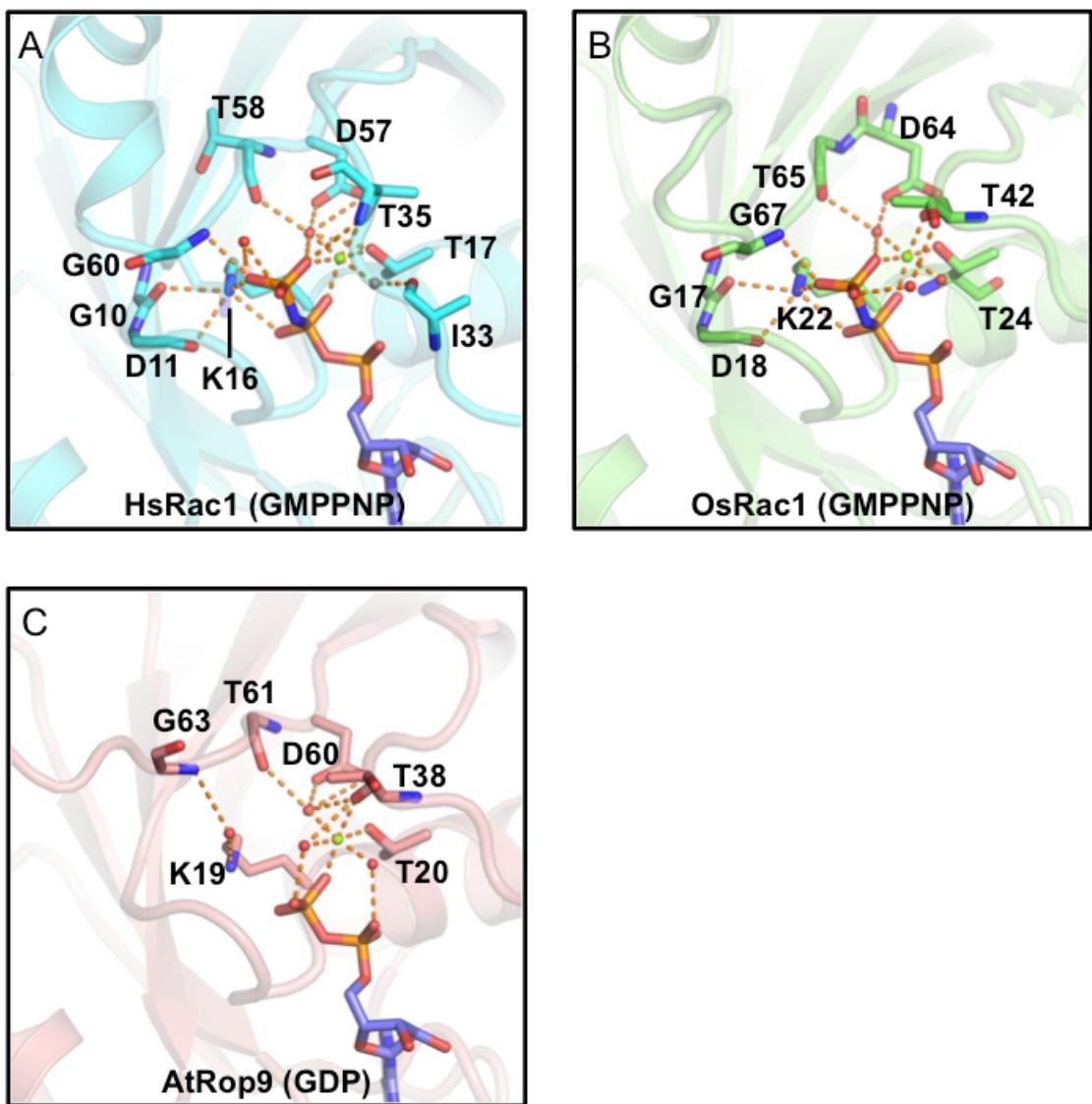
**Figure 4-1. Comparison of the γ-phosphate binding site of small GTPase.** (A) HsRac1(GMPPNP) (PDB code: 1MH1), (B) OsRac1(GMPPNP) (PDB code: 4U5X) and (C) AtRop9(GDP) (PDB code: 2J0V, chain B). The GMPPNP and GDP were shown in the stick model (red, deep blue, and orange indicates O, N, and P atoms, respectively). The $Mg^{2+}$ ion and water molecules were shown as green sphere and red sphere, respectively.
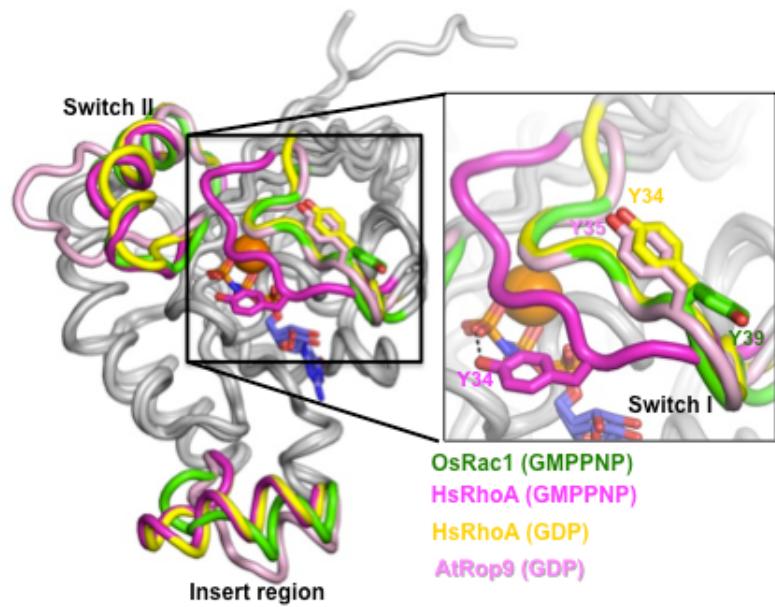
**Figure 4-2. Superimposition of the crystal structures of OsRac1(GMPPNP) (PDB code: 4U5X), HsRhoA(GMPPNP) (PDB code: 1KMQ), HsRhoA(GDP) (PDB code: 1FTN) and AtRop9(GDP) (PDB code: 2J0V, chain B).** Switch I, II and Insert regions are colored as indicated in the protein labels. GDP and GMPPNP are shown in the stick model (red, oxygen; blue, nitrogen; orange, phosphorus). The $Mg^{2+}$ ion is shown as an orange sphere. Models were generated using PyMOL.
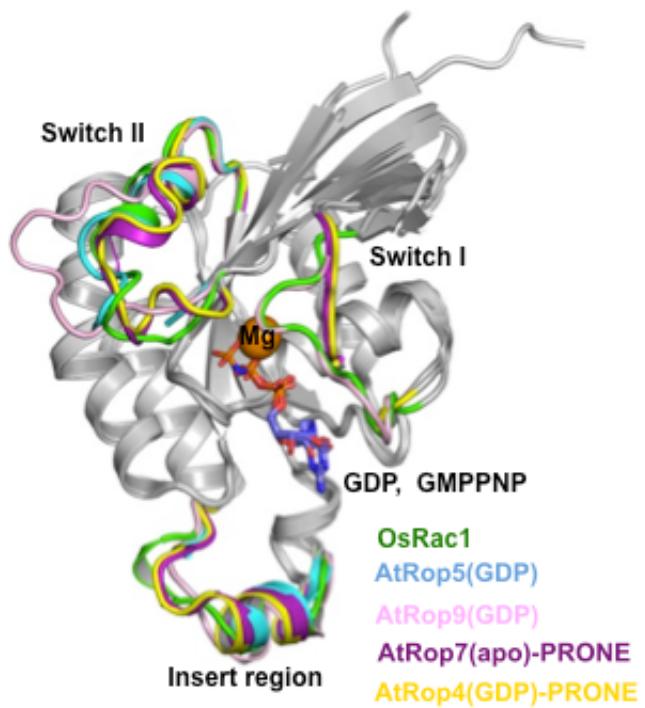
**Figure 4-3. Comparison of the overall structures of OsRac1(GMPPNP) and AtRop proteins.** Main chains of the OsRac1(GMPPNP) (PDB code: 4U5X), AtRop4(GDP) (PDB code: 2NTY, chain B), AtRop5(GDP) (PDB code: 3BWD), AtRop7(apo)-PRONE complex (PDB code: 2WBL, chain C), and AtRop9(GDP) (PDB code:2J0V, chain B) were superimposed by using program PyMOL. The Switch I, Switch II, and the Insert region are colored as indicated in the inset legend. The GMPPNP and GDP were shown in the stick model (red, deep blue, and orange indicates O, N, and P atoms, respectively). The Mg$^{2+}$ ion was shown as orange sphere.
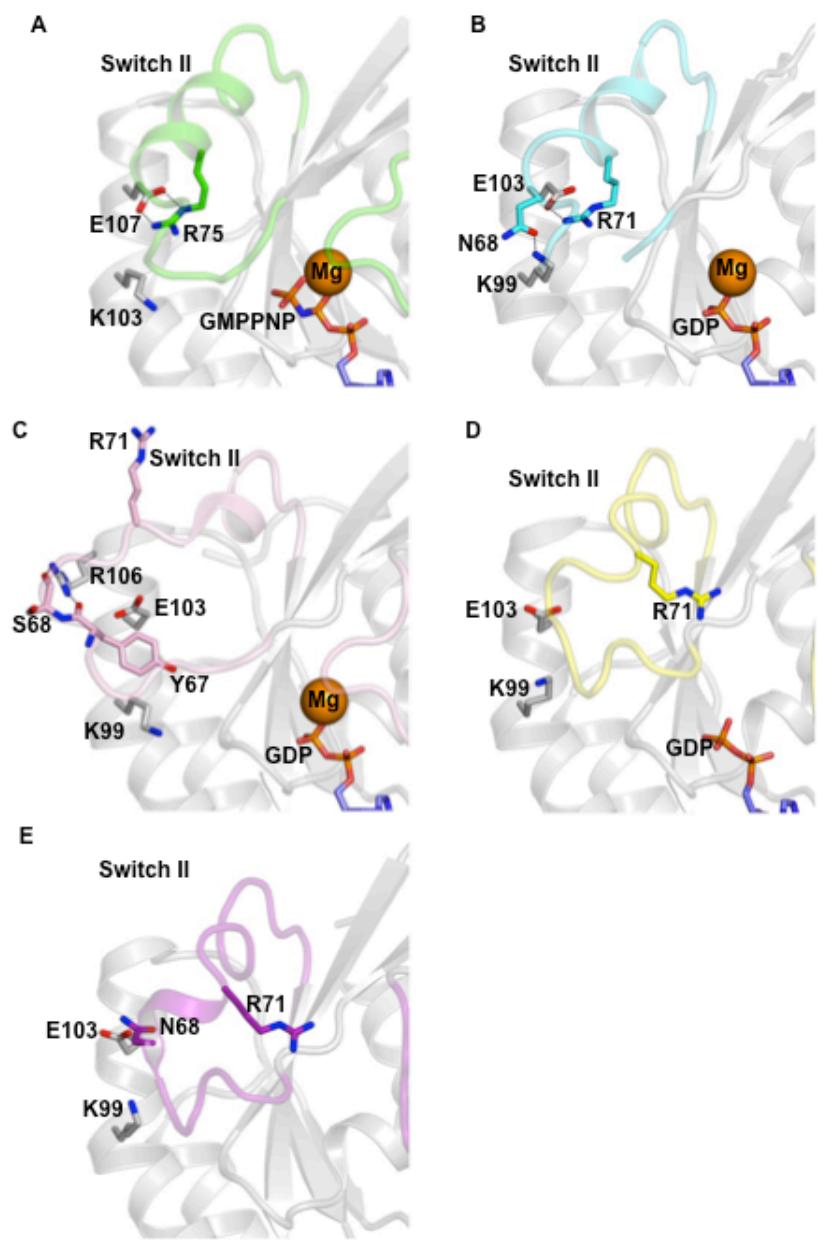
**Figure 4-4. Comparison of the structures of plant small GTPase on Switch II.** (A) Ribbon drawing of OsRac1(GMPPNP) (PDB code: 4U5X). (B) Ribbon drawing of AtRop5(GDP) (PDB code: 3BWD). (C) Ribbon drawing of AtRop9(GDP) (pdbPDB code:2J0V, chain B). (D) Ribbon drawing of AtRop4(GDP)-PRONE8 complex (PDB code: 2NTY, chain B). (E) Ribbon drawing of AtRop7(apo)-PRONE complex (PDB code: 2WBL, chain C). The GMPPNP and GDP were shown in the stick model (red, deep blue, and orange indicates O, N, and P atoms, respectively). The Mg$^{2+}$ ion was shown as orange sphere.
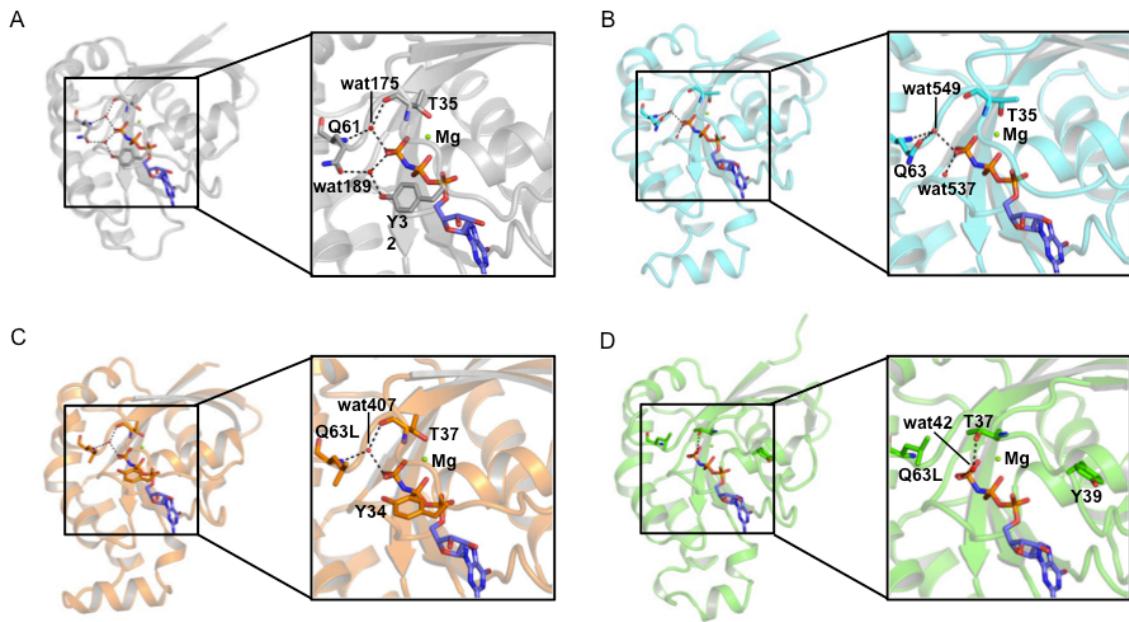
**Figure 4-5. Structural difference in active site by Gln to Lue mutation between (A) Ras (GMPPNP) (PDB code: 3K8Y), (B) HsRac1(GMPPNP) (PDB code: 1MH1), (C) RhoA<sup>Q63L</sup>(GMPPNP) (PDB code: 1KMQ) and (D) OsRac1 (GMPPNP) (PDB code: 4U5X).** The GMPPNP and GDP were shown in the stick model (red, deep blue, and orange indicates O, N, and P atoms, respectively). The Mg$^{2+}$ ion and water molecules were shown as green sphere and red sphere, respectively.
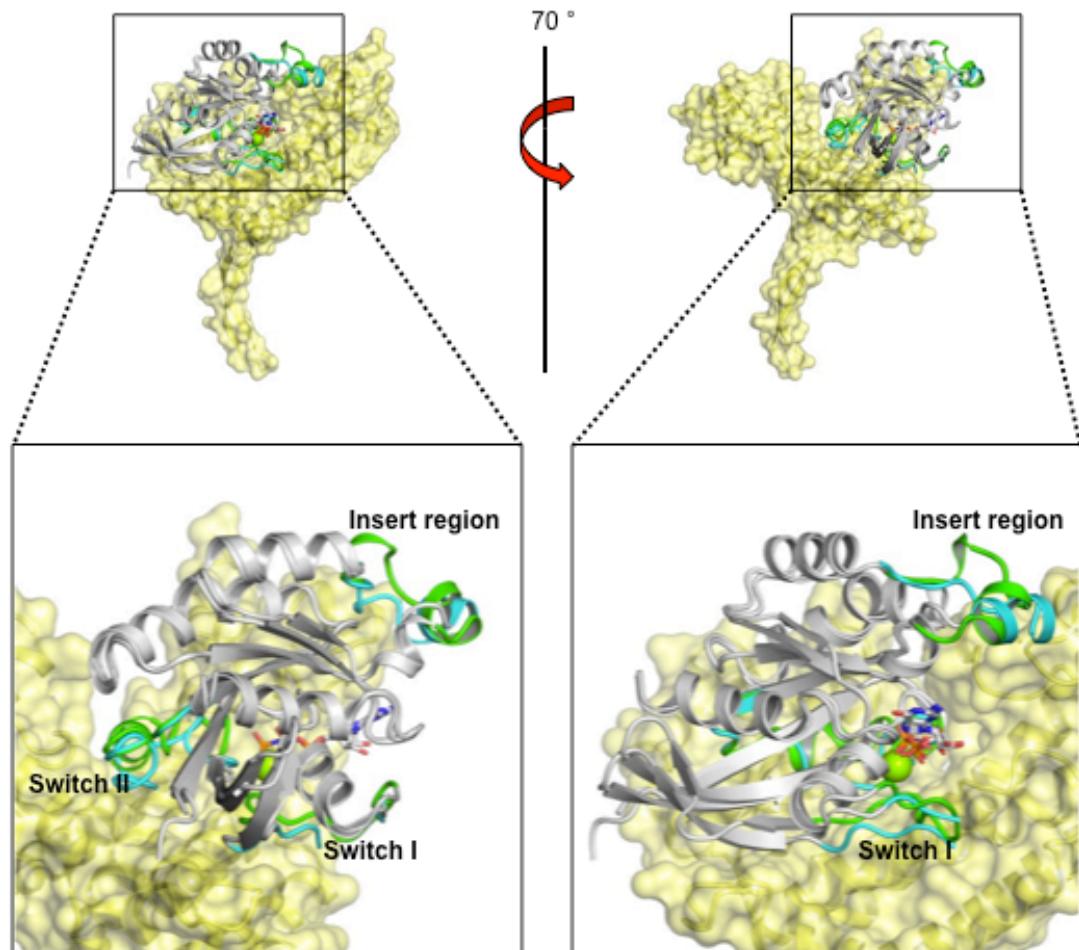
**Figure 4-6. Superimposition of the crystal structures of OsRac1(GMPPNP) (PDB code: 4U5X) and AtRop4(GDP)-PRONE8 complex (PDB code: 2NTY).** Switch I, II and Insert regions of OsRac1 and AtRop4(GDP) are colored as green and light blue, respectively. GDP and GMPPNP are shown in the stick model (red, oxygen; blue, nitrogen; orange, phosphorus). The $Mg^{2+}$ ion is shown as a green sphere. Models were generated using PyMOL.

A

```
                        10        20        30        40        50
   OsGAP1/1-444      1  MATAMSRSQGE----------------------AAARRRALQDSKRRRRRRR  30
   OsGAP3/1-450      1  MTGVVVVSPSGCKGGGGGGG----------GGVGKKRGSGEEERERERQQ    39
AtRopGAP1/1-466      1  MTEVLHFPSSPSASHSSSSSSSSSPSPSSLSYASRSNATLLISSDHNRRNPVAR 53
AtRopGAP2/1-430      1  MTGLVMMTKGGG-CGGGGK-------------GGRRKSTAEEEEEEEQNQQQ   38
AtRopGAP3/1-455      1  MTNFSRSKSTGTIGFPEFKPTRP----------GPDKYENIHNDDODEYEEGHS 43
AtRopGAP2/1-430      1  MTGLVMMTKGGG-CGGGGK-------------GGRRKSTAEEEEEEEQNQQQ   38

                        60        70        80        90        100
   OsGAP1/1-444     31  RRGGRSWRCCL--------SCCGSRCS---------                   49
   OsGAP3/1-450     40  LSVLEVLLAAV------RRSVVACRVE-REGGGGWGEEGEAEAEE--------- 77
AtRopGAP1/1-466     54  FDQDVDFHASIEEQDLRRRSSTDGGEEDDGGEDQISLLALLVAIFRRSLIS-- 104
AtRopGAP2/1-430     39  LSLVEFLLTAL------RKSVVSCRVDNRQDDGGVG----------------  68
AtRopGAP3/1-455     44  TTSTDYYDAST------PLSSHASRSGNGSGSGQLTVVDLLAAVLRKSLVMSC  90
AtRopGAP2/1-430     39  LSLVEFLLTAL------RKSVVSCRVDNRQDDGGVG----------------  68

                        110       120       130       140       150
   OsGAP1/1-444     50  ---GAVRCRRAAASAGWRLGGRRMCSTWHTSPS-----TGSMDSSASPWSSSP  94
   OsGAP3/1-450     78  ---GDAAAEVGEMEIGWPTDVRHVAHVTFDRFHGFLGLPVEFEVEMPCRVPSA 127
AtRopGAP1/1-466    105  --CKSNRRELCSMEIGWPTNVRHVAHVTFDRFNGFLGLPVEFEPEVPRRAPSA 155
AtRopGAP2/1-430     69  ---GGISSAVHHMEIGWPTNVRHITHVTFDRFHGFLGLPHELQVEIPCRVPSA 118
AtRopGAP3/1-455     91  AMERGEDDVVASMDIGWPTEVKHVSHVTFDRFNGFLGLPSELEPEVPPRAPSA 143
AtRopGAP2/1-430     69  ---GGISSAVHHMEIGWPTNVRHITHVTFDRFHGFLGLPHELQVEIPCRVPSA 118

                        160       170       180       190       200       210
   OsGAP1/1-444     95  RFPAGLPVRESMQCSYDSRGNSVPTILLMMQRRLYEQGGLRAEGIFRINAENS 147
   OsGAP3/1-450    128  SASVFGVSAESMQCTYDGKGNSVPTILLHMQERLYAQGGLKAEGIFRINPEND 180
AtRopGAP1/1-466    156  SATVFGVSTESMQLSYDSRGNCVPTILLLMQNCLYSQGGLQAEGIFRLTAENS 208
AtRopGAP2/1-430    119  SVSVFGVSAESMQCSYDEKGNSVPTILLLMQERLYSQQGLKAEGIFRINPENS 171
AtRopGAP3/1-455    144  SVSVFGVSAKSMQCSYDDRGNSVPTILLRMQKRLYTEGGLKAEGIFRINPDNG 196
AtRopGAP2/1-430    119  SVSVFGVSAESMQCSYDEKGNSVPTILLLMQERLYSQQGLKAEGIFRINPENS 171

                        220       230       240       250       260
   OsGAP1/1-444    148  QEEFVRDQLNSGIVPDGIDIHCLSGLIKAWFRELPSGVLDSIPPEQVMQCQSE 200
   OsGAP3/1-450    181  QEEHVRDQLNKGVVPEDIDVHCLASLIKAWFRELPEGVLDSLSPEQVLQCNSE 233
AtRopGAP1/1-466    209  EEEAVREQLNRGFIPERIDVHCLAGLIKAWFRELPTSVLDSLSPEQVMQCQTE 261
AtRopGAP2/1-430    172  QEEHVRDQLNRGIVPENIDVHCLAGLIKAWFRELPSGVLDGLSPEEVLNCNTE 224
AtRopGAP3/1-455    197  KEEHVRRQLNCGVVPRGIDVHCLAGLIKAWFRELPTGVLDVLTPEQVMRCNTE 249
AtRopGAP2/1-430    172  QEEHVRDQLNRGIVPENIDVHCLAGLIKAWFRELPSGVLDGLSPEEVLNCNTE 224

                        270       280       290       300       310
   OsGAP1/1-444    201  EDCARVAKCLPPAEAALLEWAVNLMADVVQEEQINKMNARNIAMVFAPNMTQM 253
   OsGAP3/1-450    234  GEFLELVTLLRPTQAALLNWAVELMADVVEETELNKMNARNIAMVFAPNMTQM 286
AtRopGAP1/1-466    262  EENVELVRLLPPTEAALLDWAINLMADVVQYEHLNKMNSRNIAMVFAPNMTQM 314
AtRopGAP2/1-430    225  DESVELIKQLKPTESALLNWAVDLMADVVEETESNKMNARNIAMVFAPNMTQM 277
AtRopGAP3/1-455    250  EDCSRLVILLPPVESAILDWAIGLMADVVEHEQFNKMNARNVAMVFAPNMTQM 302
AtRopGAP2/1-430    225  DESVELIKQLKPTESALLNWAVDLMADVVEETESNKMNARNIAMVFAPNMTQM 277

                        320       330       340       350       360
   OsGAP1/1-444    254  SDPLTALMYAVQVMNFLKMLIQKTLKGRQESNLEDTSLPHKDPSDESGHHKPC 306
   OsGAP3/1-450    287  SDPLTALMHAVQVMNFLKTLILRTLRERDDAASGDYTPYSSPASSSQQNDAEY 339
AtRopGAP1/1-466    315  DDPLTALMYAVQVMNFLKTLIEKTLRERQDSVVEQAHAFPLEPSDESGHQSPS 367
AtRopGAP2/1-430    278  TDPLTALMHAVQVMNLLKTLITKTLAEREENATGSEG-YSPSHSSNSQTDSDS 329
AtRopGAP3/1-455    303  ADPLTALIHAVQVMNFLKTLILMNLKERENADAKARWLKKQTSDPSEEWESQH 355
AtRopGAP2/1-430    278  TDPLTALMHAVQVMNLLKTLITKTLAEREENATGSEG-YSPSHSSNSQTDSDS 329

                        380       390       400       410       420
   OsGAP1/1-444    307  LTLESLLEEESRRPSFVEEEPILNSPAHGTGYNPIEVNPVQGKTAASIAQTSE 359
   OsGAP3/1-450    340  YGSERDMDRSCE--------------------MSDMHSEISRSGRQVDFLVR  371
AtRopGAP1/1-466    368  Q--SLAFNTSEQ--------------------SEETQSDNIENAENQSSSSE  397
AtRopGAP2/1-430    330  D-NAQDMEVSCE--------------------SQATDSECGEE-EEVEEVEQ  359
AtRopGAP3/1-455    356  S----EILSPEK--------------------PNNNNPKFLRVATLCRLEAD  383
AtRopGAP2/1-430    330  D-NAQDMEVSCE--------------------SQATDSECGEE-EEVEEVEQ  359

                        430       440       450       460       470
   OsGAP1/1-444    360  VQTIIEGSSSCSRPSLTDPPATADPVCAEAANSLQRKGSRSLNSRRTRKGKGQ 412
   OsGAP3/1-450    372  YNTCFDSEQEGVDPLSDVEEGFLRQLEHDLEADKREESAKKQHEISSEIMAVK 424
AtRopGAP1/1-466    398  ISDELTLENNACE----QRETDFGKYRTGRLSDSSQQVVLNLDPPAQWPVGRT 446
AtRopGAP2/1-430    360  HQEHLSRHSTHED---ETDIGSLCSIEKCFLNQLNNNAARVSNTSISEDWSPK 409
AtRopGAP3/1-455    384  NEEEFWNIKKRND-----HEGVLDTSSGN--GNIGPVQRLCKHPLFQLSKSTK 429
AtRopGAP2/1-430    360  HQEHLSRHSTHED---ETDIGSLCSIEKCFLNQLNNNAARVSNTSISEDWSPK 409

                        480       490       500
   OsGAP1/1-444    413  SGTSATSSAEKSKGTSIVSRINSKIERIEAWR                      444
   OsGAP3/1-450    425  DVQAELKVEAKAAGNTQKEEGAGSLQ------                      450
AtRopGAP1/1-466    447  KGLTNLSRVGSRVERTEAWR-                                 466
AtRopGAP2/1-430    410  AFPLVSFTENKS--NTLSSSTSD---------                      430
AtRopGAP3/1-455    430  KAFVSNRDEGRKGREAWSSRLSSLPW------                      455
AtRopGAP2/1-430    410  AFPLVSFTENKS--NTLSSSTSD---------                      430
```

B

```
OsGAP3     PTILLHMQERLYAQGGLKAEGIFRINPENDQEEHVRDQL-------NKGVVPEDI-DVHCL
AtRopGAP1  PTILLLMQNCLYSQGGLQAEGIFRLTAENSEEEAVREQL-------NRGFIPERI-DVHCL
p50RhoGAP1 PIVLRETVAYLQAHA-LTTEGIFRRSANTQVVREVQQKYN------MGLPVDFDQYNELHLP
chimerin   PMVVDMCIREIESRG-LNSEGLYRVSGFSDLIEDVKMAFDRDGEKADISVNMYE--DINII
BCR        PYIVRQCVEEIERRG-MEEVGIYRVSGVATDIQALKAAFDVNNK--DVSVMMSEM-DVNAI

OsGAP3     ASLIKAWFRELPEGVLDSLSPEQVLQCNSEGE-------FLELVTLLRPTQAALLNWAVEL
AtRopGAP1  AGLIKAWFRELPTSVLDSLSPEQVMQCQTEEE-------NVELVRLLPPTEAALLDWAINL
p50RhoGAP1 AVILKTFLRELPEPLLTFDLYPHVVGFLNIDES-QRVPATLQVLQTLPEENYQVLRFLTAF
chimerin   TGALKLYFRDLPIPLITYDAYPKFIESAKIMDPDEQLETLHEALKLLPPAHCETLRYLMAH
BCR        AGTLKLYFRELPEPLFTDEFYPNFAEGIALSDPVAKESCMLNLLLSLPEANLLTFLFLLDH

OsGAP3     MADVVEEEELNKMNARNIAMVFAPNMTQMSDP-LTALMHAVQVMNFLKTLILRTLRE
AtRopGAP1  MADVVQYEHLNKMNSRNIAMVFAPNMTQMDDP-LTALMYAVQVMNFLKTLIEKTLRE
p50RhoGAP1 LVQISAHSDQNKMTNTNLAVVFGPNLLWAKDA--AITLKAINPINTFTKFLLDHQGE
chimerin   LKRVTLHEKENLMNAENLGIVFGPTLMRSPELDAMAALNDIR----YQRLVVELLIK
BCR        LKRVAEKEAVNKMSLHNLATVFGPTLLRPSEKESKLPANPSQPITMTDSWSLEVMSQ
```

**Figure 4-7. Comparison of primary sequences between six RopGAPs and their conserved domains.** (A) Amino acid alignment of the RopGAPs. (B) Amino acid alignment of the GAP-like domain of RopGAPs with various RhoGAPs. O.s., *Oryza sativa*; A.t., *Arabidopsis*; Sequence alignment was performed by using the Clustal W program.
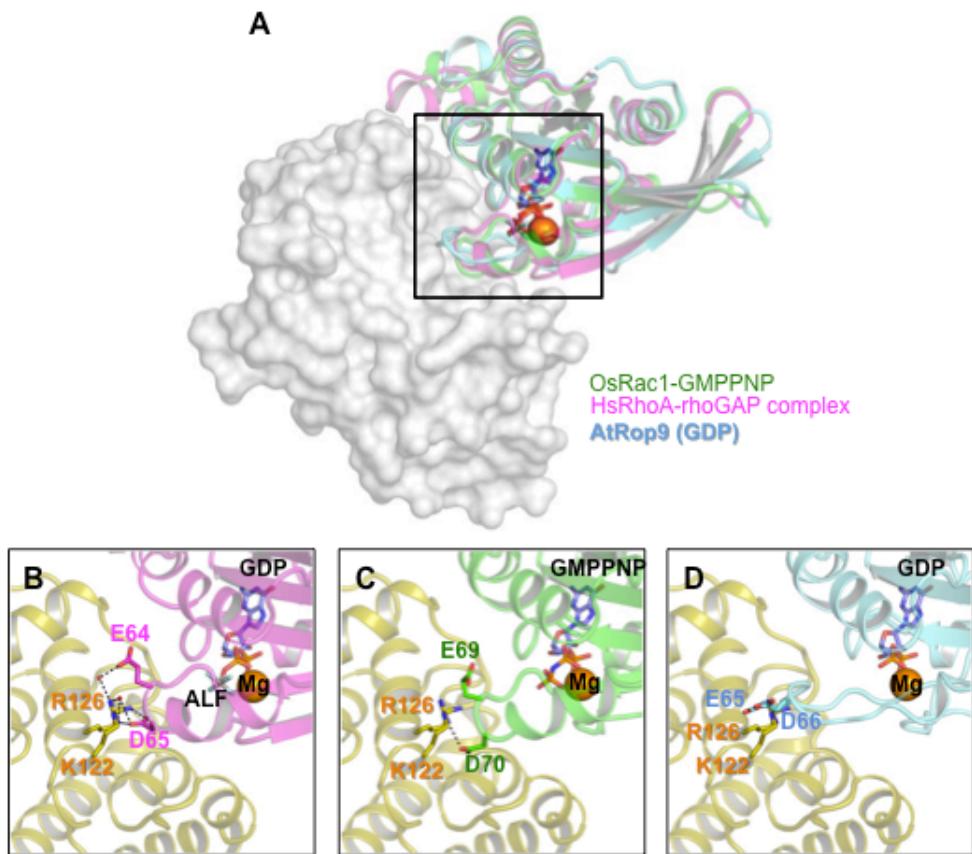
**Figure 4-8. Structural models of the Osrac1•GAP complex.** (A) Superimposition of the crystal structures of OsRac1(GMPPNP) (PDB code: 4U5X), HsRhoA-RhoGAP complex (PDB code: 1TX4) and AtRop9(GDP) (PDB code: 2J0V, chain B). (B) The crystal structure of HsRhoA-RhoGAP domain complex (PDB code: 1TX4). AlFx is shown in the stick model. (C) Superimposition of the crystal structures of OsRac1(GMPPNP) (PDB code: 4U5X) and HsRhoA-RhoGAP complex (PDB code: 1TX4). (D) Superimposition of the crystal structures of HsRhoA-RhoGAP complex (PDB code: 1TX4) and AtRop9(GDP) (PDB code: 2J0V, chain B). GDP and GMPPNP are shown in the stick model (red, oxygen; blue, nitrogen; orange, phosphorus). The $Mg^{2+}$ ion is shown as an orange sphere. Models were generated using PyMOL.
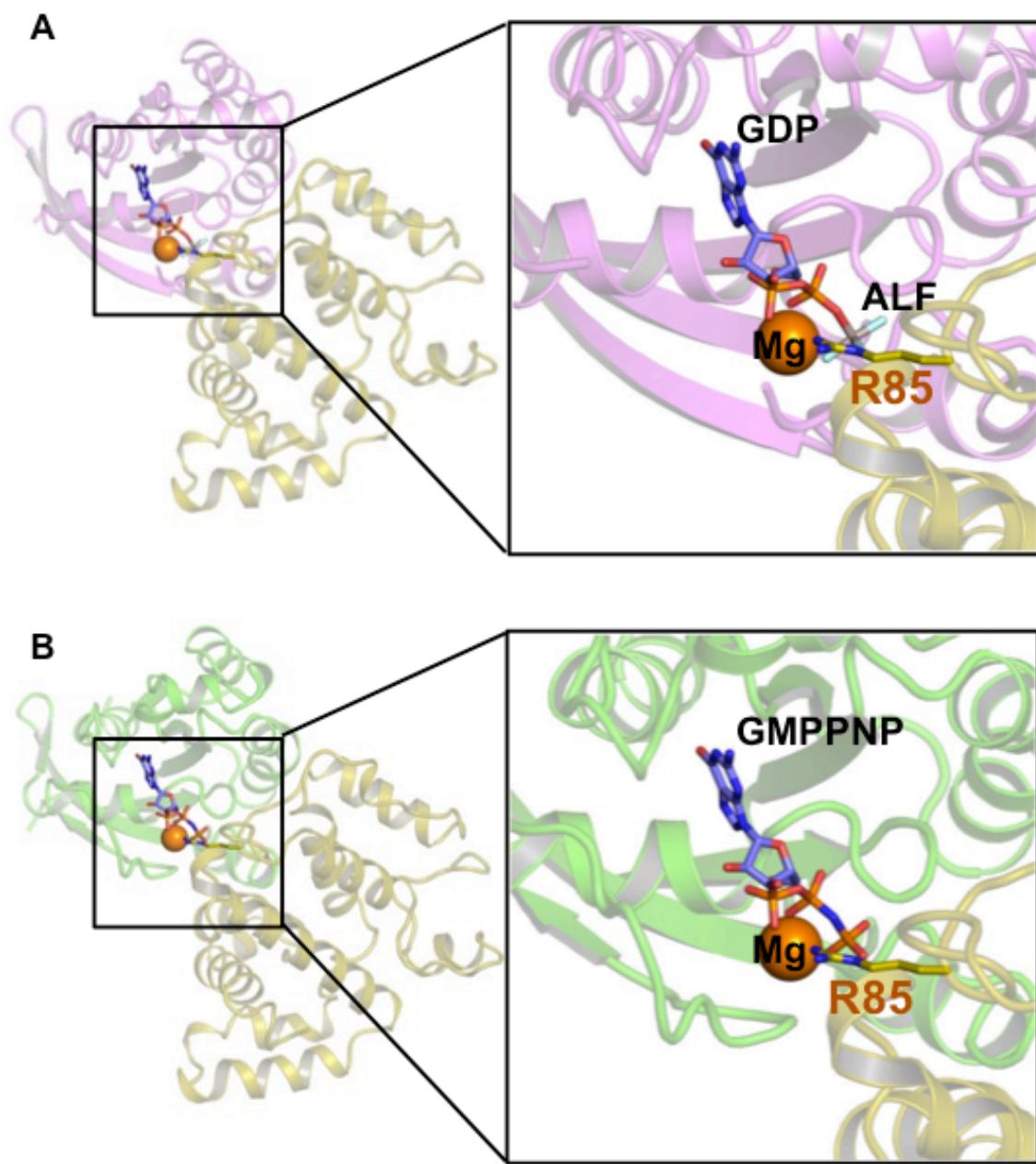
**Figure 4-9. Structural models of the mechanism of GTP hydrolysis by GAP.**

(A) The crystal structure of HsRhoA-RhoGAP domain complex (PDB code: 1TX4). AlFx is shown in the stick model. (B) Superimposition of the crystal structures of OsRac1(GMPPNP) (PDB code: 4U5X) and HsRhoA-RhoGAP complex (PDB code: 1TX4). The ribbon cartoons are rotated by 180° about the Y axis compared with the depiction in Figure 4-8.GDP and GMPPNP are shown in the stick model (red, oxygen; blue, nitrogen; orange, phosphorus). The $Mg^{2+}$ ion is shown as an orange sphere. Models were generated using PyMOL.
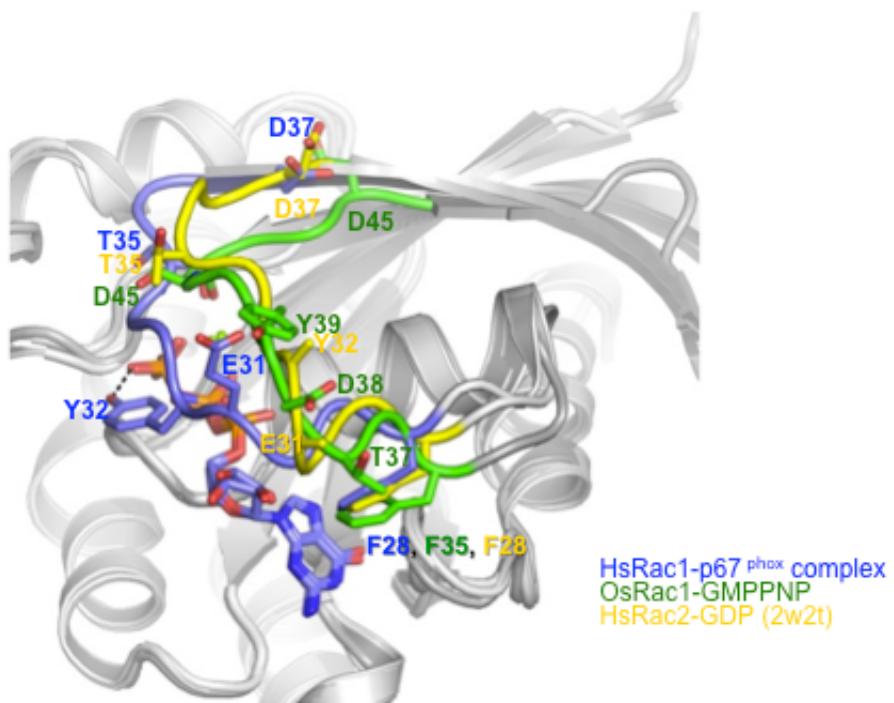
**Figure 4-10. Structural difference in SwitchI of OsRac1, HsRac1 and AtRop9 for the NADPH oxidase interaction.** Main chains of the HsRac1-p67[phox] complex (PDB code: 1E96), OsRac1(GMPPNP) (PDB code: 4U5X) and AtRop9(GDP) (pdbPDB code:2J0V, chain B) and were superimposed by using program PyMOL. The Switch I are colored as indicated in the inset legend. The GMPPNP and GDP were shown in the stick model (red, deep blue, and orange indicates O, N, and P atoms, respectively). The Mg$^{2+}$ ion was shown as orange sphere.

**References**

1. Sørmo, C. G., Leiros, I., Brembu, T., Winge, P., Os, V., and Bones, A. M. (2006) The crystal structure of Arabidopsis thaliana RAC7/ROP9: the first RAS superfamily GTPase from the plant kingdom. *Phytochemistry,* **67**, 2332-2340.

2. Scheidig, A. J., Burmester, C., Goody, R. S. (1999) The pre-hydrolysis state of p21(ras) in complex with GTP: new insights into the role of water molecules in the GTP hydrolysis reaction of ras-like proteins. *Structure* **7**, 1311-24.

3. Berken, A. (2006) ROPs in the spotlight of plant signal transduction. *Cell. Mol. Life Sci.* **63**, 2446–2459.

4. Akamatsu, A., Wong, H. L., Fujiwara, M., Okuda, J., Nishide, K., Uno, K., Imai, K., Umemura, K., Kawasaki, T., Kawano, Y., and Shimamoto, K. (2013) An OsCEBiP/OsCERK1-OsRacGEF1-OsRac1 module is an essential early component of chitin-induced rice immunity. *Cell Host Microbe* **13**, 465-476.

5. Thomas, C., Fricke, I., Scrima, A., Berken, A., and Wittinghofer, A. (2007) Structural evidence for a common intermediate in small G protein-GEF reactions. *Mol. Cell* **25**, 141-149.

6. Rittinger, K., Walker, P. A., Eccleston, J. F., Smerdon, S. J., and Gamblin, S. J. (1997) Structure at 1.65 A of RhoA and its GTPase-activating protein in complex with a transition-state analogue. *Nature* **389**, 758-762

7. Xu, X., Barry, D. C., Settleman, J., Schwartz, M. A., and Bokoch, G. M. (1994) Differing structural requirements for GTPase-activating protein responsiveness and NADPH oxidase activation by Rac. *J. Biol. Chem.* **269**, 23569-23574.

8. Koga, H., Terasawa, H., Nunoi, H., Takeshige, K., Inagaki, F., and Sumimoto, H. (1999) Tetratricopeptide repeat (TPR) motifs of p67[phox] participate in interaction with

the small GTPase Rac and activation of the phagocyte NADPH oxidase. *J. Biol. Chem.* **274**, 25051-25060.

9. Lapouge, K., Smith, S. J., Walker, P. A., Gamblin, S. J., Smerdon, S. J., and Rittinger, K. (2000) Structure of the TPR domain of p67[phox] in complex with Rac-GTP. *Mol. Cell* **6**, 899-907.

# CHAPTER 5

# GENERAL CONCLUSION

## 5. GENERAL CONCLUSION

In rice, small GTPase OsRac1 has emerged as a key activator of rice innate immunity. OsRac1 plays an important role in regulating the production of reactive oxygen species (ROS) by the NADPH oxidase OsRbohB during innate immunity.

In this thesis, the crystals of OsRac1$^{Q68L}$ mutant was obtained (Chapter 2, Figure 2-2) and structure of OsRac1 was determined as the first active-form structure of a plant small GTPase (Chapter 3, Figure 3-1 A). The structure of OsRac1 had a typical G domain fold structure. The overall structure of OsRac1 was similar to the GDP-bound form plant small GTPase proteins. However, structural differences were observed in the Switch I, Switch II and Insert regions (Chapter 3, Figure 3-2).

The interaction analysis between OsRac1 and OsRbohB shown Tyr39, Val43, Phe44 and Asp45 residues of OsRac1 was important in the interaction with OsRbohB[138-313] (Chapter 3, Figure 3-9). Two of these, the Tyr39Ala and Asp45Ala mutants were markedly decreased in the levels of ROS (Chapter 3, Figure 3-8). NMR data also indicated that the tertiary structures of the Y39A and D45A mutants are folded (Chapter 3, Figure 3-6 D). These mutation sites (Tyr39, Val43, Phe44 and Asp45) were locating on the C-terminal region of switch I of OsRac1 and these results strongly suggest that C-terminal region of switch I of OsRac1 is interaction site with OsRbohB.

**List of Publications**

1. Ken-ichi Kosami, Izuru Ohki, Kokoro Hayashi, Ryo Tabata, Sayaka Usugi, Tsutomu Kawasaki, Toshimichi Fujiwara, Atsushi Nakagawa, Ko Shimamoto, and Chojiro Kojima, Purification, crystallization and preliminary X-ray crystallographic analysis of a rice Rac/Rop GTPase, OsRac1, *Acta Crystallographica*, F70, 113-115 (2014)

2. Ken-ichi Kosami, Izuru Ohki, Minoru Nagano, Kyoko Furuita, Toshihiko Sugiki, Yoji Kawano, Tsutomu Kawasaki, Toshimichi Fujiwara, Atsushi Nakagawa, Ko Shimamoto, and Chojiro Kojima, The crystal structure of the plant small GTPase OsRac1 reveals its mode of binding to NADPH oxidase, *J. Biol. Chem.*, 289:28569-78 (2014)